# Evaluating the Technology Design Space for Long-Duration Energy Storage and Role in Deep Decarbonization of Power Systems: Supplementary Information

**Nestor A. Sepulveda[1,2,*], Jesse D. Jenkins[3], Aurora Edington[1], Dharik Mallapragada[1], and Richard K. Lester[4]**

[1]Massachusetts Institute of Technology, MIT Energy Initiative, Cambridge, MA
[2]Massachusetts Institute of Technology, Department of Nuclear Science and Engineering, Cambridge, MA
[3]Princeton University, Andlinger Center for Energy and the Environment and Department of Mechanical and Aerospace Engineering, Princeton, NJ
[4]Massachusetts Institute of Technology, Office of the Provost, Cambridge, MA
[*]Corresponding Author nsep@mit.edu

## Contents

**Supplementary Figures** **2**
- LDES Space . . . 2
- Cost Reduction . . . 2
- LDES Operation . . . 5
- Firm Reduction . . . 7
- Li-ion Reduction . . . 9
- LDES Energy-to-Power Ratio . . . 17
- LDES Duration . . . 21
- LDES Charge/Discharge Balance . . . 25
- Disaggregated Plots . . . 27

**Supplementary Methods** **46**
- Reference Case Descriptors . . . 46
- Model Configuration . . . 48
- Economic and Operational Parameters . . . 49
- Variable Renewable and Demand Assumptions . . . 52
- GenX Overview . . . 55

**References** **70**

# Supplementary Figures

## LDES Space

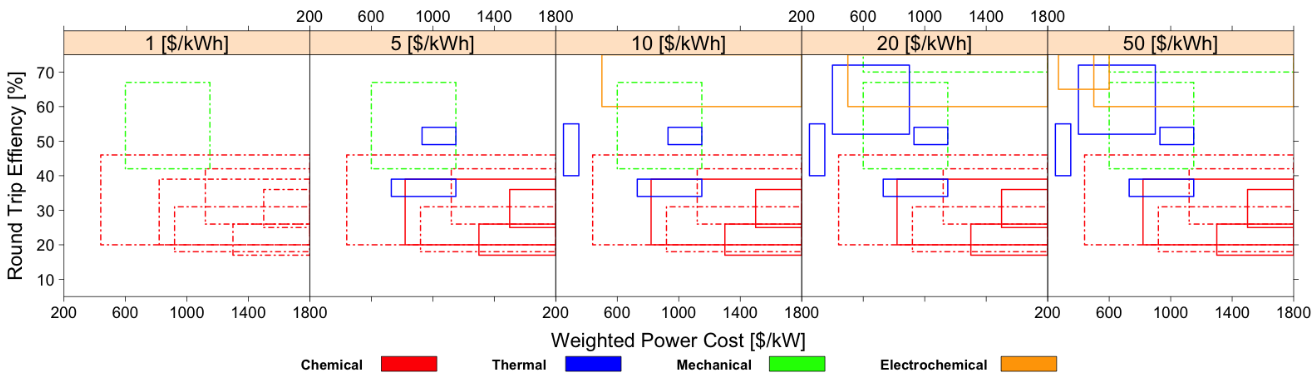


Each column represents a specific Energy Capacity Cost [$/kWh] assumption in the "LDES Technology Space". Within each subplot the x-axis represents the Weighted Power Capacity Cost and the y-axis the Round-Trip Efficiency. Dash-dotted lines depict technologies subject to geological and geographic constraints.

**Figure SI-1.** Intersection between LDES Technology Space and Future Projections in Table 2

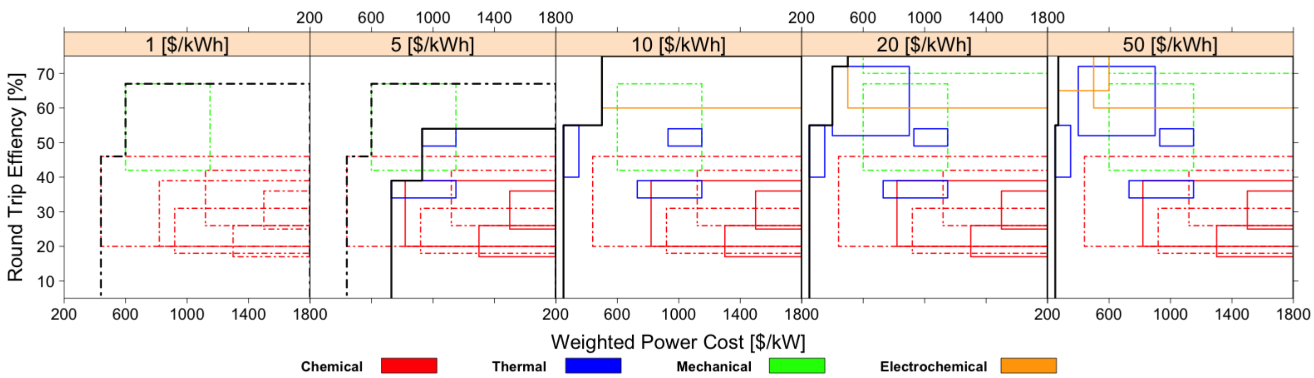


Each column represents a specific Energy Capacity Cost [$/kWh] assumption in the "LDES Technology Space". Within each subplot the x-axis represents the Weighted Power Capacity Cost and the y-axis the Round-Trip Efficiency. Dash-dotted lines depict technologies subject to geological and geographic constraints. Feasibility lines in black correspond to the convex-hull of the lowest weighted power cost and highest round-trip efficiency regions of different geological and geographic constrained and unconstrained LDES projected technologies. For cases with the unconstrained feasibility line reaching higher efficiency and lower power cost levels than the constrained one, only the unconstrained line is shown.

**Figure SI-2.** Feasibility Lines Based on the Intersection between LDES Technology Space and Future Projections in Table 2

## Cost Reduction

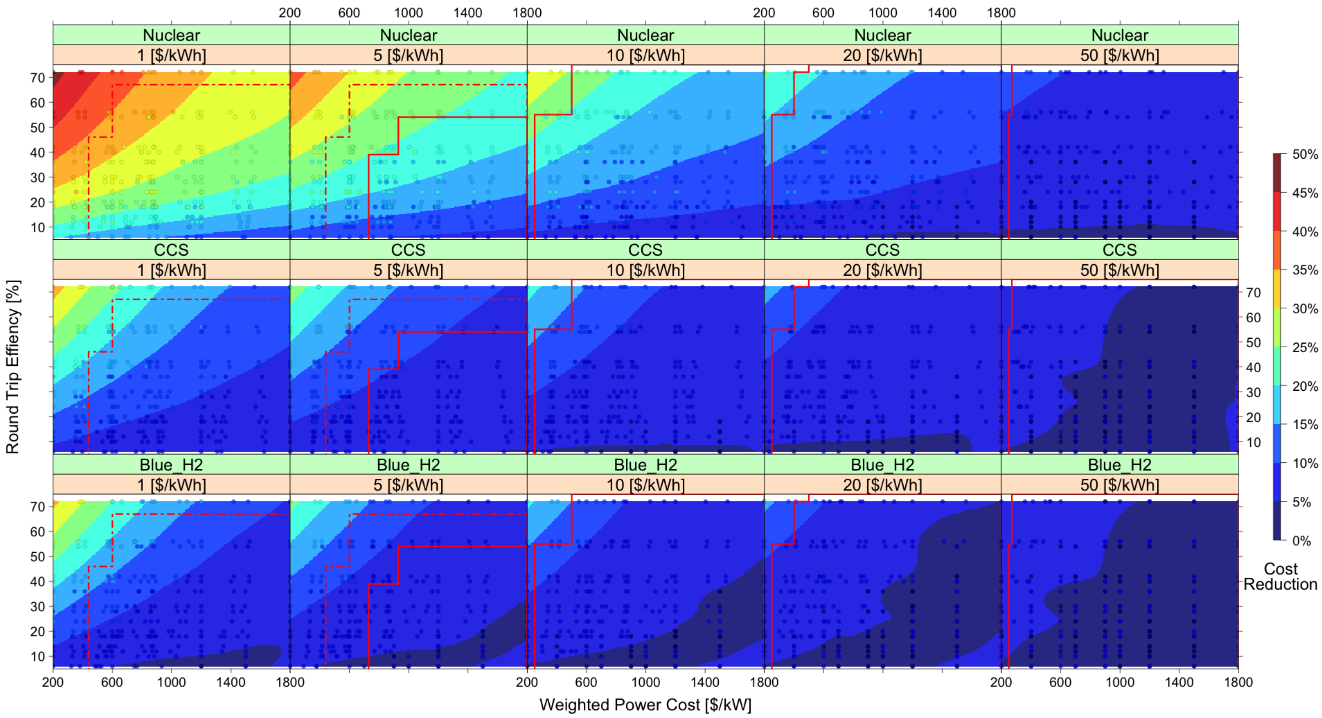


Each row of plots represents a different scenario using a different firm low-carbon technology, and consequently a different reference case was used to calculate the percentage change in system costs. "Future feasible regions" for known LDES technologies from Figure SI-1 are plotted to the right of the dash-dotted lines for each row. Each column represents a specific LDES energy capacity cost ($/kWh) assumption in the LDES parameter combination. Within each subplot the x-axis represents the weighted power capacity cost and the y-axis the round-trip efficiency. Total annualized system costs for the reference cases (in USD per MWh) are as follows: nuclear - $67.90; gas w/CCS - $53.14; Blue $H_2$ - $52.12.

**Figure SI-3.** Southern System: Percentage Cost Reduction as Function of LDES Parameter Combination Compared to Reference Cases (Scenarios 1-3 Table 4)

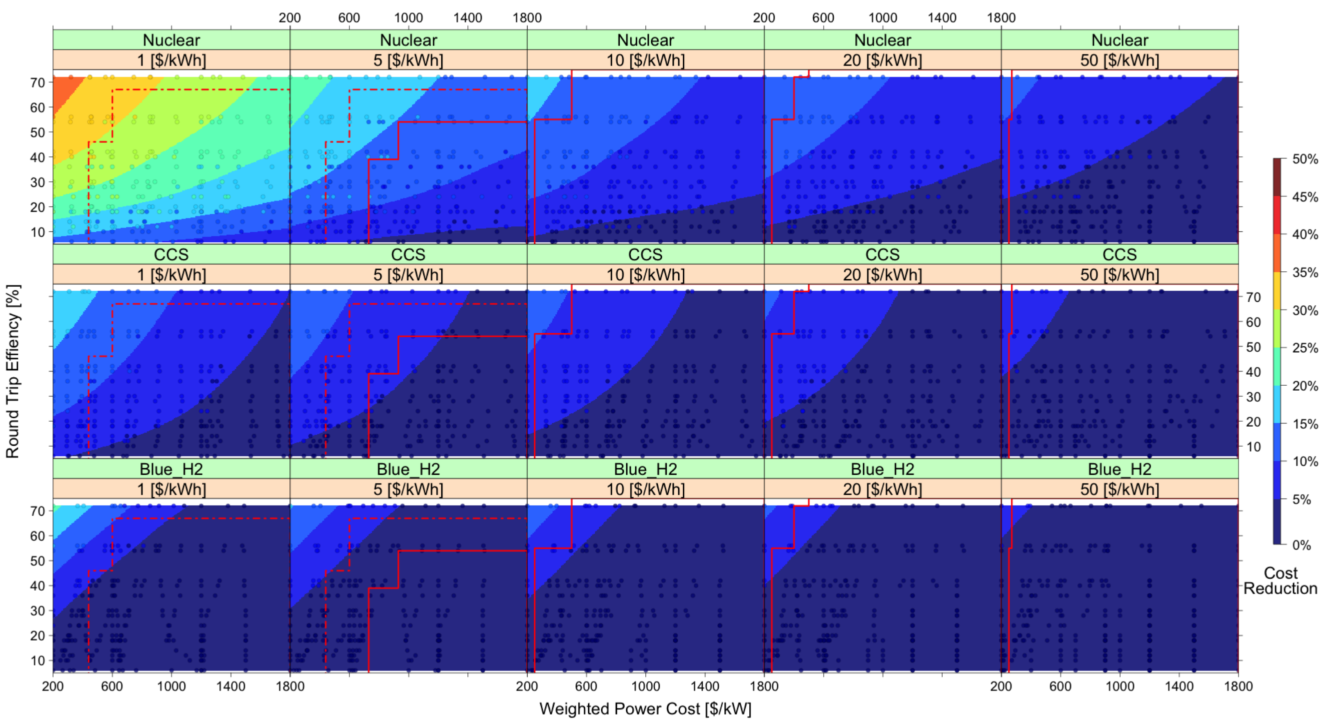


Each row of plots represents a different scenario using a different firm low-carbon technology, and consequently a different reference case was used to calculate the percentage change in system costs. "Future feasible regions" for known LDES technologies from Figure SI-1 are plotted to the right of the dash-dotted lines for each row. Each column represents a specific LDES energy capacity cost ($/kWh) assumption in the LDES parameter combination. Within each subplot the x-axis represents the weighted power capacity cost and the y-axis the round-trip efficiency. Total annualized system costs for the reference cases (in USD per MWh) are as follows: nuclear - $108.48; gas w/CCS - $82.66; Blue $H_2$ - $86.69.

**Figure SI-4.** Northern System with Electrified Load and Medium Cost for VRE and Li-ion: Percentage Cost Reduction as Function of LDES Parameter Combination Compared to Reference Cases (Scenarios 12-14 Table 4)

## LDES Operation

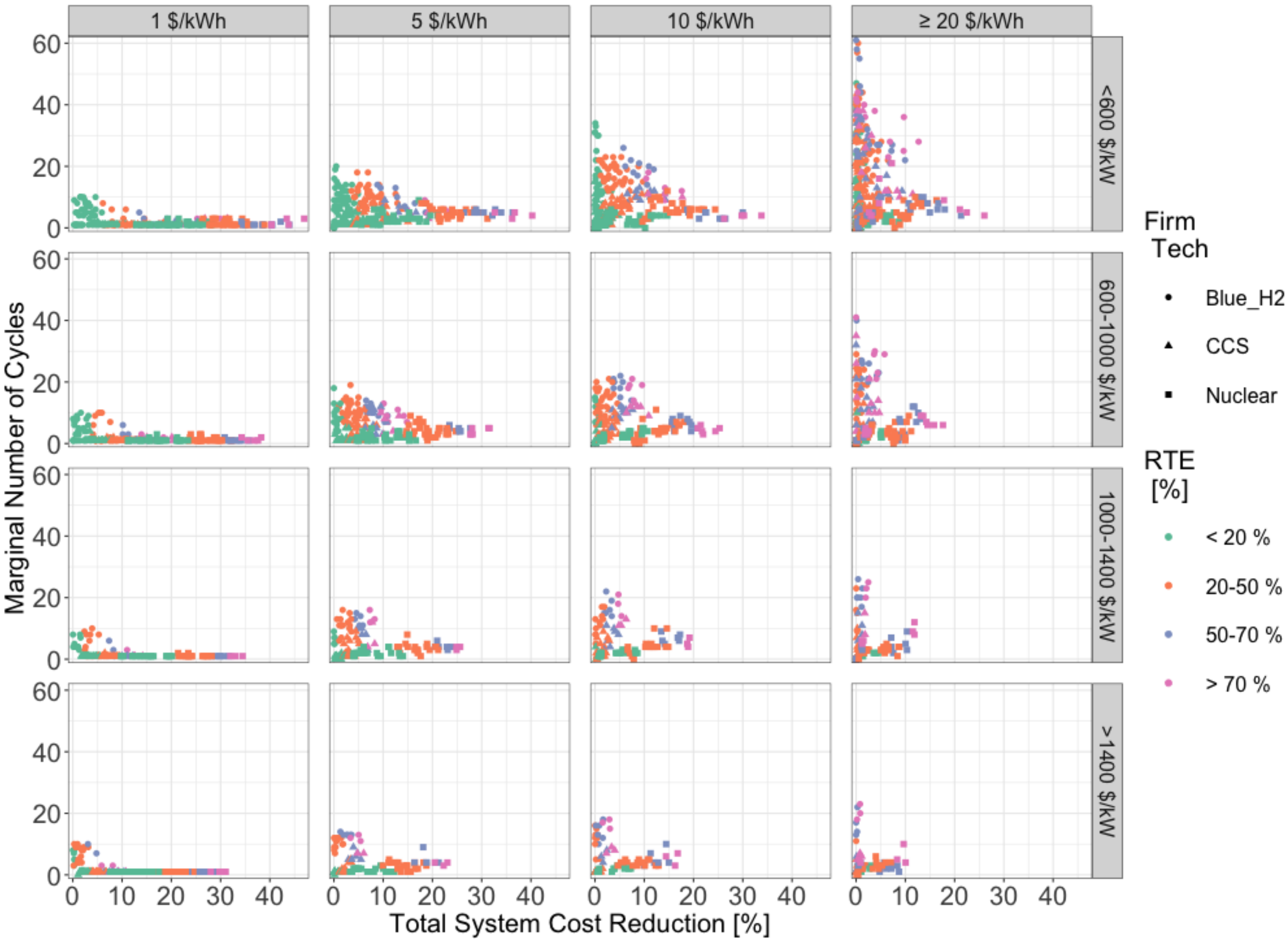


The figure shows the marginal number of cycles which is calculated as the minimum number of cycles over the year across every 1% of energy capacity of the system. For each 1% of energy capacity the number of full charge and full discharge (a cycle) is calculated for the full year by looking at the hours that specific energy capacity level is above and below that energy capacity level. Panels going left-right indicate different energy capacity cost levels and panels going bottom-up indicate different weighted power cost levels

**Figure SI-5.** Northern System: Marginal number of cycles of LDES energy storage capacity versus system value of LDES (Scenarios 1-3 Table 4)

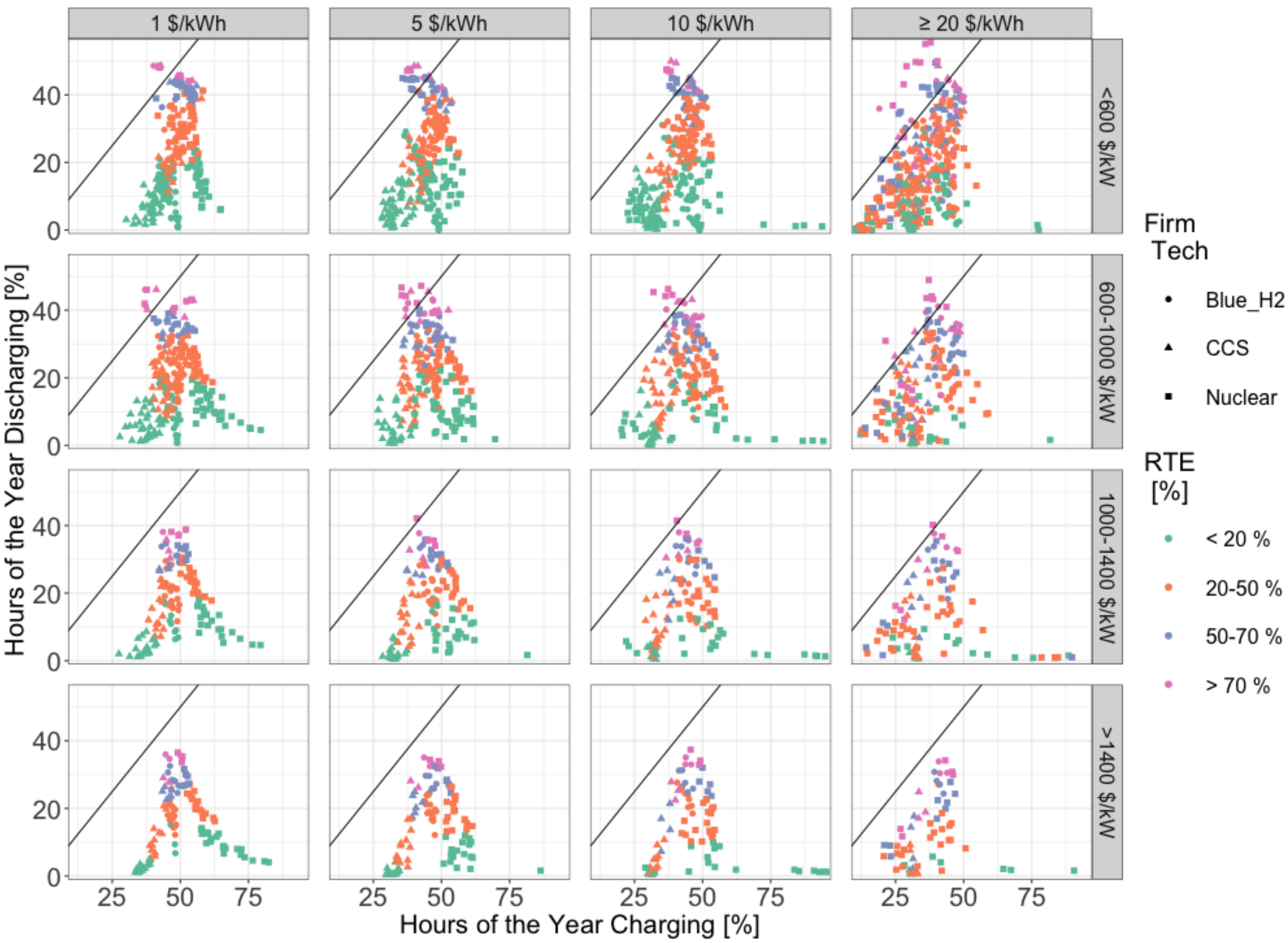


The figure shows the percentage of the hours of the year the LDES system is charging (x-axis) and discharging (y-axis). The solid line denotes with the same percentage for charge and discharge. For the space below the line charging is more frequent than discharge. For the space above the line discharge is more frequent. Panels going left-right indicate different energy capacity cost levels and panels going bottom-up indicate different weighted power cost levels

**Figure SI-6.** Northern System: Charge versus discharge frequency (Scenarios 1-3 Table 4)

## Firm Reduction

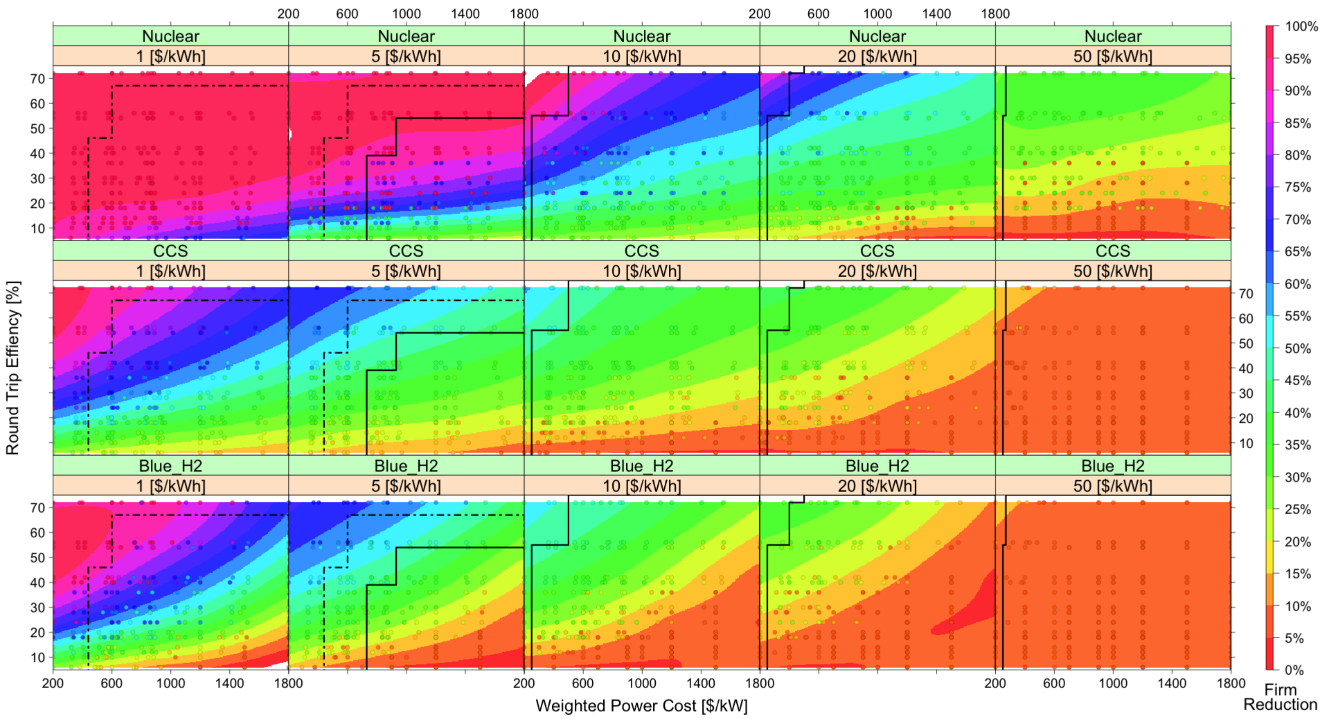


Each row of plots represents a different scenario using a different firm low-carbon technology, and consequently a different reference case was used to calculate the percentage change in firm capacity. "Future feasible regions" for known LDES technologies from Figure SI-1 are plotted to the right of the dash-dotted lines for each row. Each column represents a specific LDES energy capacity cost ($/kWh) assumption in the LDES parameter combination. Within each subplot the x-axis represents the weighted power capacity cost and the y-axis the round-trip efficiency. Total firm capacity for the reference cases normalized by peak demand (in %) are as follows: nuclear - 31.9%; gas w/CCS - 36.3%; Blue $H_2$ - 32.9%.

**Figure SI-7.** Southern System: Percentage Firm Capacity Reduction as Function of LDES Parameter Combination Compared to Reference Cases (Scenarios 1-3 Table 4)

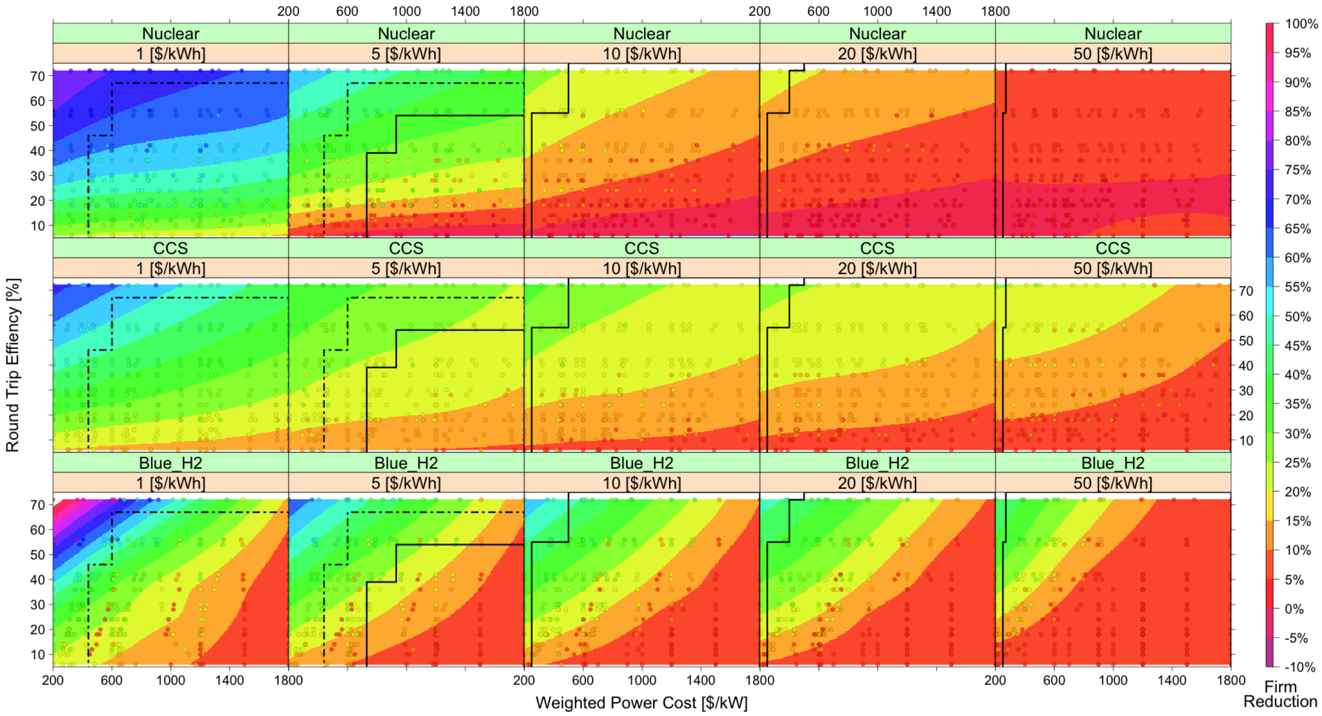


Each row of plots represents a different scenario using a different firm low-carbon technology, and consequently a different reference case was used to calculate the percentage change in firm capacity. "Future feasible regions" for known LDES technologies from Figure SI-1 are plotted to the right of the dash-dotted lines for each row. Each column represents a specific LDES energy capacity cost ($/kWh) assumption in the LDES parameter combination. Within each subplot the x-axis represents the weighted power capacity cost and the y-axis the round-trip efficiency. Total firm capacity for the reference cases normalized by peak demand (in %) are as follows: nuclear - 57.5%; gas w/CCS - 64.0%; Blue $H_2$ - 67.5%.

**Figure SI-8.** Northern System with Electrified Load and Medium Cost for VRE and Li-ion: Percentage Firm Capacity Reduction as Function of LDES Parameter Combination Compared to Reference Cases (Scenarios 12-14 Table 4)

## Li-ion Reduction

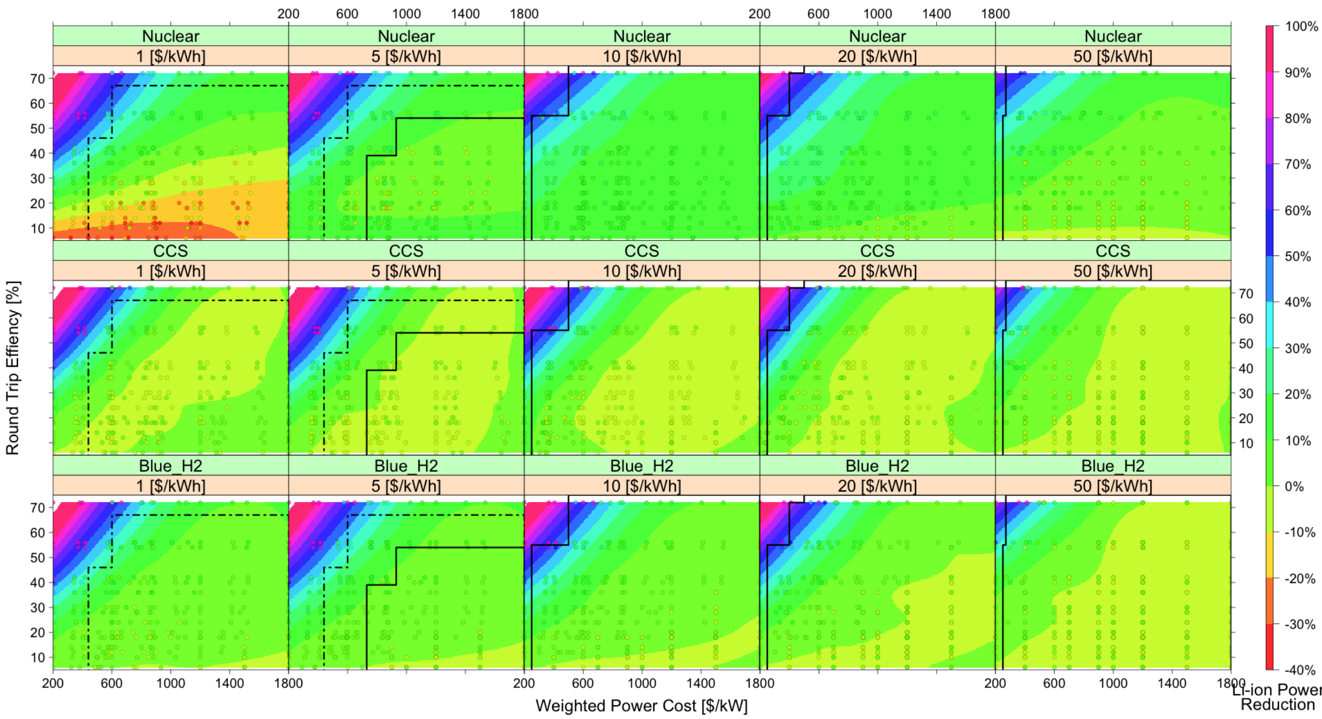


Each row of plots represents a different scenario using a different firm low-carbon technology, and consequently a different reference case was used to calculate the percentage change in Li-ion power capacity. "Future feasible regions" for known LDES technologies from Figure SI-1 are plotted to the right of the dash-dotted lines (geographically constrained) and solid lines (unconstrained) for each row. Each column represents a specific LDES energy capacity cost ($/kWh) assumption in the LDES parameter combination. Within each subplot the x-axis represents the weighted power capacity cost and the y-axis the round-trip efficiency. Total Li-ion power capacity for the reference cases normalized by peak demand (in %) and duration (in hours) are as follows: nuclear - 39.2%-10h; gas w/CCS - 31.2% -7.8h; Blue $H_2$ - 35%-8.8h.

**Figure SI-9.** Southern System: Percentage Li-ion Power Capacity Reduction as Function of LDES Parameter Combination Compared to Reference Cases (Scenarios 1-3 Table 4)

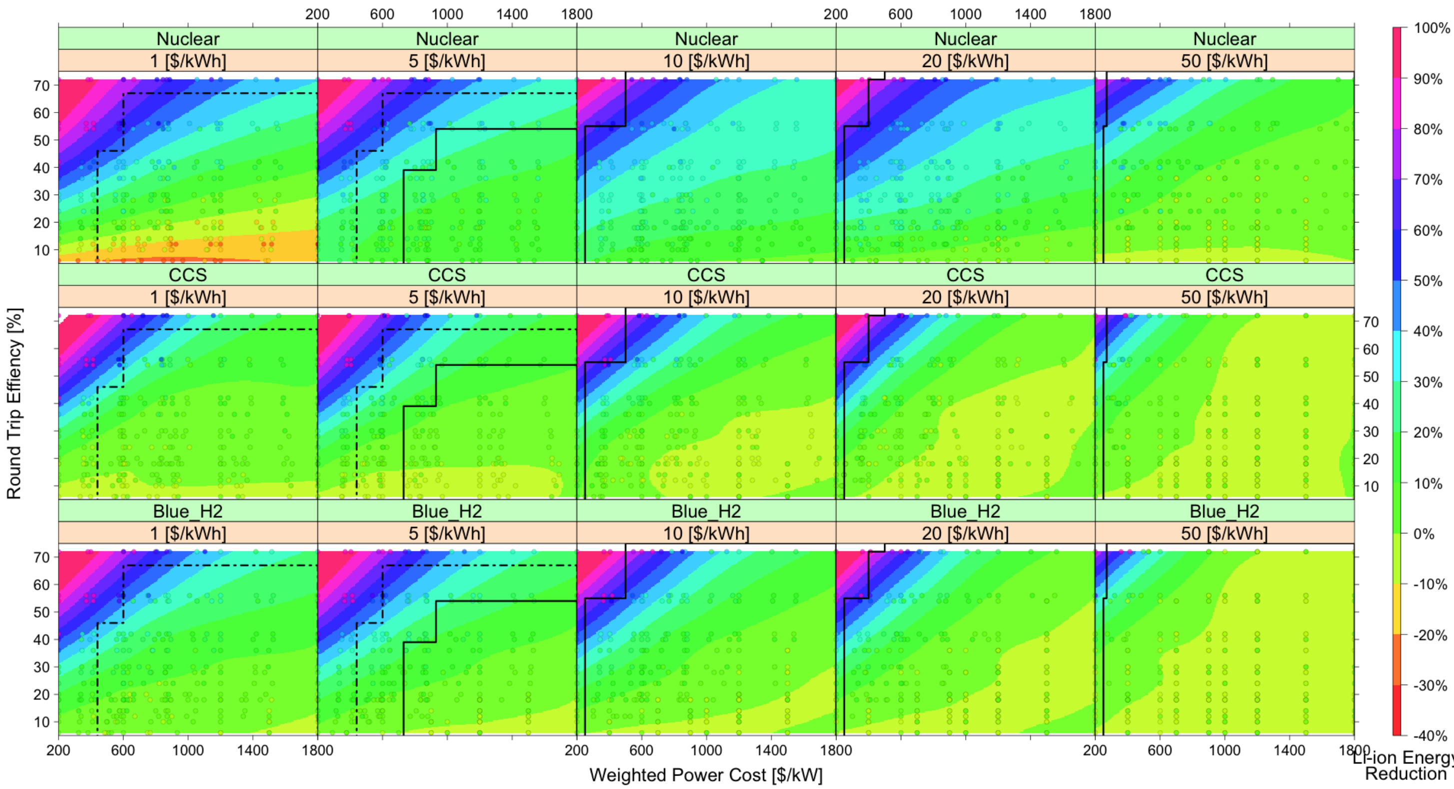


Each row of plots represents a different scenario using a different firm low-carbon technology, and consequently a different reference case was used to calculate the percentage change in Li-ion energy capacity. "Future feasible regions" for known LDES technologies from Figure SI-1 are plotted to the right of the dash-dotted lines (geographically constrained) and solid lines (unconstrained) for each row. Each column represents a specific LDES energy capacity cost ($/kWh) assumption in the LDES parameter combination. Within each subplot the x-axis represents the weighted power capacity cost and the y-axis the round-trip efficiency. Total Li-ion power capacity for the reference cases normalized by peak demand (in %) and duration (in hours) are as follows: nuclear - 39.2%-10h; gas w/CCS - 31.2% -7.8h; Blue $H_2$ - 35%-8.8h.

**Figure SI-10.** Southern System: Percentage Li-ion Energy Capacity Reduction as Function of LDES Parameter Combination Compared to Reference Cases (Scenarios 1-3 Table 4)

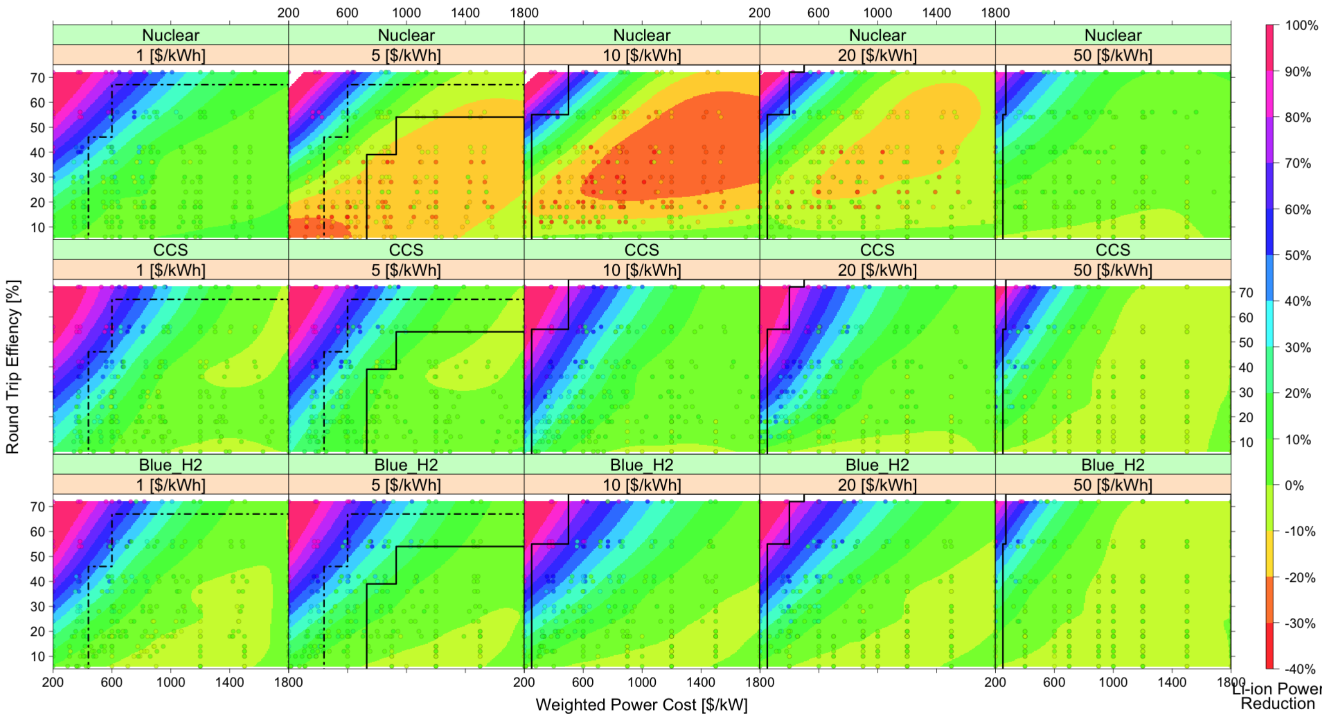


Each row of plots represents a different scenario using a different firm low-carbon technology, and consequently a different reference case was used to calculate the percentage change in Li-ion power capacity. "Future feasible regions" for known LDES technologies from Figure SI-1 are plotted to the right of the dash-dotted lines (geographically constrained) and solid lines (unconstrained) for each row. Each column represents a specific LDES energy capacity cost ($/kWh) assumption in the LDES parameter combination. Within each subplot the x-axis represents the weighted power capacity cost and the y-axis the round-trip efficiency. Total Li-ion power capacity for the reference cases normalized by peak demand (in %) and duration (in hours) are as follows: nuclear - 37.5%-10h; gas w/CCS - 27.9% -8.4h; Blue $H_2$ - 31%-8.3h.

**Figure SI-11.** Northern System: Percentage Li-ion Power Capacity Reduction as Function of LDES Parameter Combination Compared to Reference Cases (Scenarios 4-6 Table 4)

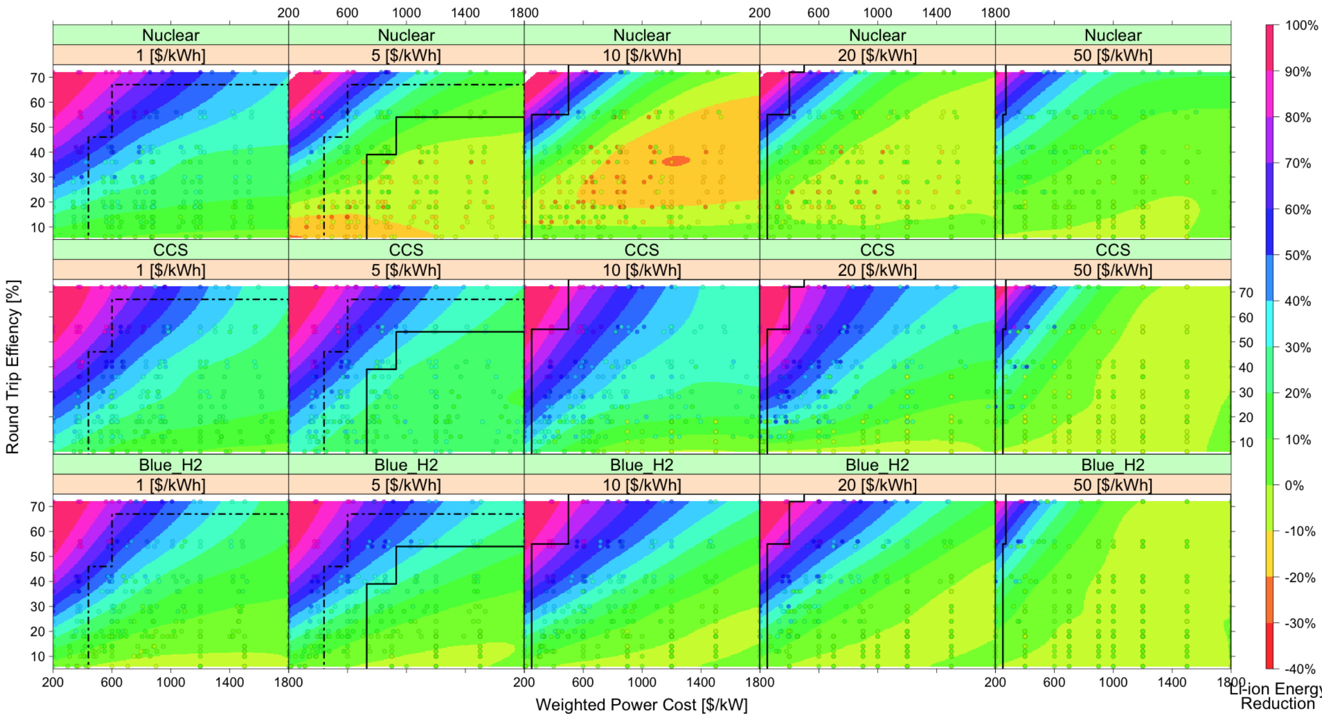


Each row of plots represents a different scenario using a different firm low-carbon technology, and consequently a different reference case was used to calculate the percentage change in Li-ion energy capacity. "Future feasible regions" for known LDES technologies from Figure SI-1 are plotted to the right of the dash-dotted lines (geographically constrained) and solid lines (unconstrained) for each row. Each column represents a specific LDES energy capacity cost ($/kWh) assumption in the LDES parameter combination. Within each subplot the x-axis represents the weighted power capacity cost and the y-axis the round-trip efficiency. Total Li-ion power capacity for the reference cases normalized by peak demand (in %) and duration (in hours) are as follows: nuclear - 37.5%-10h; gas w/CCS - 27.9% -8.4h; Blue $H_2$ - 31%-8.3h.

**Figure SI-12.** Northern System: Percentage Li-ion Energy Capacity Reduction as Function of LDES Parameter Combination Compared to Reference Cases (Scenarios 4-6 Table 4)

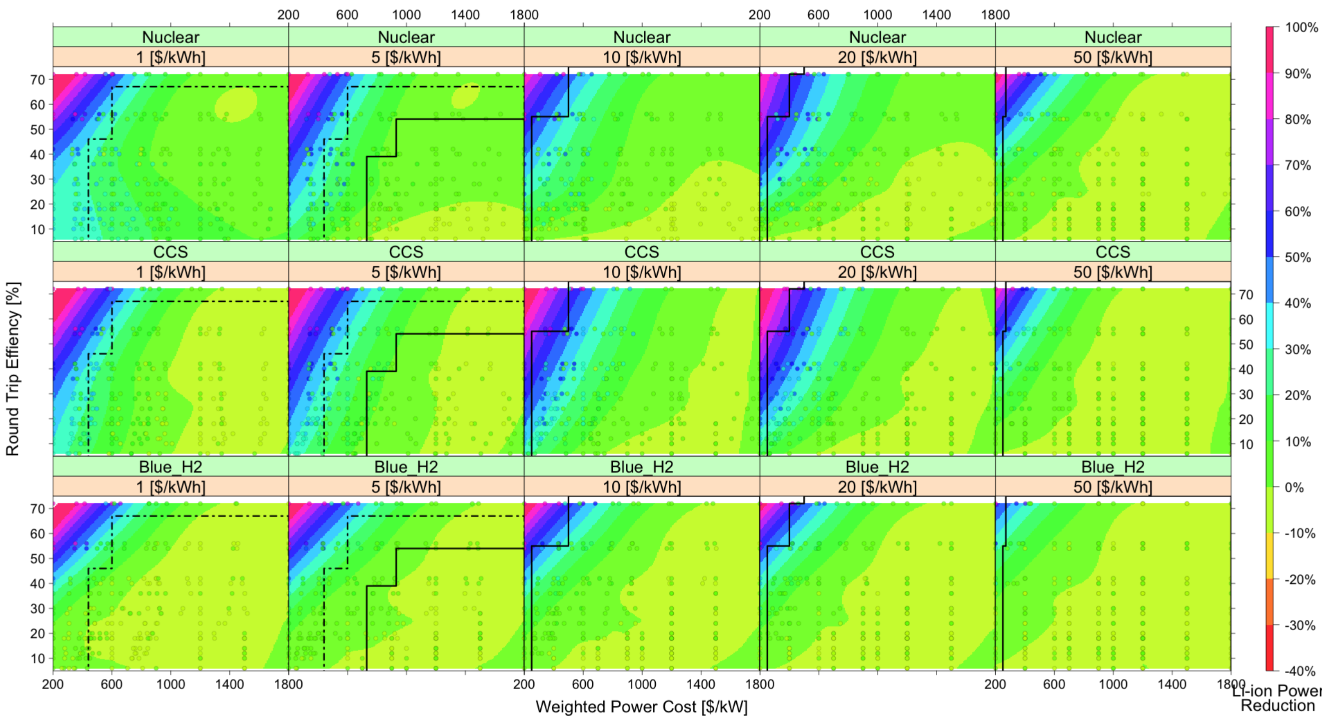


Each row of plots represents a different scenario using a different firm low-carbon technology, and consequently a different reference case was used to calculate the percentage change in Li-ion power capacity. "Future feasible regions" for known LDES technologies from Figure SI-1 are plotted to the right of the dash-dotted lines (geographically constrained) and solid lines (unconstrained) for each row. Each column represents a specific LDES energy capacity cost ($/kWh) assumption in the LDES parameter combination. Within each subplot the x-axis represents the weighted power capacity cost and the y-axis the round-trip efficiency. Total Li-ion power capacity for the reference cases normalized by peak demand (in %) and duration (in hours) are as follows: nuclear - 36.8%-10h; gas w/CCS - 33.9% -5.6h; Blue $H_2$ - 37.8%-7.4h.

**Figure SI-13.** Northern System with Electrified Load: Percentage Li-ion Power Reduction as Function of LDES Parameter Combination Compared to Reference Cases (Scenarios 7-9 Table 4)

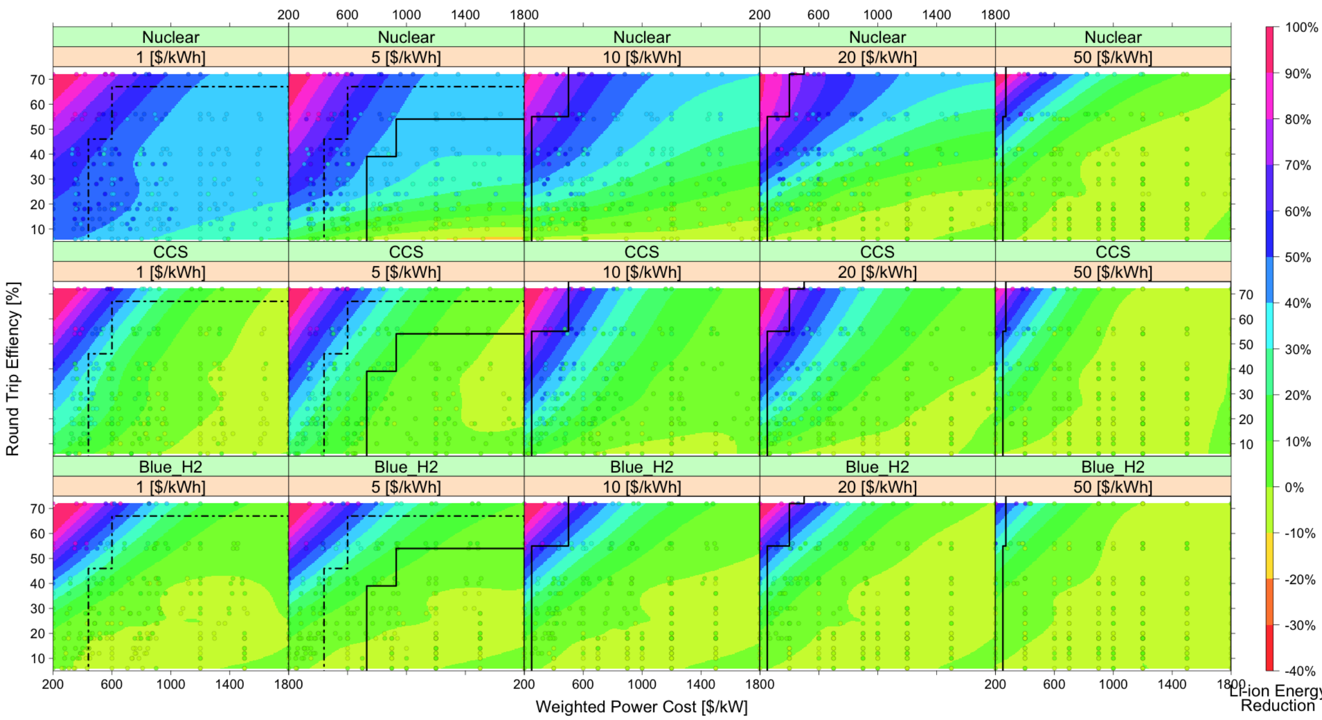


Each row of plots represents a different scenario using a different firm low-carbon technology, and consequently a different reference case was used to calculate the percentage change in Li-ion energy capacity. "Future feasible regions" for known LDES technologies from Figure SI-1 are plotted to the right of the dash-dotted lines (geographically constrained) and solid lines (unconstrained) for each row. Each column represents a specific LDES energy capacity cost ($/kWh) assumption in the LDES parameter combination. Within each subplot the x-axis represents the weighted power capacity cost and the y-axis the round-trip efficiency. Total Li-ion power capacity for the reference cases normalized by peak demand (in %) and duration (in hours) are as follows: nuclear - 36.8%-10h; gas w/CCS - 33.9% -5.6h; Blue $H_2$ - 37.8%-7.4h.

**Figure SI-14.** Northern System with Electrified Load: Percentage Li-ion Energy Reduction as Function of LDES Parameter Combination Compared to Reference Cases (Scenarios 7-9 Table 4)

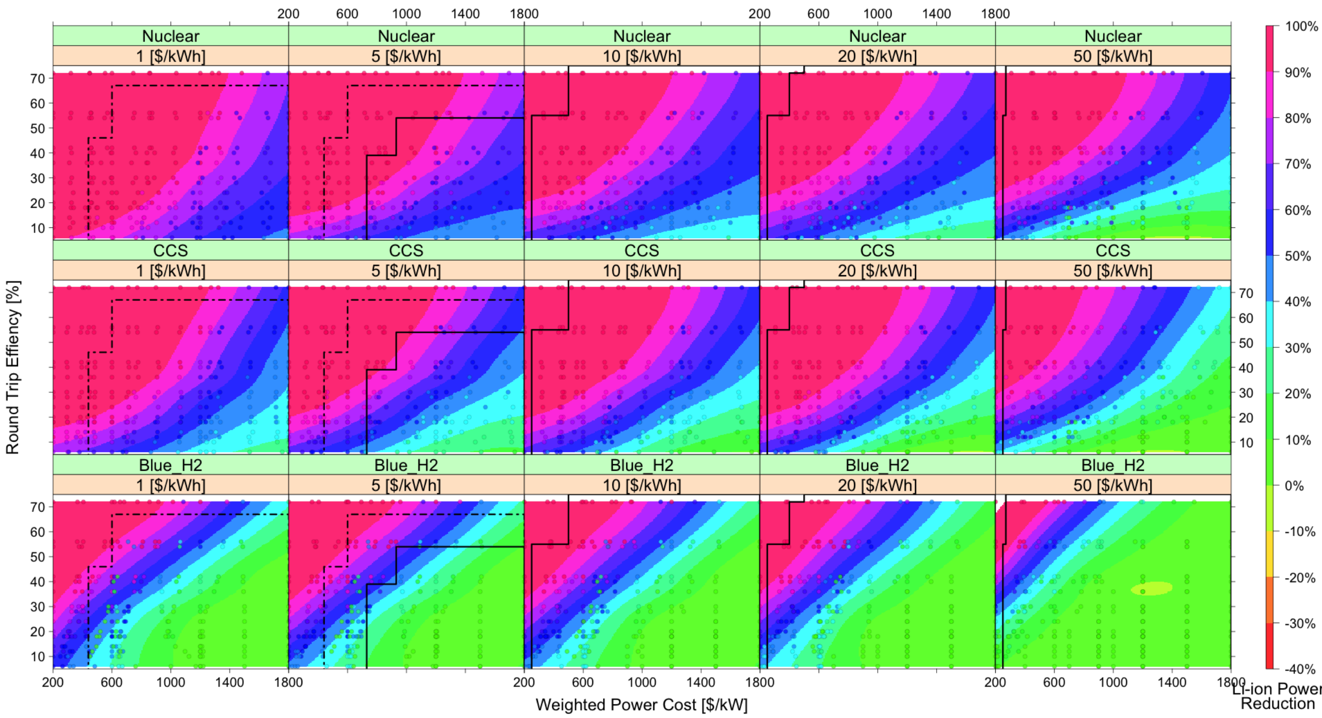


Each row of plots represents a different scenario using a different firm low-carbon technology, and consequently a different reference case was used to calculate the percentage change in Li-ion power capacity. "Future feasible regions" for known LDES technologies from Figure SI-1 are plotted to the right of the dash-dotted lines (geographically constrained) and solid lines (unconstrained) for each row. Each column represents a specific LDES energy capacity cost ($/kWh) assumption in the LDES parameter combination. Within each subplot the x-axis represents the weighted power capacity cost and the y-axis the round-trip efficiency. Total Li-ion power capacity for the reference cases normalized by peak demand (in %) and duration (in hours) are as follows: nuclear - 29.3%-4.8h; gas w/CCS - 22.4% -3.4h; Blue $H_2$ - 17.7%-2.9h.

**Figure SI-15.** Northern System with Electrified Load and Medium Cost for VRE and Li-ion: Percentage Li-ion Power Reduction as Function of LDES Parameter Combination Compared to Reference Cases (Scenarios 12-14 Table 4)

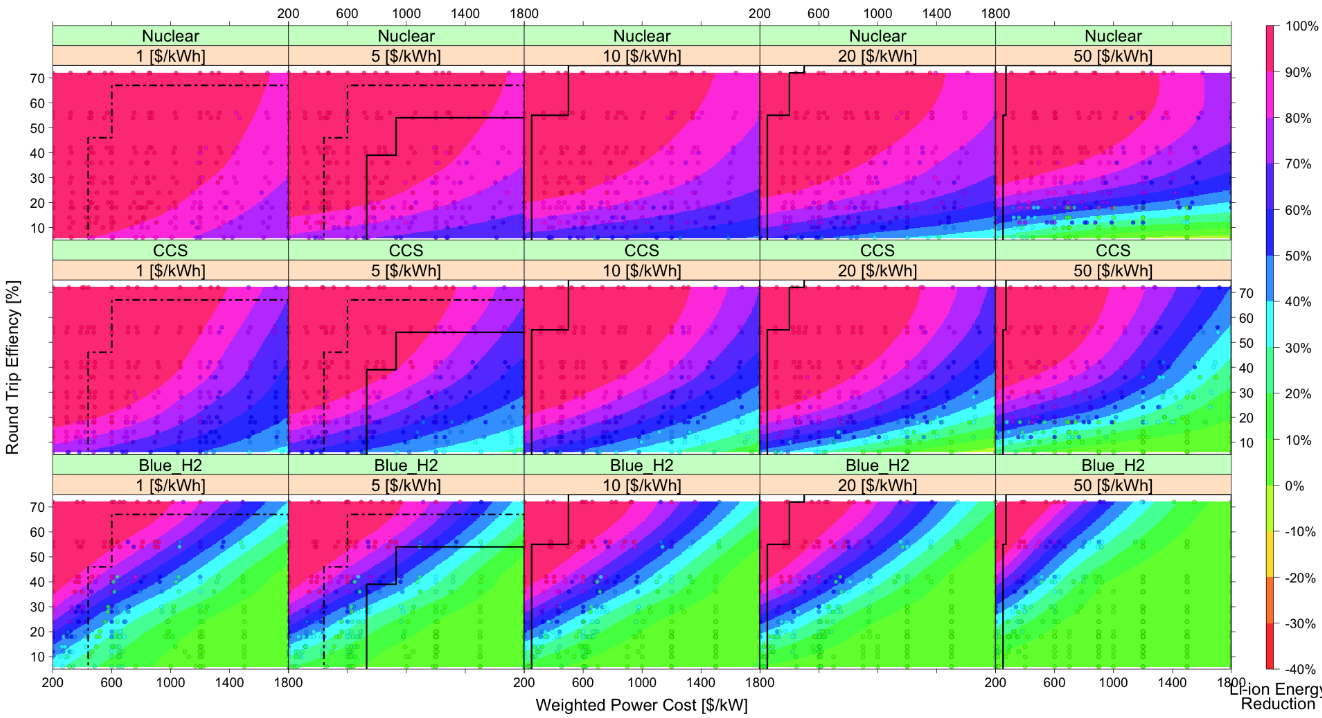


Each row of plots represents a different scenario using a different firm low-carbon technology, and consequently a different reference case was used to calculate the percentage change in Li-ion energy capacity. "Future feasible regions" for known LDES technologies from Figure SI-1 are plotted to the right of the dash-dotted lines (geographically constrained) and solid lines (unconstrained) for each row. Each column represents a specific LDES energy capacity cost ($/kWh) assumption in the LDES parameter combination. Within each subplot the x-axis represents the weighted power capacity cost and the y-axis the round-trip efficiency. Total Li-ion power capacity for the reference cases normalized by peak demand (in %) and duration (in hours) are as follows: nuclear - 29.3%-4.8h; gas w/CCS - 22.4% -3.4h; Blue $H_2$ - 17.7%-2.9h.

**Figure SI-16.** Northern System with Electrified Load and Medium Cost for VRE and Li-ion: Percentage Li-ion Energy Reduction as Function of LDES Parameter Combination Compared to Reference Cases (Scenarios 12-14 Table 4)

## LDES Energy-to-Power Ratio

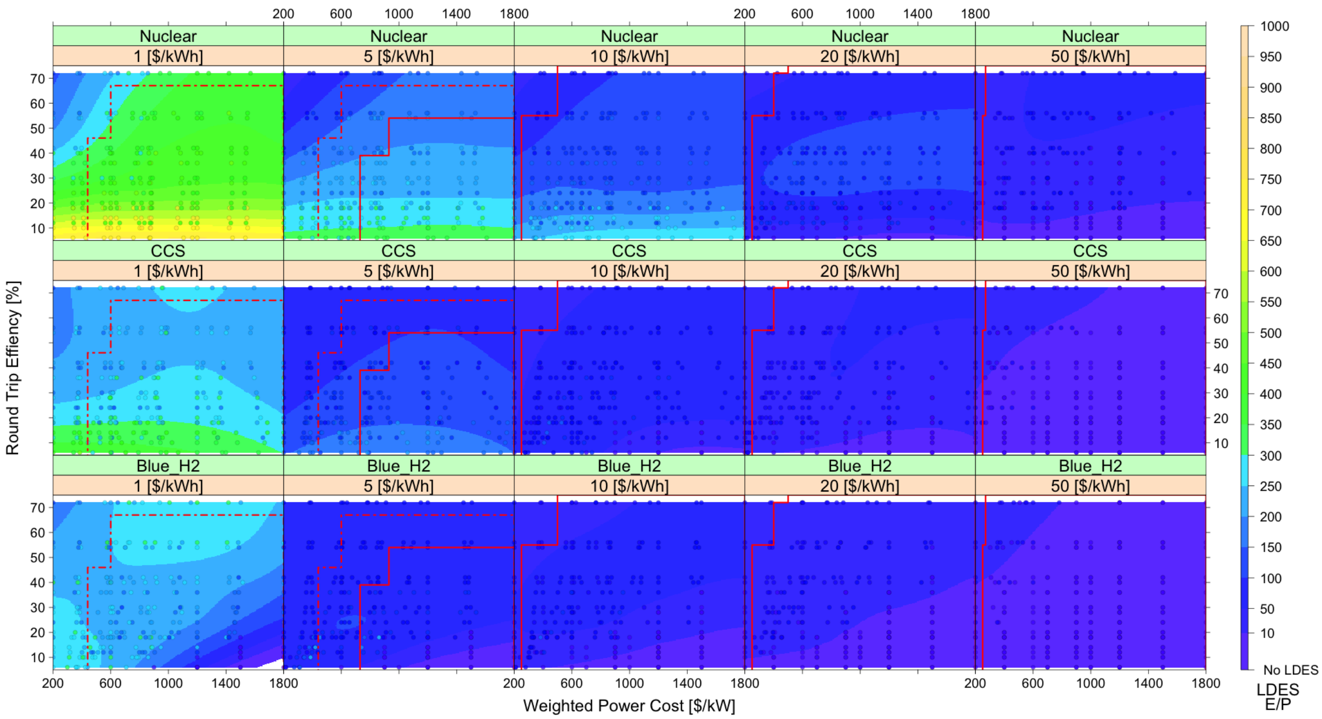


Each row of plots represents a different scenario using a different firm low-carbon technology. "Future feasible regions" for known LDES technologies from Figure SI-1 are plotted to the right of the dash-dotted lines (geographically constrained) and solid lines (unconstrained) for each row. Each column represents a specific LDES energy capacity cost ($/kWh) assumption in the LDES parameter combination. Within each subplot the x-axis represents the weighted power capacity cost and the y-axis the round-trip efficiency.

**Figure SI-17.** Northern System: LDES energy-to-power ratio (Energy Capacity/Discharge Capacity)) for optimal deployment of LDES

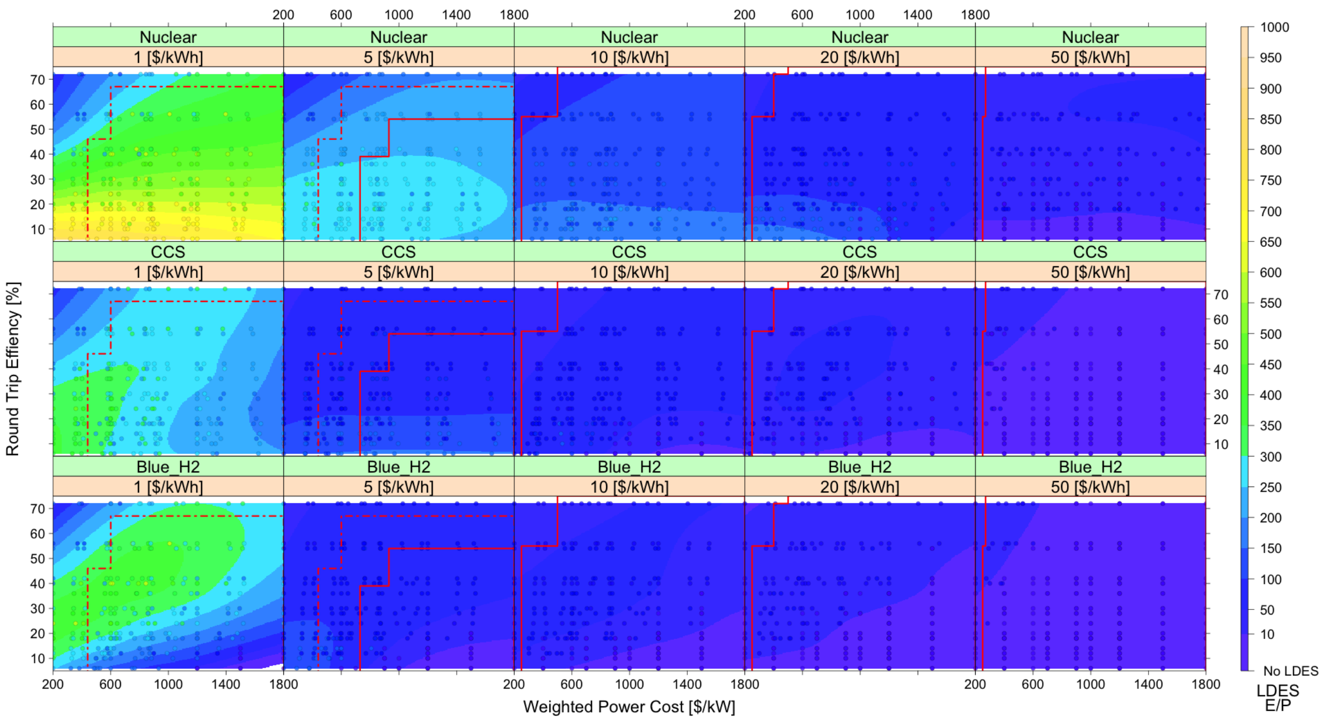


Each row of plots represents a different scenario using a different firm low-carbon technology. "Future feasible regions" for known LDES technologies from Figure SI-1 are plotted to the right of the dash-dotted lines (geographically constrained) and solid lines (unconstrained) for each row. Each column represents a specific LDES energy capacity cost ($/kWh) assumption in the LDES parameter combination. Within each subplot the x-axis represents the weighted power capacity cost and the y-axis the round-trip efficiency.

**Figure SI-18.** Southern System: LDES energy-to-power ratio (Energy Capacity/Discharge Capacity) for optimal deployment of LDES

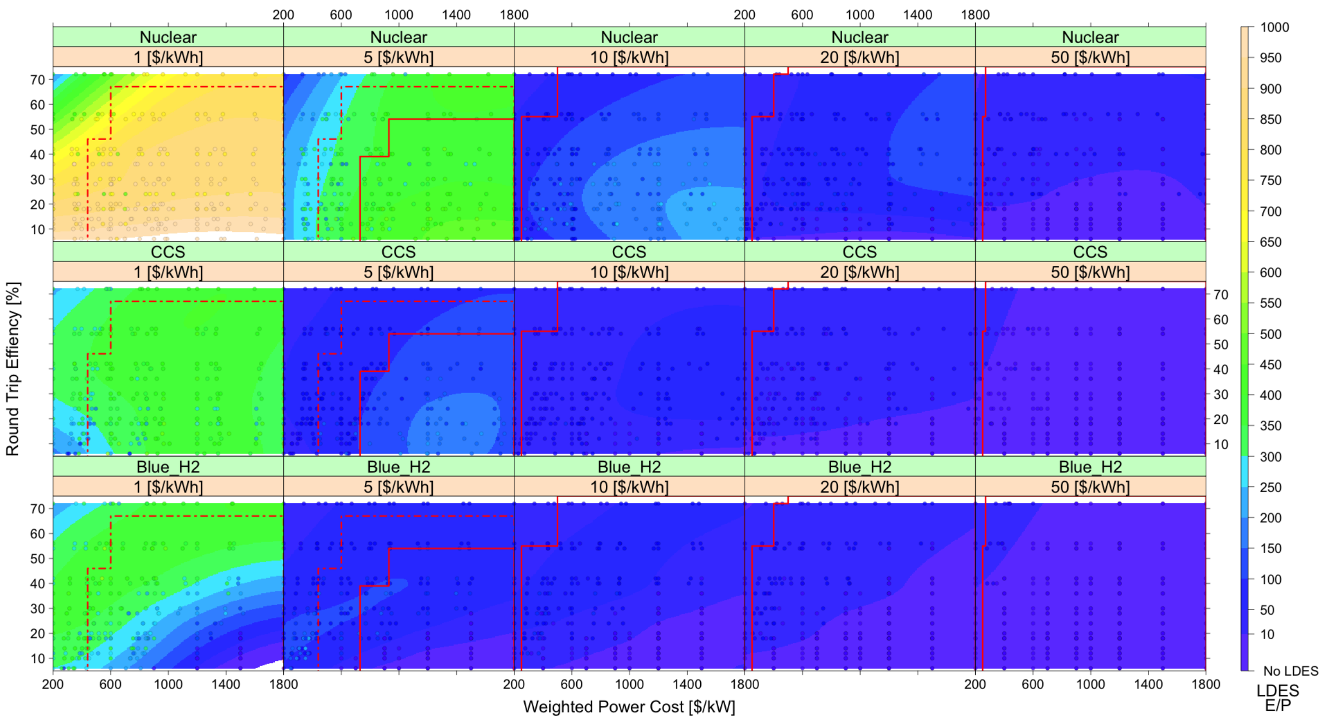


Each row of plots represents a different scenario using a different firm low-carbon technology. "Future feasible regions" for known LDES technologies from Figure SI-1 are plotted to the right of the dash-dotted lines (geographically constrained) and solid lines (unconstrained) for each row. Each column represents a specific LDES energy capacity cost ($/kWh) assumption in the LDES parameter combination. Within each subplot the x-axis represents the weighted power capacity cost and the y-axis the round-trip efficiency.

**Figure SI-19.** Northern System with Electrified Load: LDES energy-to-power ratio (Energy Capacity/Discharge Capacity) for optimal deployment of LDES

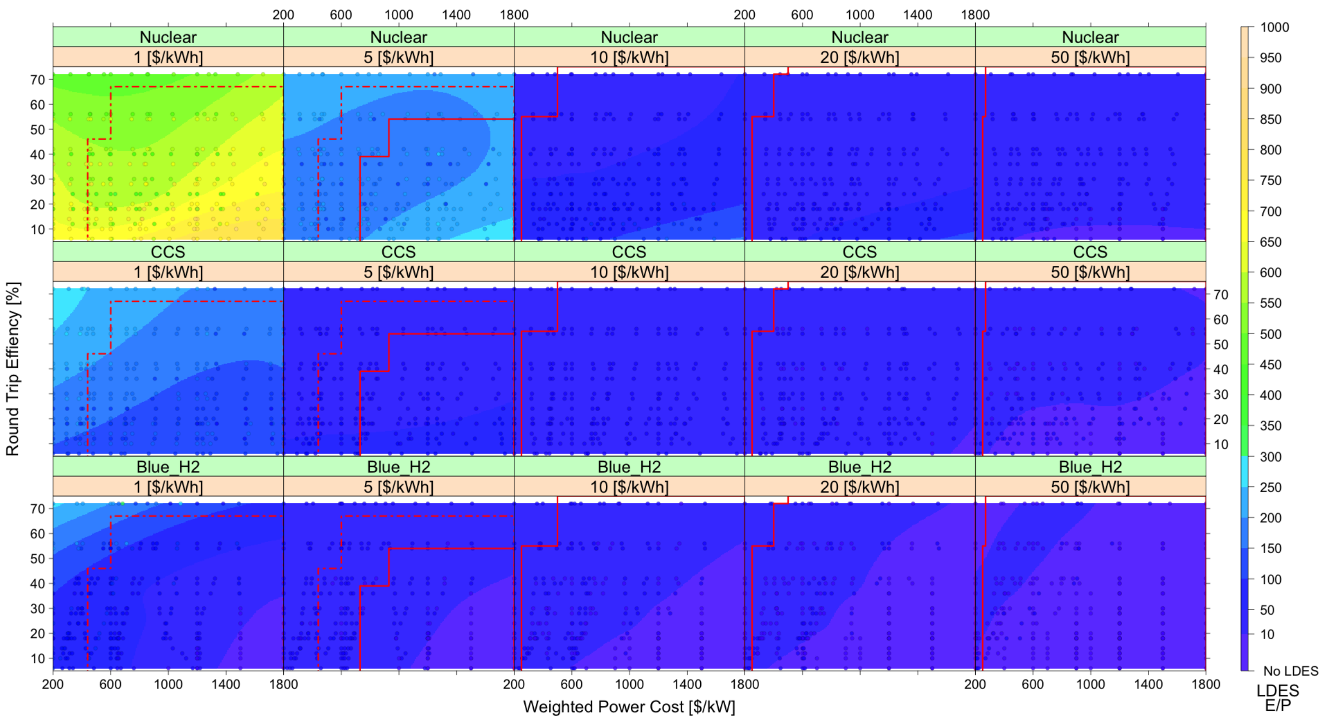


Each row of plots represents a different scenario using a different firm low-carbon technology. "Future feasible regions" for known LDES technologies from Figure SI-1 are plotted to the right of the dash-dotted lines (geographically constrained) and solid lines (unconstrained) for each row. Each column represents a specific LDES energy capacity cost ($/kWh) assumption in the LDES parameter combination. Within each subplot the x-axis represents the weighted power capacity cost and the y-axis the round-trip efficiency.

**Figure SI-20.** Northern System with Electrified Load and Medium Cost for VRE and Li-ion: LDES energy-to-power ratio (Energy Capacity/Discharge Capacity) for optimal deployment of LDES

## LDES Duration

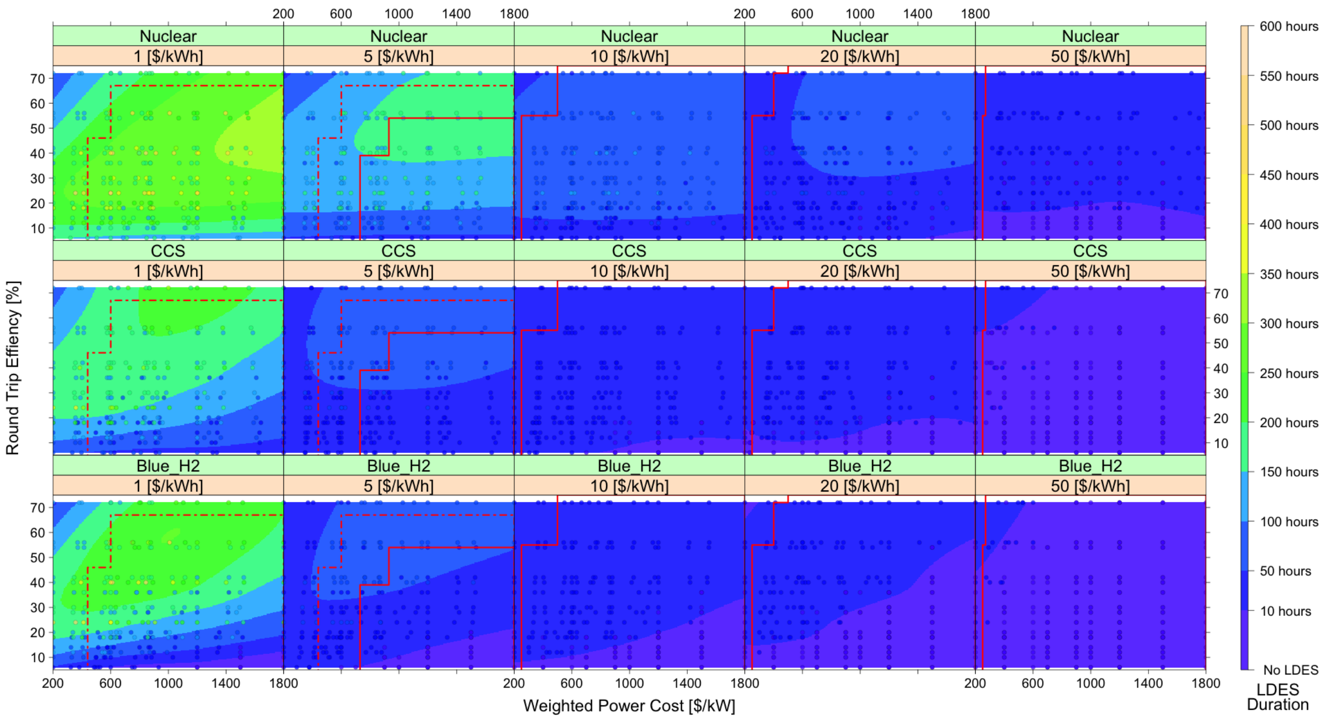


Each row of plots represents a different scenario using a different firm low-carbon technology. “Future feasible regions” for known LDES technologies from Figure SI-1 are plotted to the right of the dash-dotted lines (geographically constrained) and solid lines (unconstrained) for each row. Each column represents a specific LDES energy capacity cost ($/kWh) assumption in the LDES parameter combination. Within each subplot the x-axis represents the weighted power capacity cost and the y-axis the round-trip efficiency.

**Figure SI-21.** Southern System: LDES duration (Energy Capacity x Discharge Efficiency)/(Discharge Capacity ) in hours for optimal deployment of LDES

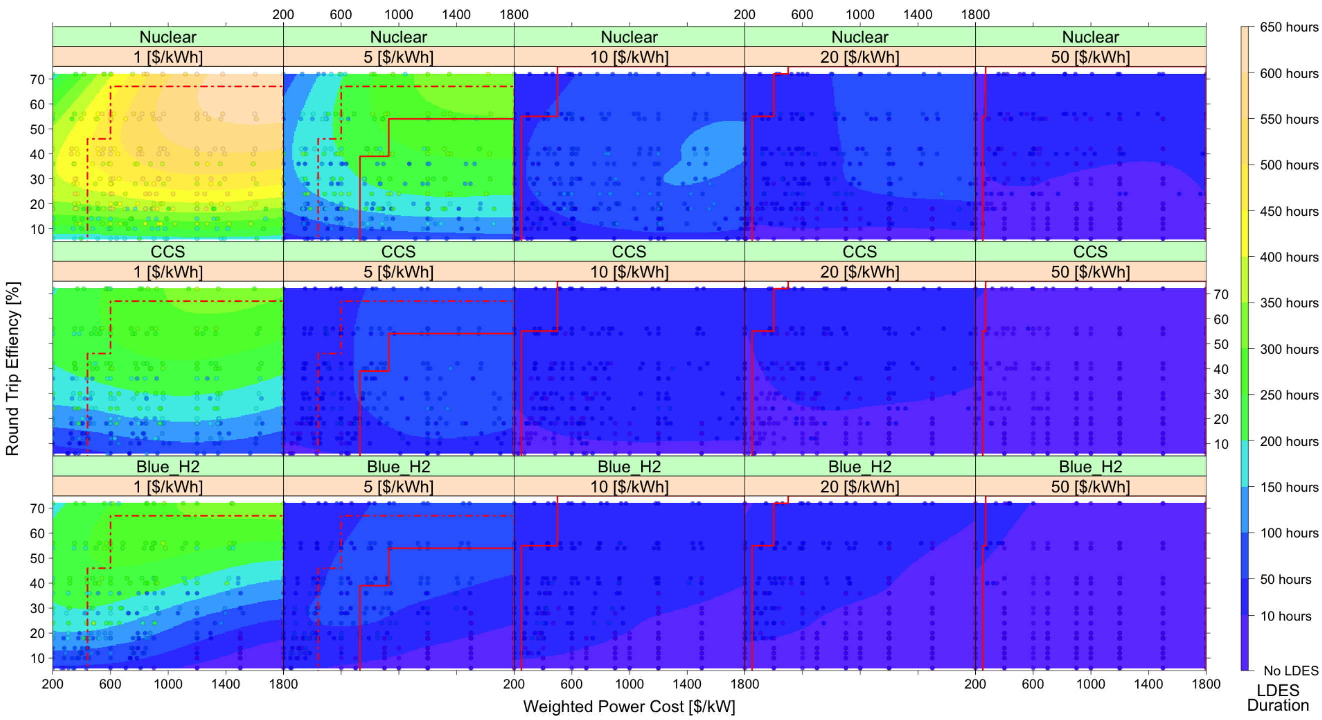


Each row of plots represents a different scenario using a different firm low-carbon technology. "Future feasible regions" for known LDES technologies from Figure SI-1 are plotted to the right of the dash-dotted lines (geographically constrained) and solid lines (unconstrained) for each row. Each column represents a specific LDES energy capacity cost ($/kWh) assumption in the LDES parameter combination. Within each subplot the x-axis represents the weighted power capacity cost and the y-axis the round-trip efficiency.

**Figure SI-22.** Northern System with Electrified Load: LDES duration (Energy Capacity x Discharge Efficiency)/(Discharge Capacity ) in hours for optimal deployment of LDES

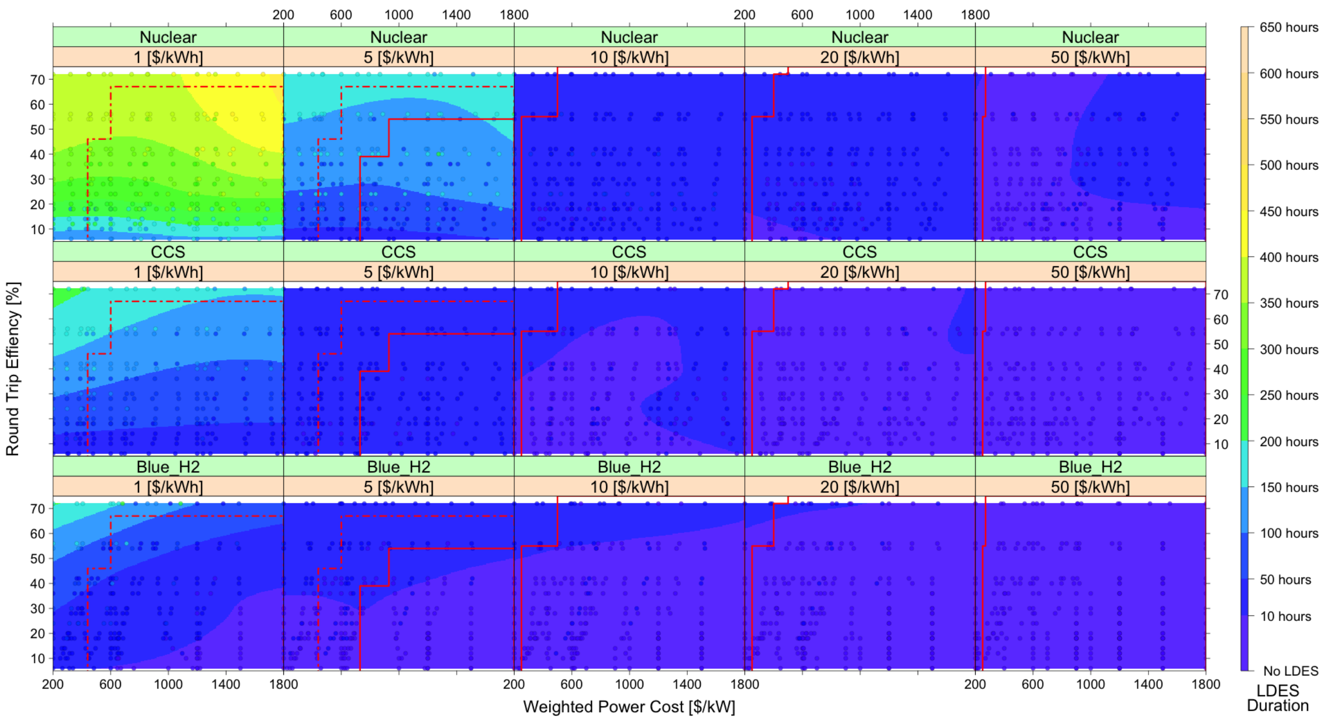


Each row of plots represents a different scenario using a different firm low-carbon technology. "Future feasible regions" for known LDES technologies from Figure SI-1 are plotted to the right of the dash-dotted lines (geographically constrained) and solid lines (unconstrained) for each row. Each column represents a specific LDES energy capacity cost ($/kWh) assumption in the LDES parameter combination. Within each subplot the x-axis represents the weighted power capacity cost and the y-axis the round-trip efficiency.

**Figure SI-23.** Northern System with Electrified Load and Medium Cost for VRE and Li-ion: LDES duration (Energy Capacity x Discharge Efficiency)/(Discharge Capacity ) in hours for optimal deployment of LDES

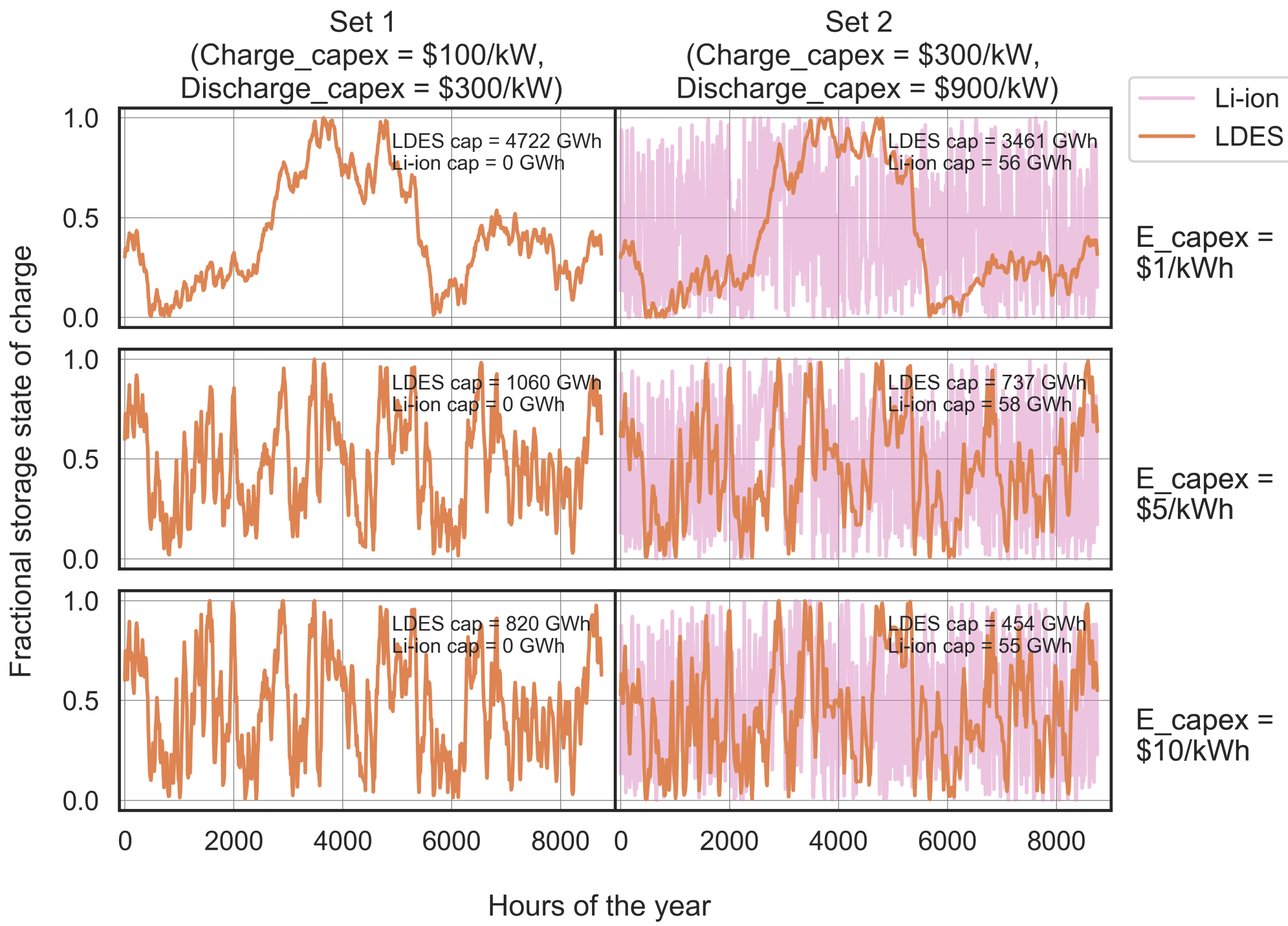


Stored energy levels are calculated by averaging stored energy over 12 hours at a time and dividing by installed energy capacity. Each row represents a different LDES energy capital cost scenario, while the two columns correspond to two sets of LDES charge and discharge power capital costs. Across all panels, charge and discharge efficiency are held constant at 90% and 60%, respectively.Within each panel the x-axis represents the chronological hours of the year and the y-axis the stored energy level.

**Figure SI-24.** Northern System with CCGT-CCS as firm technology: Variation in stored energy for LDES and Li-ion throughout the year for two sets of LDES power capital costs and 3 energy capital costs

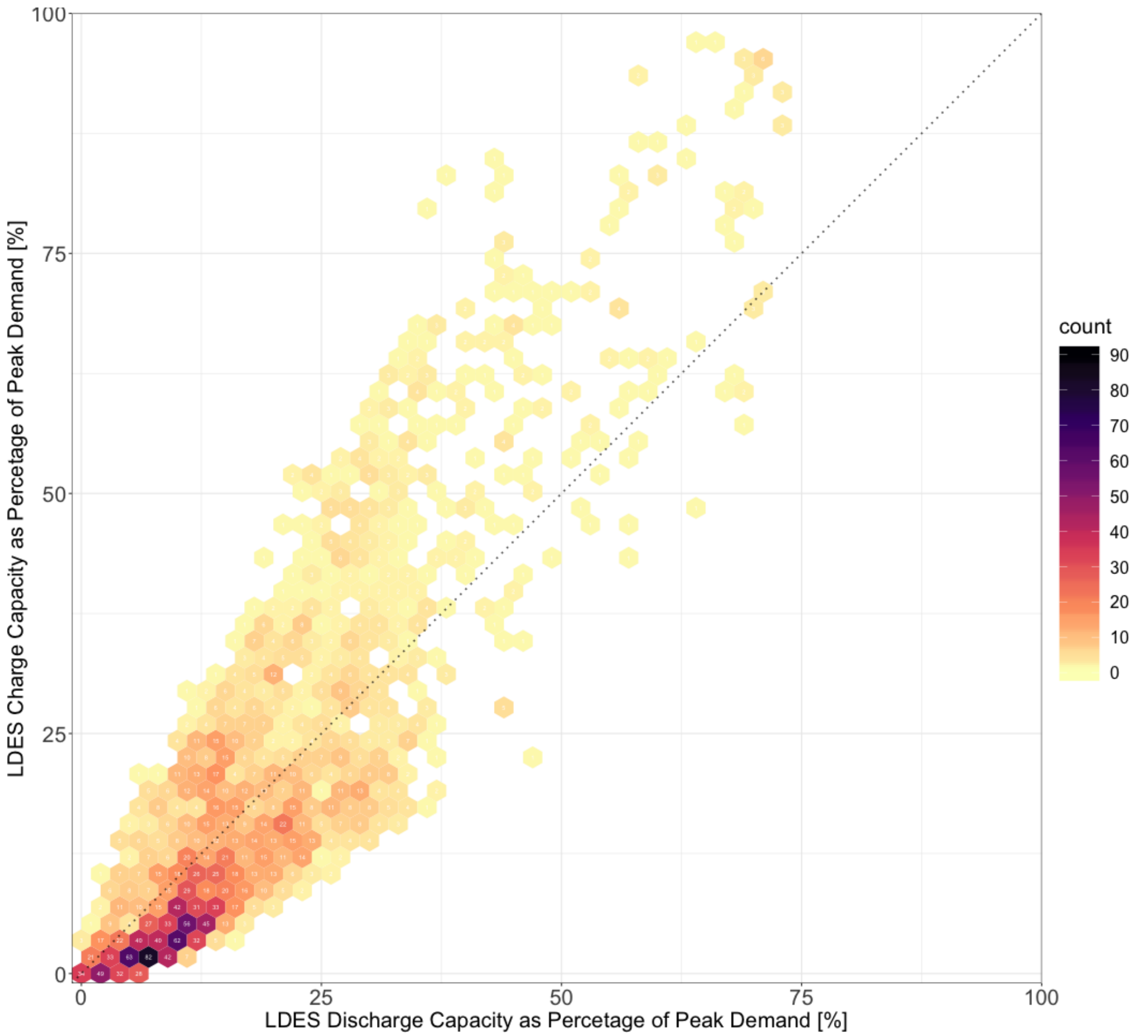


Discharge power capacity and charge power capacity are both normalized by the peak demand. The resulting values range between 0% and 100% of peak demand and the hexbins (2D bins) have a width of 2%. The dotted line indicates balanced or symmetrical charge and discharge power capacities and separates the space into two diagonal sub-spaces: the upper diagonal sub-space contains systems with more charge power capacity than discharge power capacity, and the lower diagonal space contains systems with more discharge power capacity than charge power capacity.

**Figure SI-25.** Southern System: Distribution of Discharge and Charge Power Capacities Normalized as Percent of Peak Demand

## LDES Charge/Discharge Balance

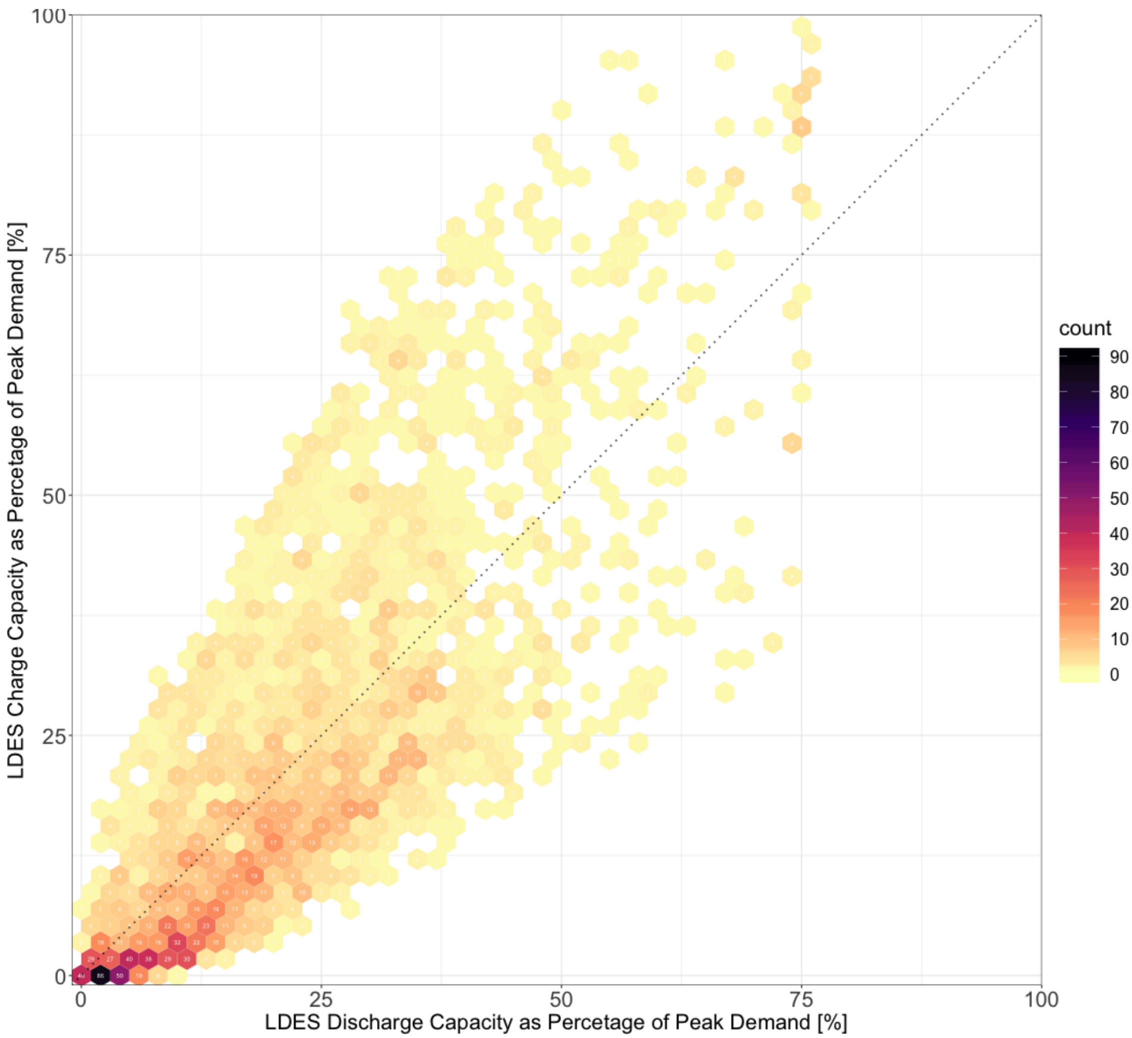


Discharge power capacity and charge power capacity are both normalized by the peak demand. The resulting values range between 0% and 100% of peak demand and the hexbins (2D bins) have a width of 2%. The dotted line indicates balanced or symmetrical charge and discharge power capacities and separates the space into two diagonal sub-spaces: the upper diagonal sub-space contains systems with more charge power capacity than discharge power capacity, and the lower diagonal space contains systems with more discharge power capacity than charge power capacity.

**Figure SI-26.** Northern System: Distribution of Discharge and Charge Power Capacities Normalized as Percent of Peak Demand

**LDES Charge/Discharge Balance**

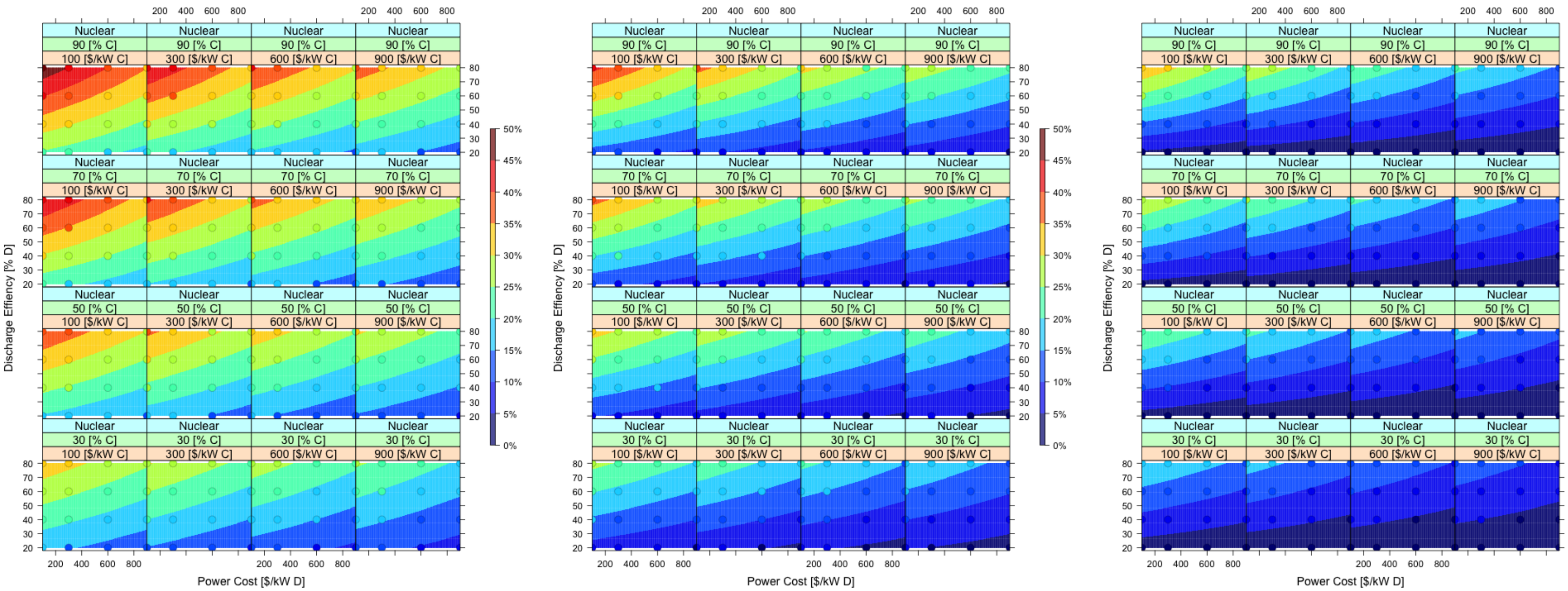


**(a)** 1 \$/kWh **(b)** 5 \$/kWh **(c)** 10 \$/kWh

All plots for the same system with the same low-carbon firm resource. Each Figure for an specific energy capacity cost level (\$/kWh). Each row of subplots represents a different level of charge efficiency (%). Each column of subplots represents a specific level for the charge power capacity cost cost (\$/kW) assumption in the LDES parameter combination. Within each subplot the x-axis represents the discharge power capacity cost (\$/kW) and the y-axis the discharge efficiency (%).

**Figure SI-27.** Northern System: Percentage cost reduction as function of LDES parameter combination in the original 5-dimensional space compared to reference cases (scenarios 4-6 Table 4) using nuclear as low-carbon firm resource

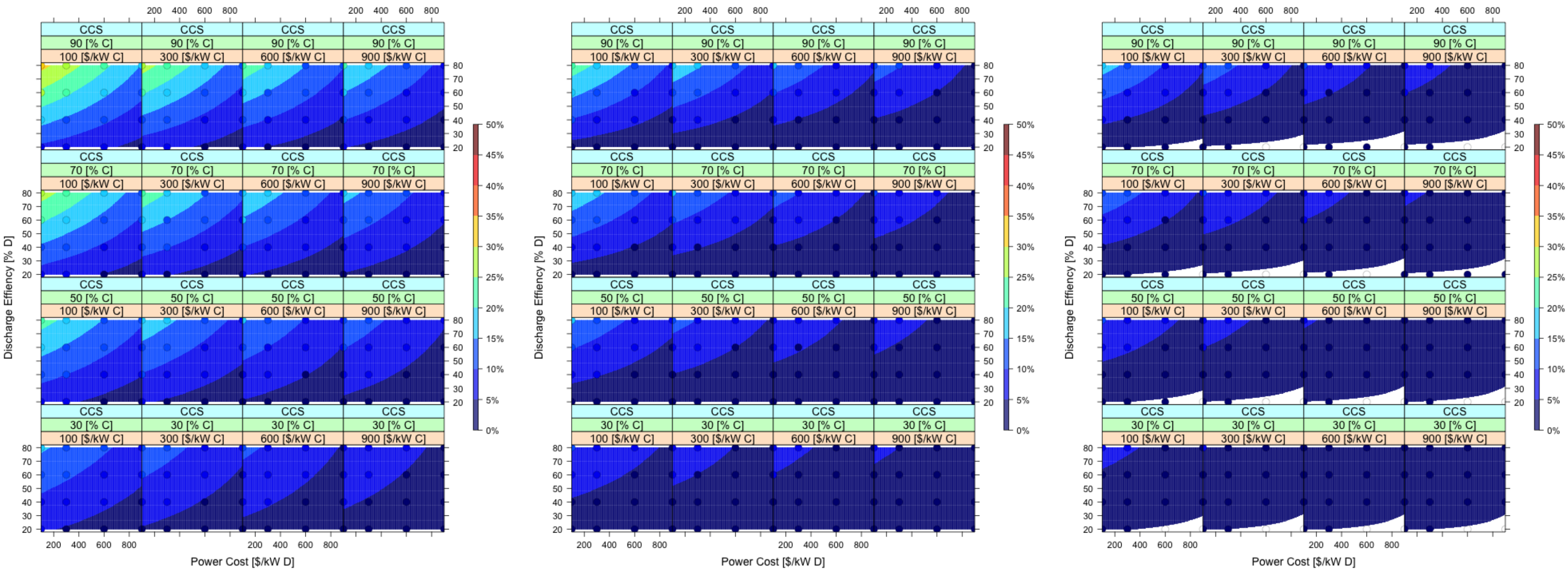


**(a)** 1 \$/kWh **(b)** 5 \$/kWh **(c)** 10 \$/kWh

All plots for the same system with the same low-carbon firm resource. Each Figure for an specific energy capacity cost level (\$/kWh). Each row of subplots represents a different level of charge efficiency (%). Each column of subplots represents a specific level for the charge power capacity cost (\$/kW) assumption in the LDES parameter combination. Within each subplot the x-axis represents the discharge power capacity cost (\$/kW) and the y-axis the discharge efficiency (%).

**Figure SI-28.** Northern System: Percentage cost reduction as function of LDES parameter combination in the original 5-dimensional space compared to reference cases (scenarios 4-6 Table 4) using gas w/CCS as low-carbon firm resource

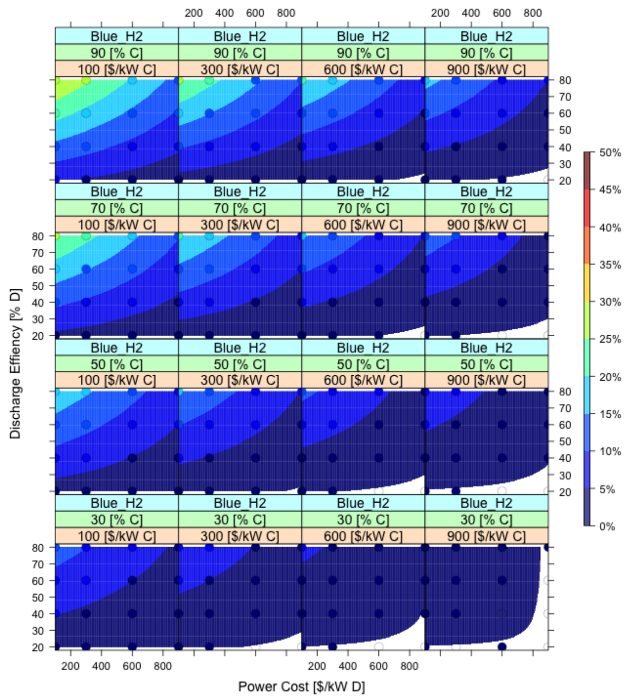


**(a)** 1 $/kWh

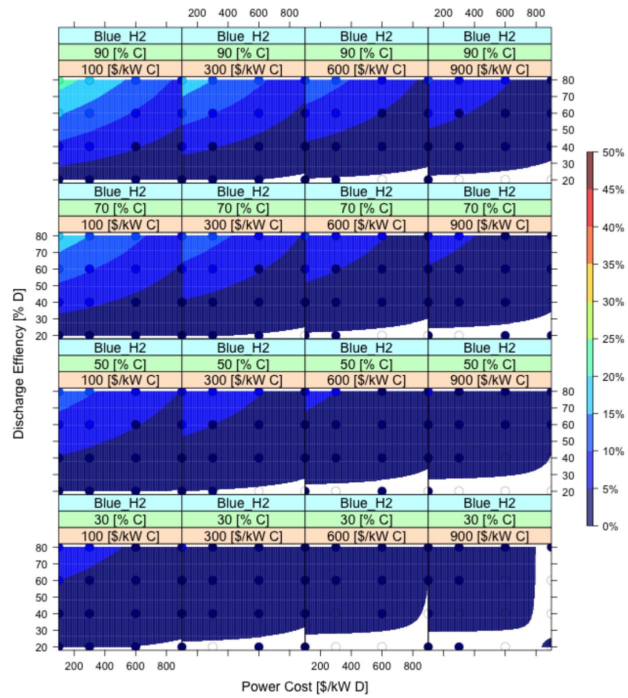

**(b)** 5 $/kWh

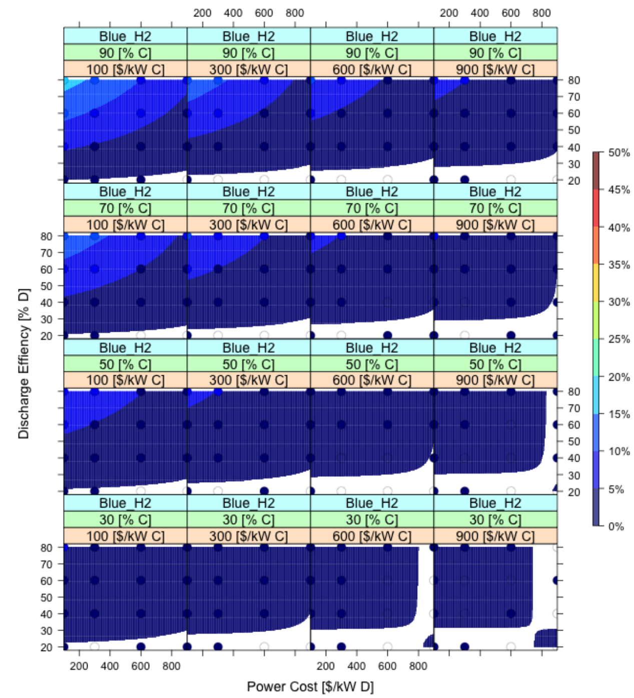

**(c)** 10 $/kWh

All plots for the same system with the same low-carbon firm resource. Each Figure for an specific energy capacity cost level ($/kWh). Each row of subplots represents a different level of charge efficiency (%). Each column of subplots represents a specific level for the charge power capacity cost ($/kW) assumption in the LDES parameter combination. Within each subplot the x-axis represents the discharge power capacity cost ($/kW) and the y-axis the discharge efficiency (%).

**Figure SI-29.** Northern System: Percentage cost reduction as function of LDES parameter combination in the original 5-dimensional space compared to reference cases (scenarios 4-6 Table 4) using blue $H_2$ as low-carbon firm resource

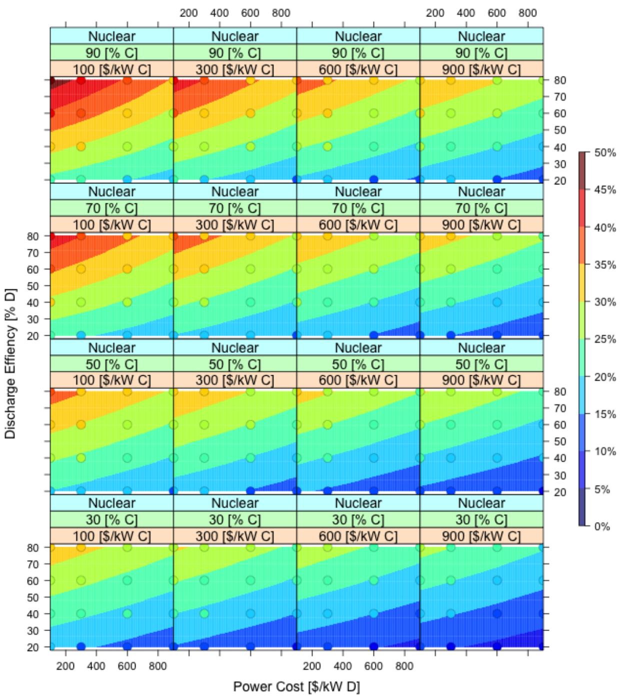


**(a)** 1 $/kWh

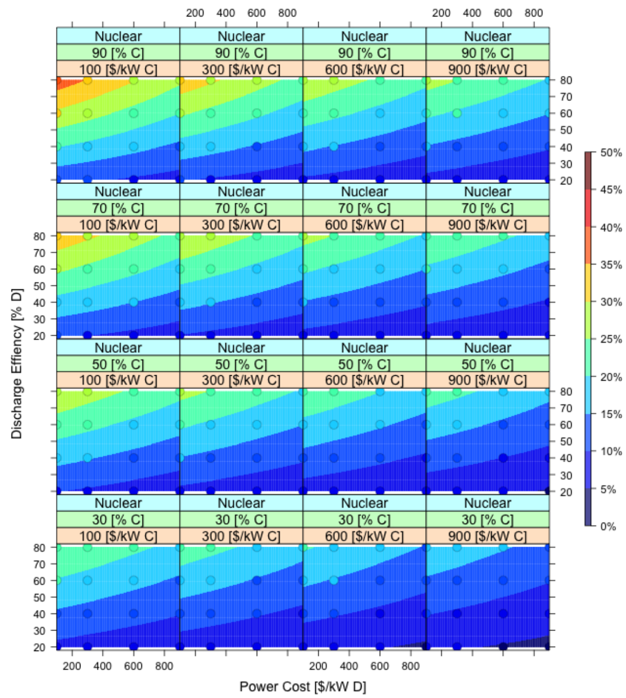


**(b)** 5 $/kWh

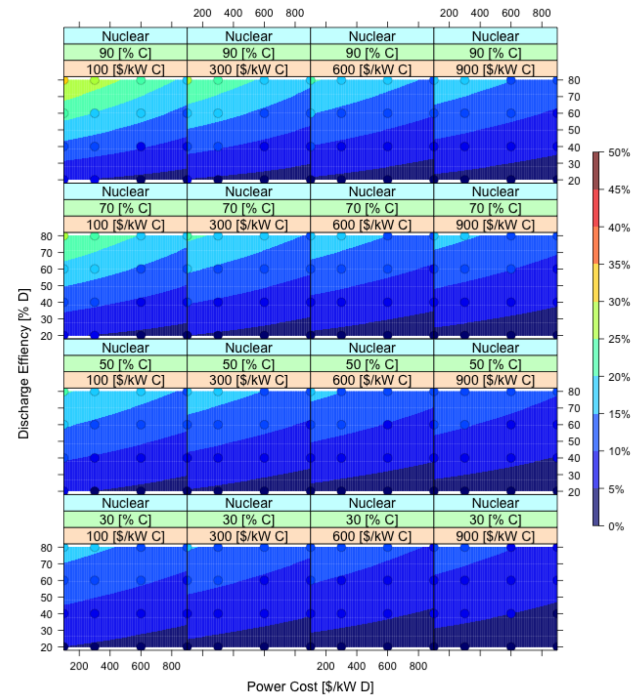


**(c)** 10 $/kWh

All plots for the same system with the same low-carbon firm resource. Each Figure for an specific energy capacity cost level ($/kWh). Each row of subplots represents a different level of charge efficiency (%). Each column of subplots represents a specific level for the charge power capacity cost ($/kW) assumption in the LDES parameter combination. Within each subplot the x-axis represents the discharge power capacity cost ($/kW) and the y-axis the discharge efficiency (%).

**Figure SI-30.** Southern System: Percentage cost reduction as function of LDES parameter combination in the original 5-dimensional space compared to reference cases (scenarios 1-3 Table 4) using nuclear as low-carbon firm resource

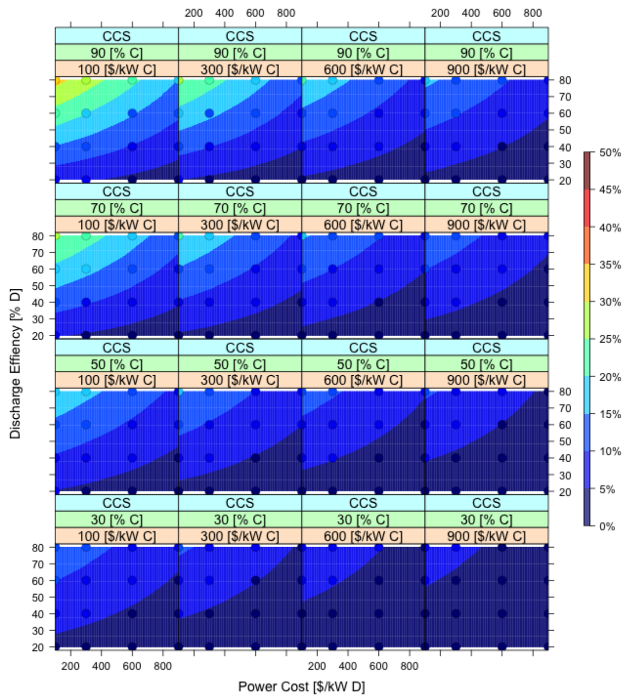


**(a)** 1 $/kWh

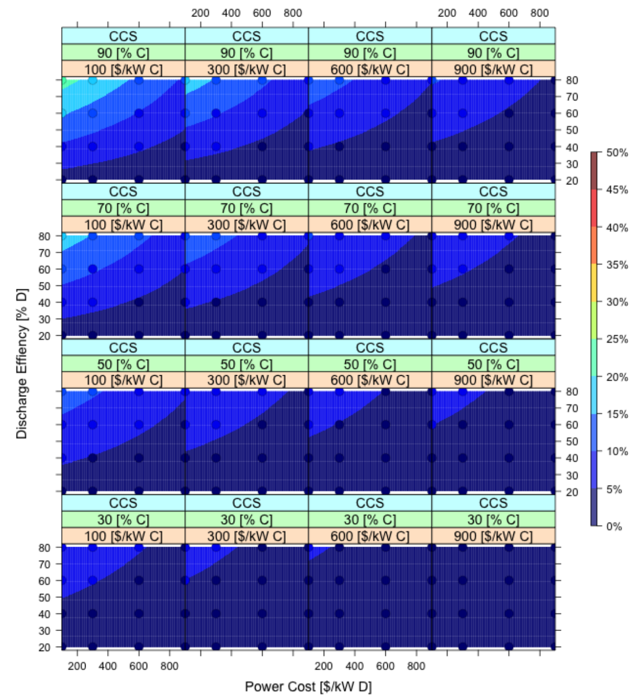


**(b)** 5 $/kWh

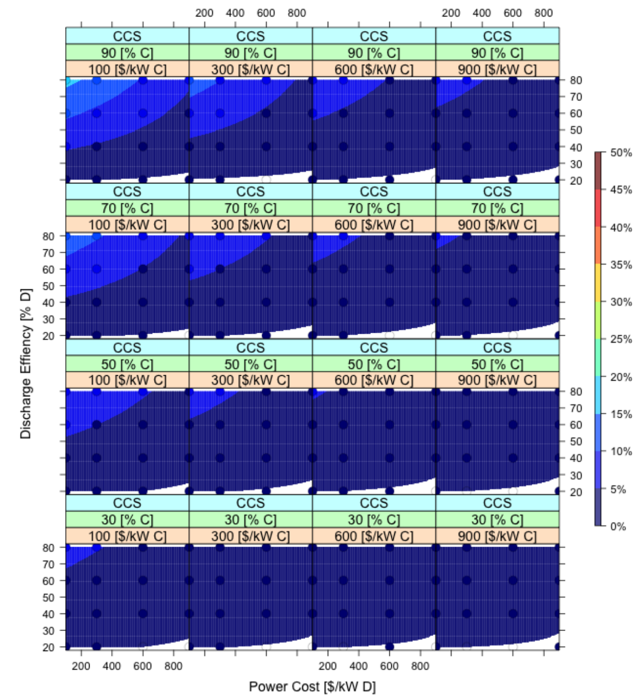


**(c)** 10 $/kWh

All plots for the same system with the same low-carbon firm resource. Each Figure for an specific energy capacity cost level ($/kWh). Each row of subplots represents a different level of charge efficiency (%). Each column of subplots represents a specific level for the charge power capacity cost ($/kW) assumption in the LDES parameter combination. Within each subplot the x-axis represents the discharge power capacity cost ($/kW) and the y-axis the discharge efficiency (%).

**Figure SI-31.** Southern System: Percentage cost reduction as function of LDES parameter combination in the original 5-dimensional space compared to reference cases (scenarios 1-3 Table 4) using gas w/CCS as low-carbon firm resource

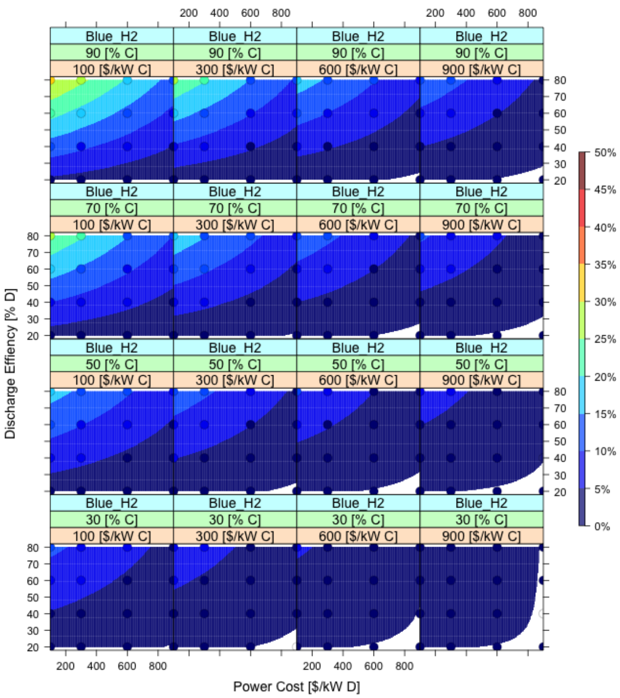


**(a)** 1 $/kWh

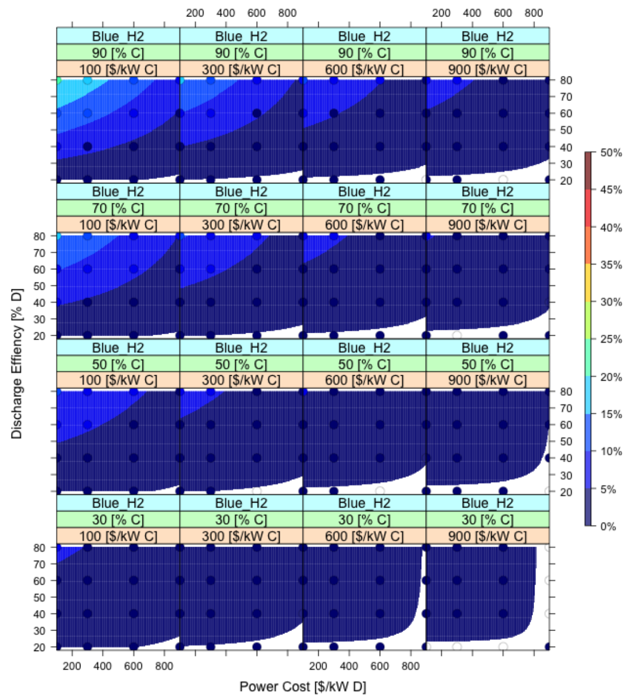


**(b)** 5 $/kWh

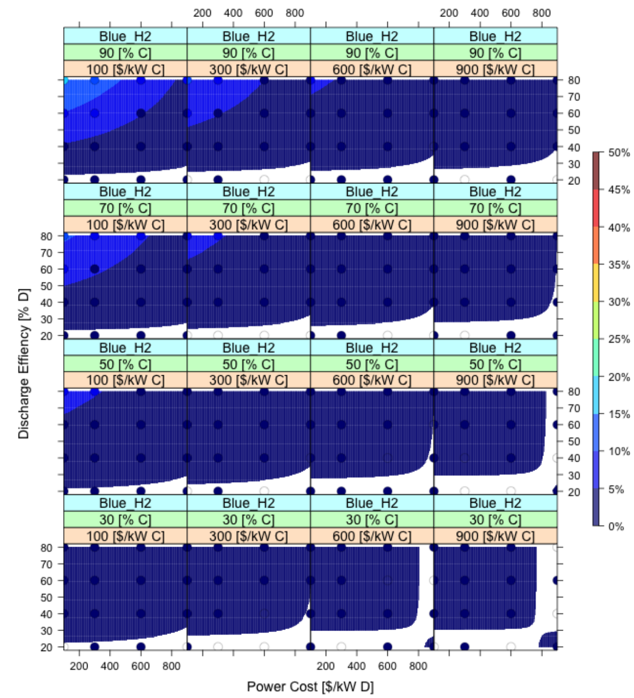


**(c)** 10 $/kWh

All plots for the same system with the same low-carbon firm resource. Each Figure for an specific energy capacity cost level ($/kWh). Each row of subplots represents a different level of charge efficiency (%). Each column of subplots represents a specific level for the charge power capacity cost ($/kW) assumption in the LDES parameter combination. Within each subplot the x-axis represents the discharge power capacity cost ($/kW) and the y-axis the discharge efficiency (%).

**Figure SI-32.** Southern System: Percentage cost reduction as function of LDES parameter combination in the original 5-dimensional space compared to reference cases (scenarios 1-3 Table 4) using blue $H_2$ as low-carbon firm resource

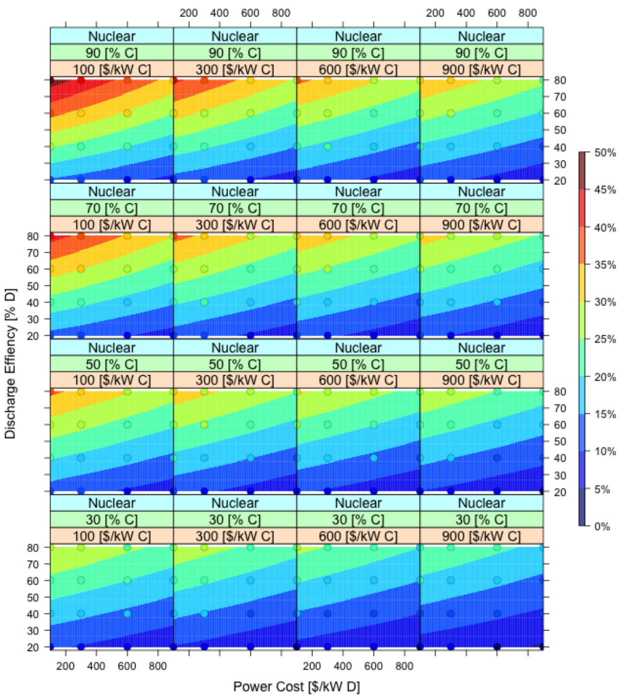


**(a)** 1 $/kWh

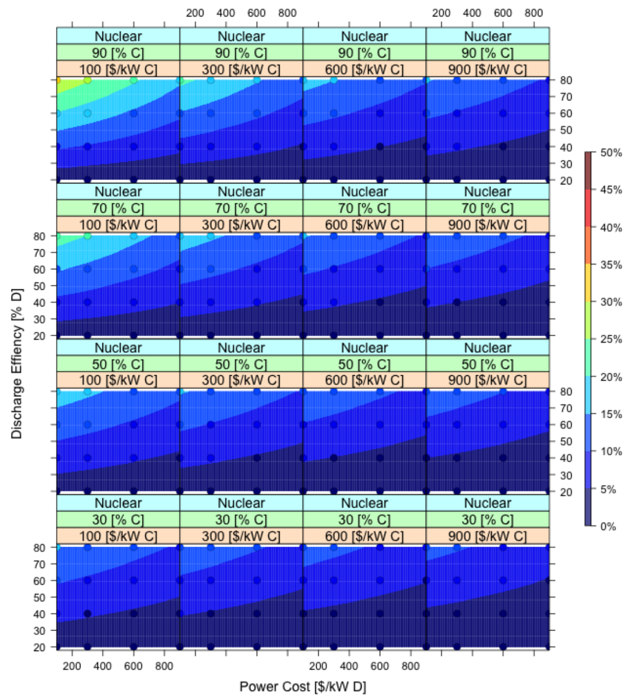


**(b)** 5 $/kWh

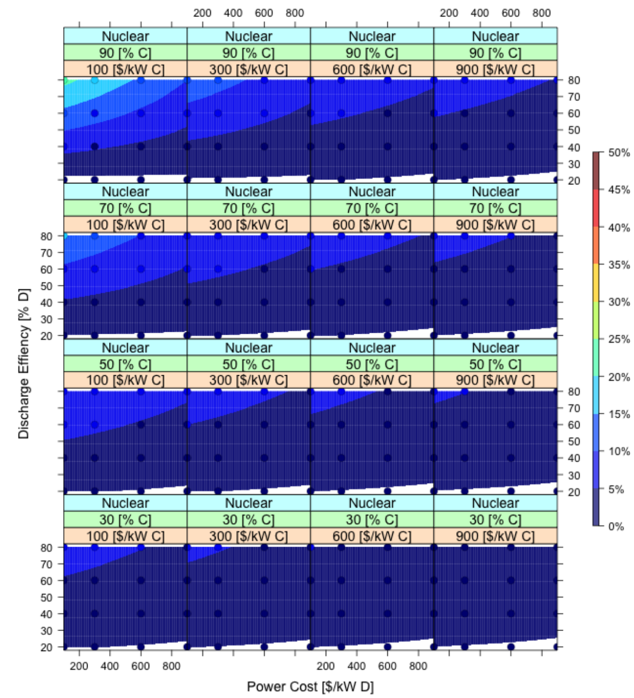


**(c)** 10 $/kWh

All plots for the same system with the same low-carbon firm resource. Each Figure for an specific energy capacity cost level ($/kWh). Each row of subplots represents a different level of charge efficiency (%). Each column of subplots represents a specific level for the charge power capacity cost ($/kW) assumption in the LDES parameter combination. Within each subplot the x-axis represents the discharge power capacity cost ($/kW) and the y-axis the discharge efficiency (%).

**Figure SI-33.** Northern System with Electrified Load: Percentage cost reduction as function of LDES parameter combination in the original 5-dimensional space compared to reference cases (scenarios 7-9 Table 4) using nuclear as low-carbon firm resource

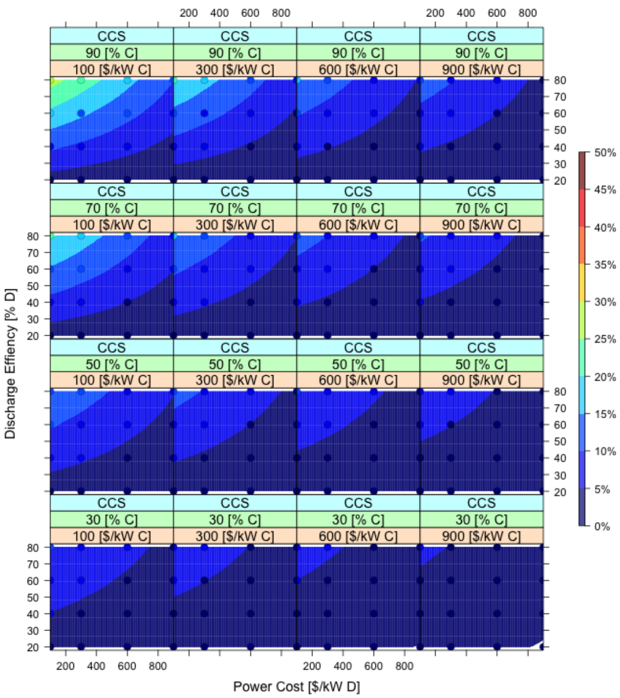


**(a)** 1 $/kWh

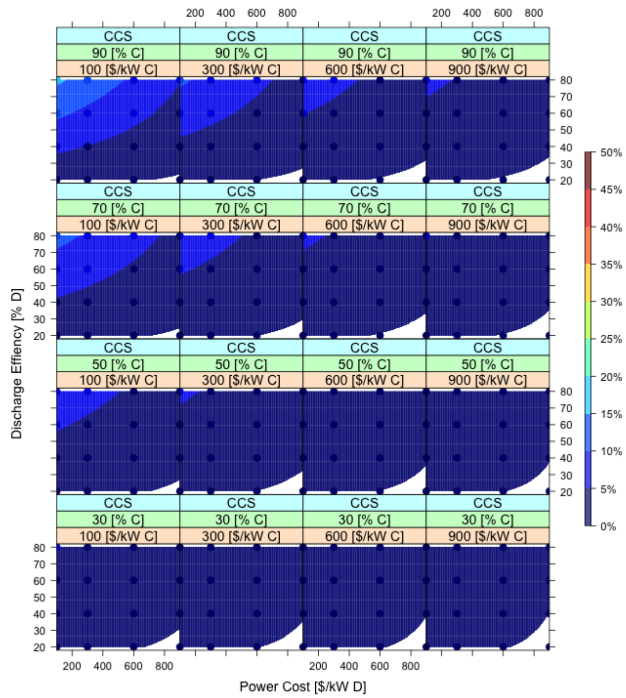


**(b)** 5 $/kWh

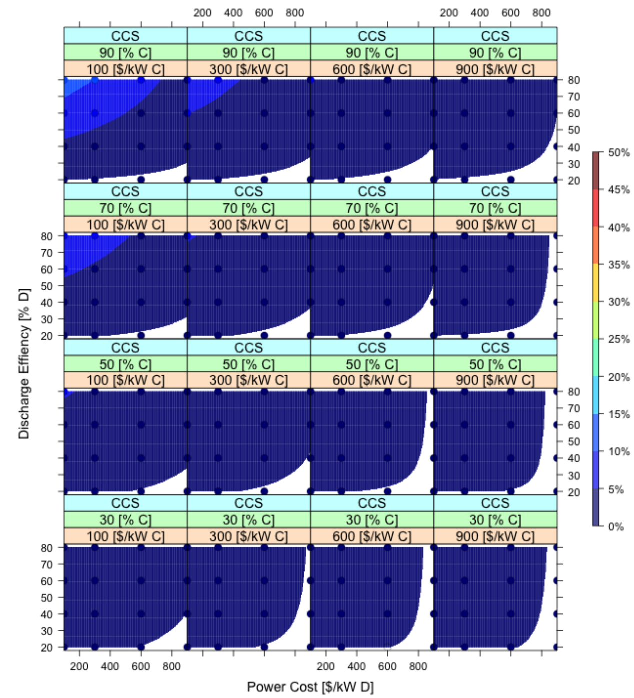


**(c)** 10 $/kWh

All plots for the same system with the same low-carbon firm resource. Each Figure for an specific energy capacity cost level ($/kWh). Each row of subplots represents a different level of charge efficiency (%). Each column of subplots represents a specific level for the charge power capacity cost ($/kW) assumption in the LDES parameter combination. Within each subplot the x-axis represents the discharge power capacity cost ($/kW) and the y-axis the discharge efficiency (%).

**Figure SI-34.** Northern System with Electrified Load: Percentage cost reduction as function of LDES parameter combination in the original 5-dimensional space compared to reference cases (scenarios 7-9 Table 4) using gas w/CCS as low-carbon firm resource

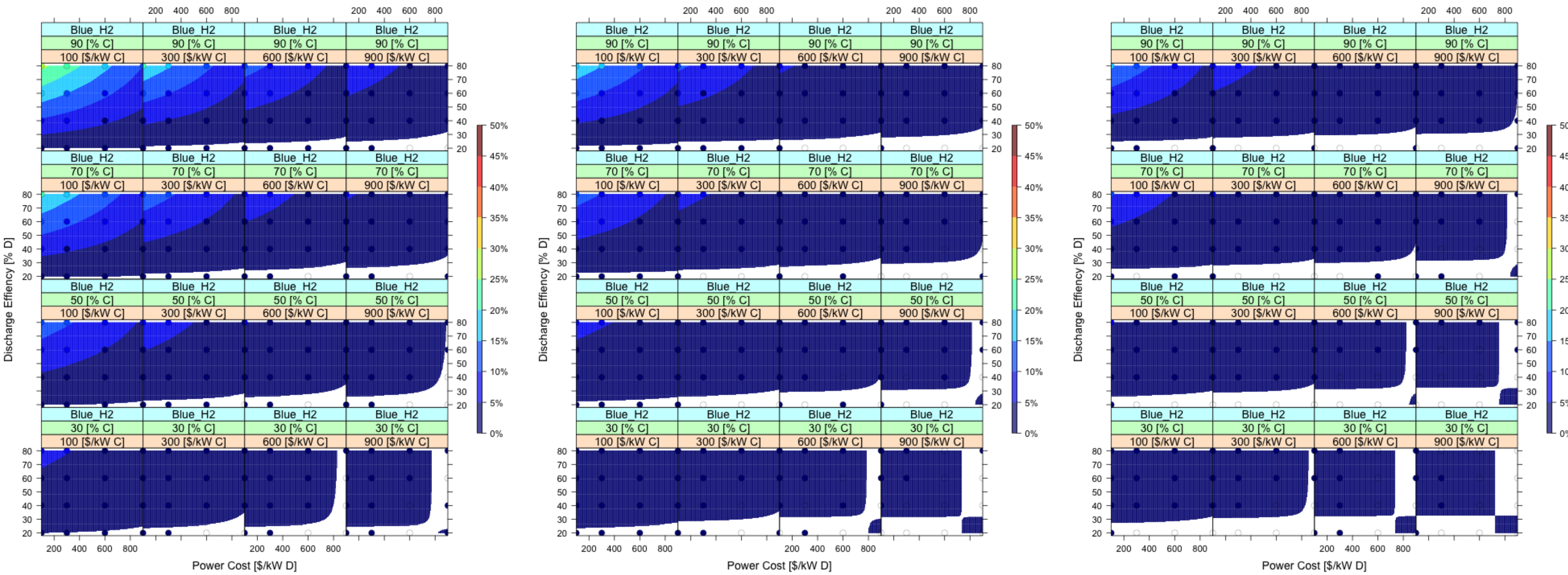


**(a)** 1 \$/kWh **(b)** 5 \$/kWh **(c)** 10 \$/kWh

All plots for the same system with the same low-carbon firm resource. Each Figure for an specific energy capacity cost level (\$/kWh). Each row of subplots represents a different level of charge efficiency (%). Each column of subplots represents a specific level for the charge power capacity cost (\$/kW) assumption in the LDES parameter combination. Within each subplot the x-axis represents the discharge power capacity cost (\$/kW) and the y-axis the discharge efficiency (%).

**Figure SI-35.** Northern System with Electrified Load: Percentage cost reduction as function of LDES parameter combination in the original 5-dimensional space compared to reference cases (scenarios 7-9 Table 4) using blue $H_2$ as low-carbon firm resource

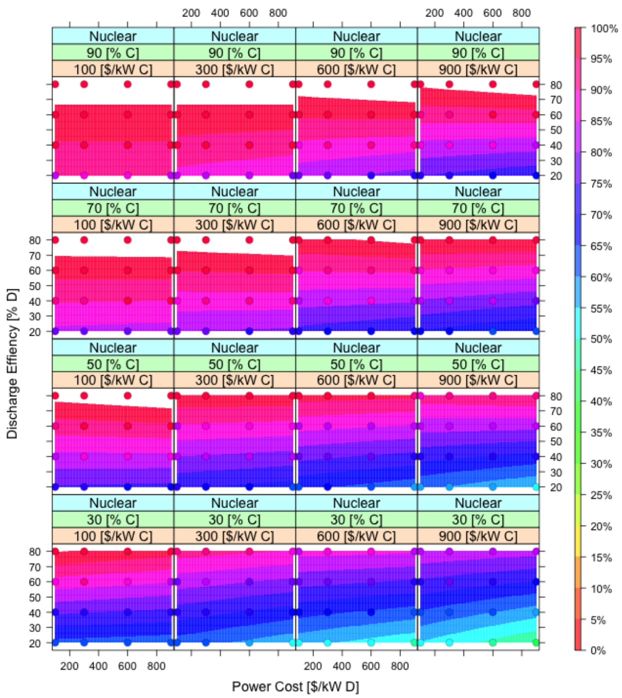


(a) 1 \$/kWh

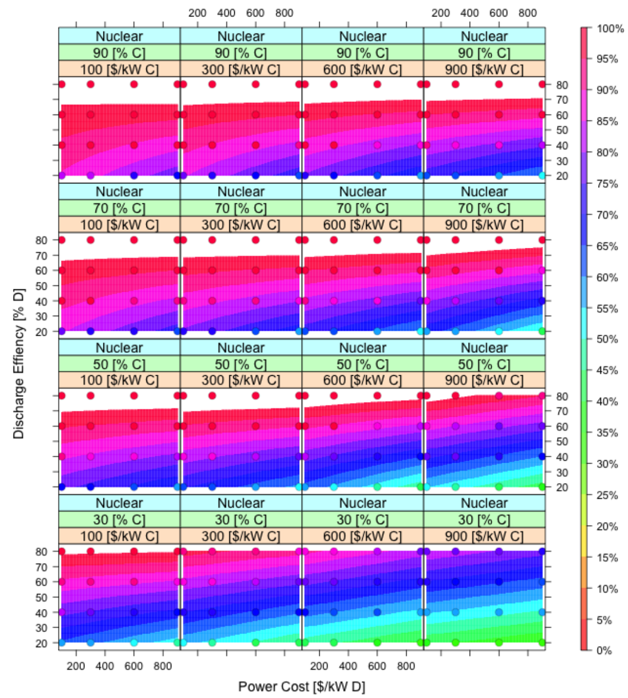


(b) 5 \$/kWh

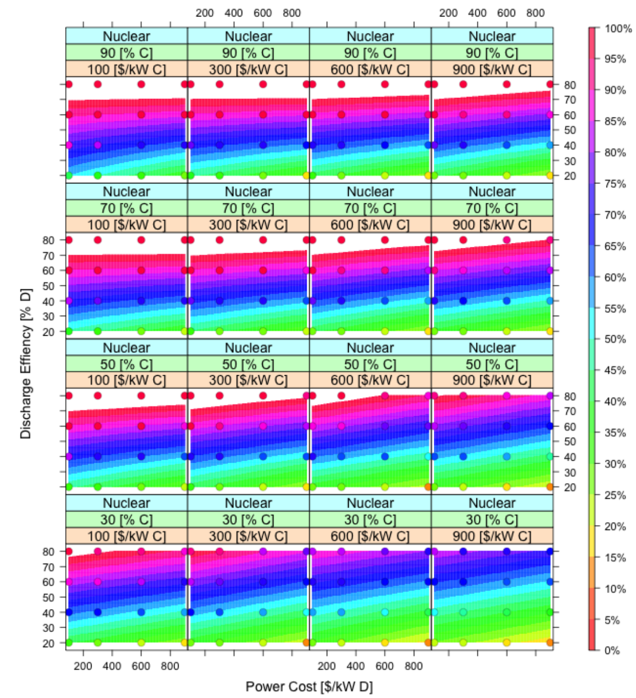


(c) 10 \$/kWh

All plots for the same system with the same low-carbon firm resource. Each Figure for an specific energy capacity cost level (\$/kWh). Each row of subplots represents a different level of charge efficiency (%). Each column of subplots represents a specific level for the charge power capacity cost cost (\$/kW) assumption in the LDES parameter combination. Within each subplot the x-axis represents the discharge power capacity cost (\$/kW) and the y-axis the discharge efficiency (%).

**Figure SI-36.** Northern System: Percentage firm reduction as function of LDES parameter combination in the original 5-dimensional space compared to reference cases (scenarios 4-6 Table 4) using nuclear as low-carbon firm resource

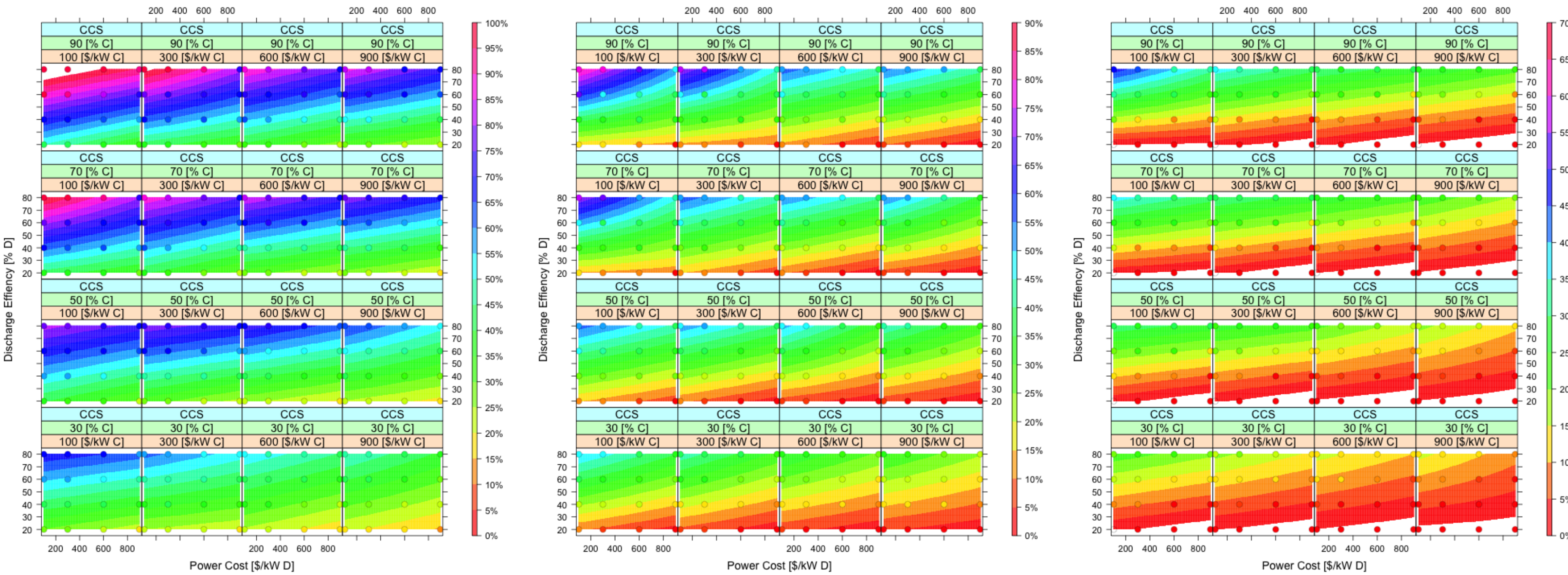


**(a)** 1 \$/kWh

**(b)** 5 \$/kWh

**(c)** 10 \$/kWh

All plots for the same system with the same low-carbon firm resource. Each Figure for an specific energy capacity cost level (\$/kWh). Each row of subplots represents a different level of charge efficiency (%). Each column of subplots represents a specific level for the charge power capacity cost (\$/kW) assumption in the LDES parameter combination. Within each subplot the x-axis represents the discharge power capacity cost (\$/kW) and the y-axis the discharge efficiency (%).

**Figure SI-37.** Northern System: Percentage firm reduction as function of LDES parameter combination in the original 5-dimensional space compared to reference cases (scenarios 4-6 Table 4) using gas w/CCS as low-carbon firm resource

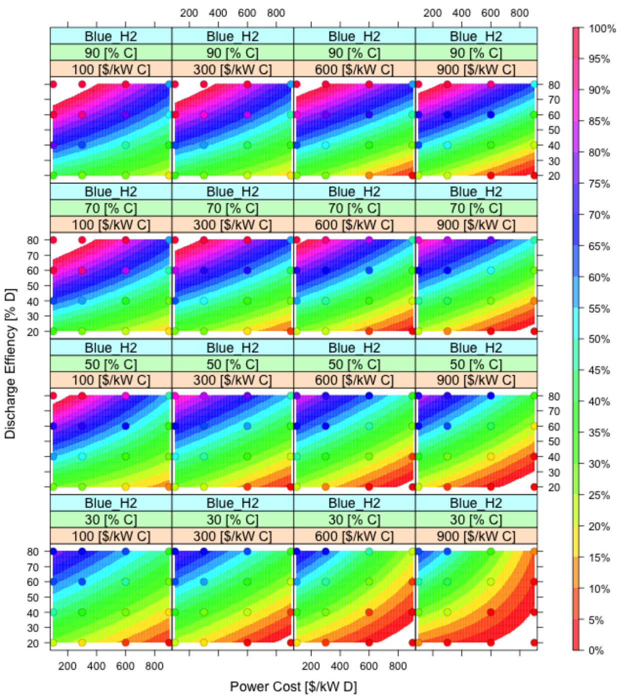


**(a)** 1 $/kWh

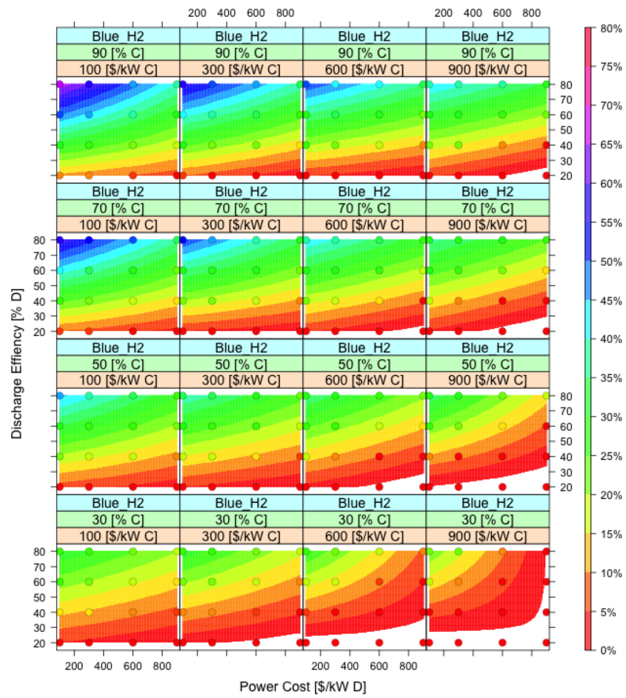


**(b)** 5 $/kWh

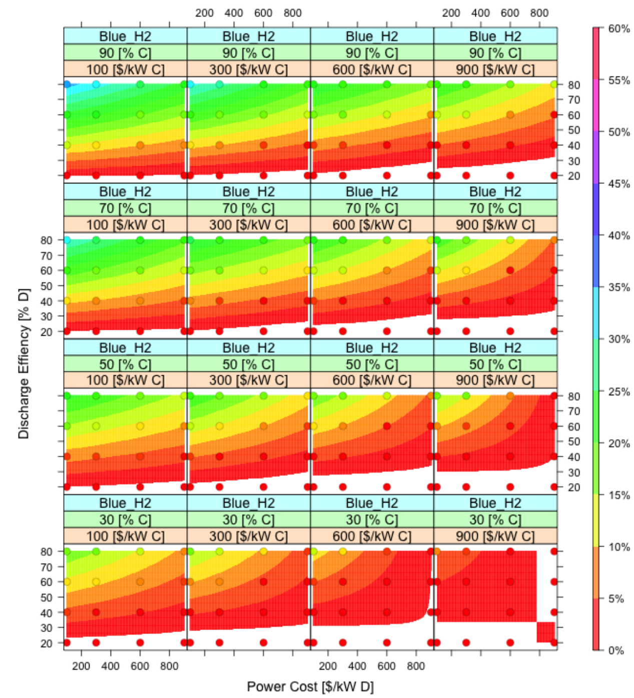


**(c)** 10 $/kWh

All plots for the same system with the same low-carbon firm resource. Each Figure for an specific energy capacity cost level ($/kWh). Each row of subplots represents a different level of charge efficiency (%). Each column of subplots represents a specific level for the charge power capacity cost ($/kW) assumption in the LDES parameter combination. Within each subplot the x-axis represents the discharge power capacity cost ($/kW) and the y-axis the discharge efficiency (%).

**Figure SI-38.** Northern System: Percentage firm reduction as function of LDES parameter combination in the original 5-dimensional space compared to reference cases (scenarios 4-6 Table 4) using blue $H_2$ as low-carbon firm resource

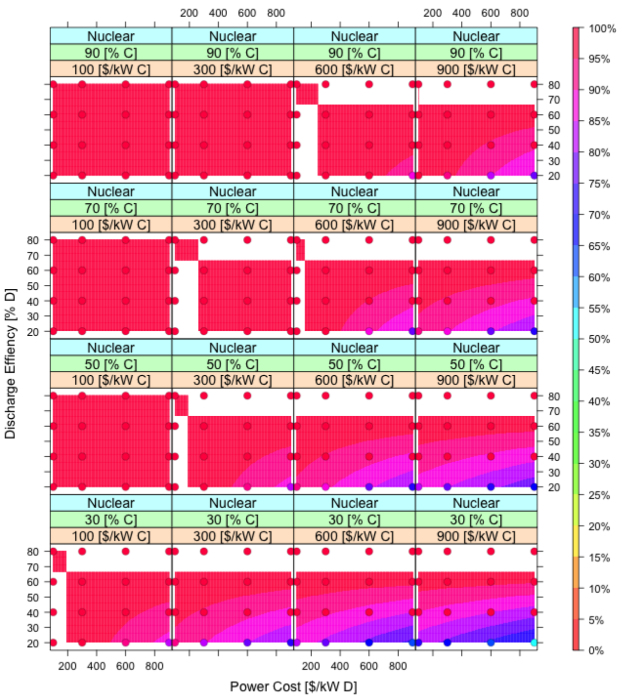


**(a)** 1 \$/kWh

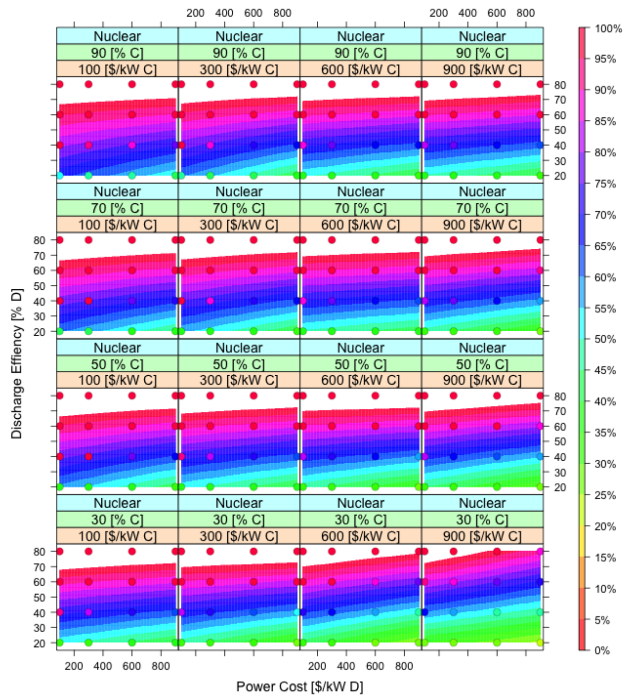


**(b)** 5 \$/kWh

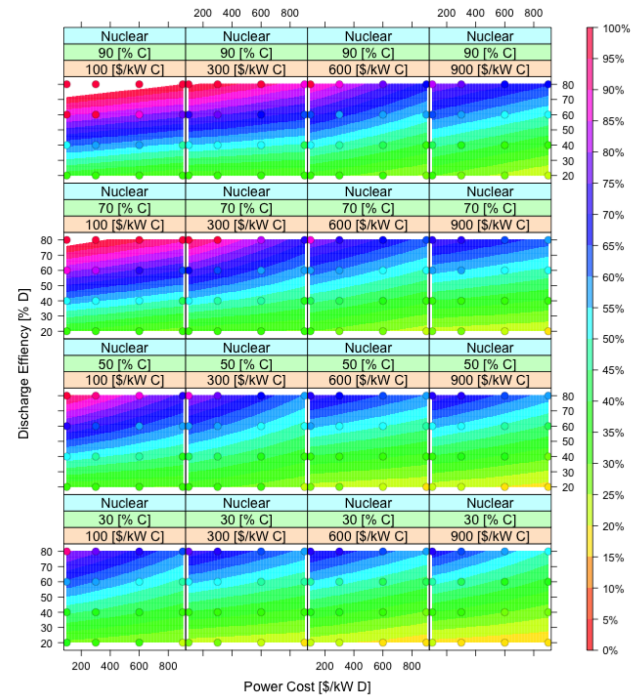


**(c)** 10 \$/kWh

All plots for the same system with the same low-carbon firm resource. Each Figure for an specific energy capacity cost level (\$/kWh). Each row of subplots represents a different level of charge efficiency (%). Each column of subplots represents a specific level for the charge power capacity cost (\$/kW) assumption in the LDES parameter combination. Within each subplot the x-axis represents the discharge power capacity cost (\$/kW) and the y-axis the discharge efficiency (%).

**Figure SI-39.** Southern System: Percentage firm reduction as function of LDES parameter combination in the original 5-dimensional space compared to reference cases (scenarios 1-3 Table 4) using nuclear as low-carbon firm resource

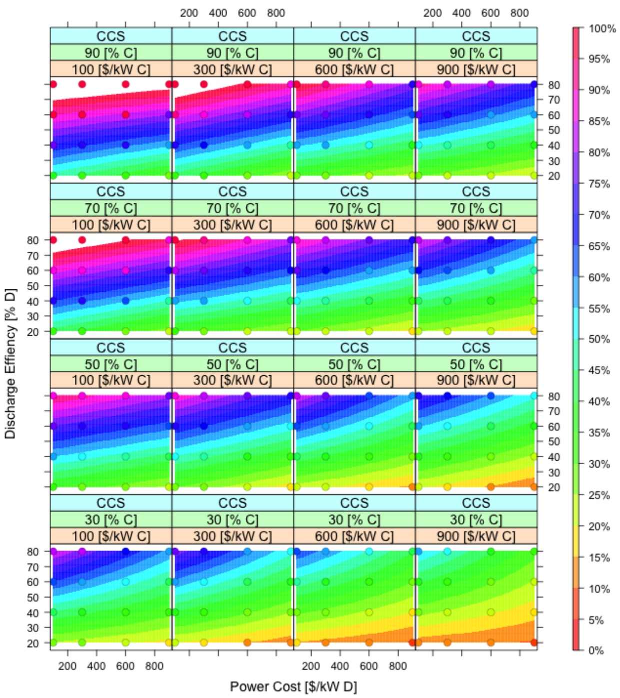


**(a)** 1 $/kWh

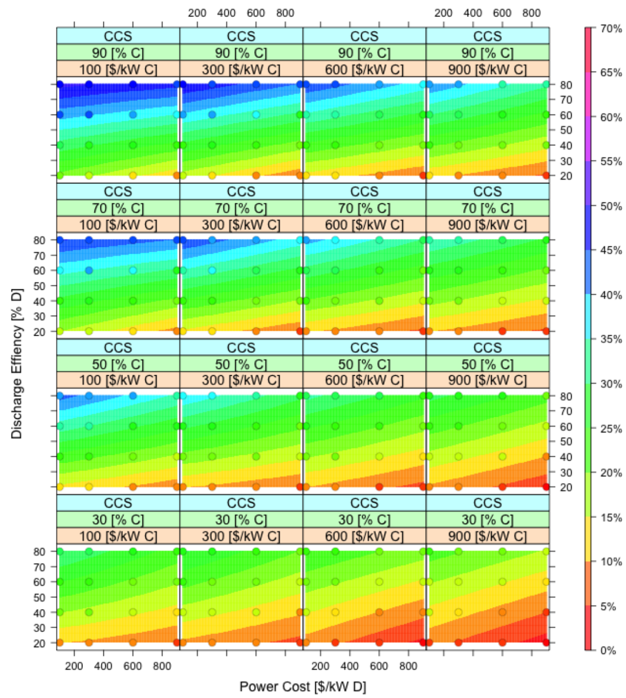


**(b)** 5 $/kWh

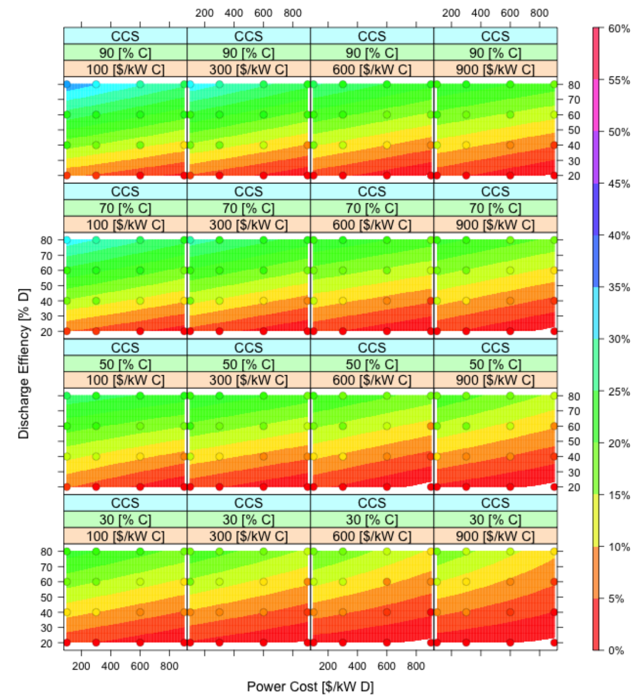


**(c)** 10 $/kWh

All plots for the same system with the same low-carbon firm resource. Each Figure for an specific energy capacity cost level ($/kWh). Each row of subplots represents a different level of charge efficiency (%). Each column of subplots represents a specific level for the charge power capacity cost ($/kW) assumption in the LDES parameter combination. Within each subplot the x-axis represents the discharge power capacity cost ($/kW) and the y-axis the discharge efficiency (%).

**Figure SI-40.** Southern System: Percentage firm reduction as function of LDES parameter combination in the original 5-dimensional space compared to reference cases (scenarios 1-3 Table 4) using gas w/CCS as low-carbon firm resource

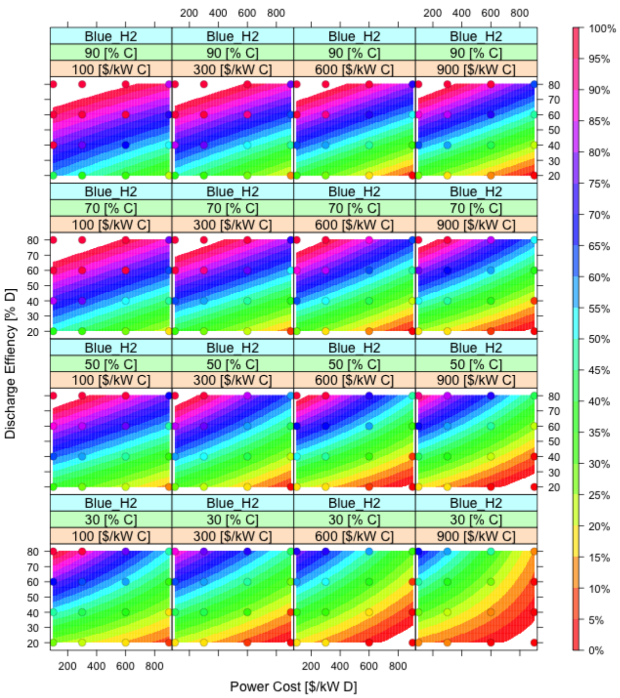


**(a)** 1 \$/kWh

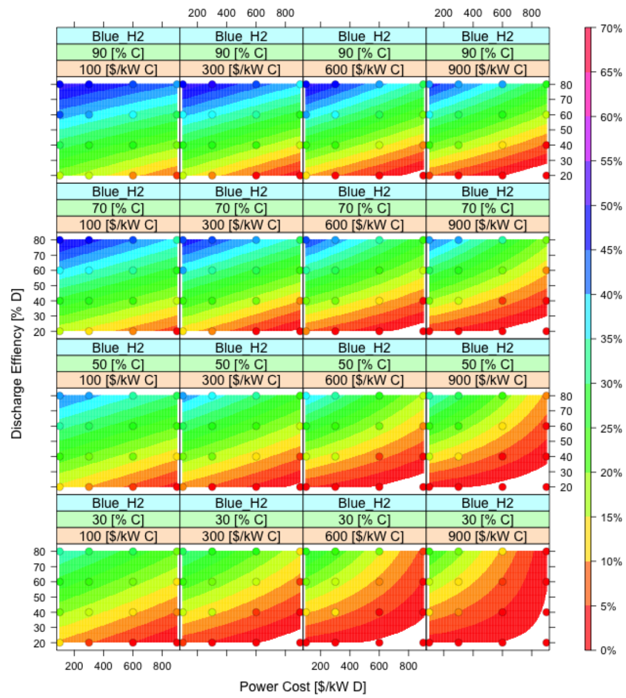


**(b)** 5 \$/kWh

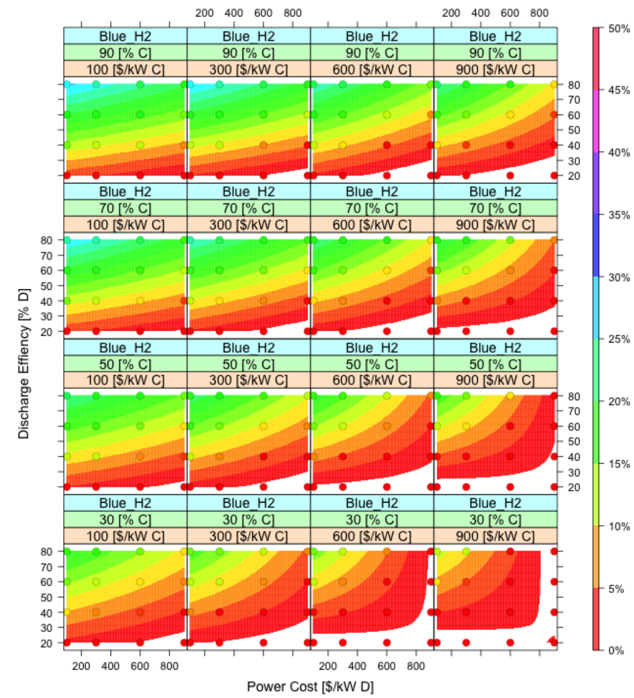


**(c)** 10 \$/kWh

All plots for the same system with the same low-carbon firm resource. Each Figure for an specific energy capacity cost level (\$/kWh). Each row of subplots represents a different level of charge efficiency (%). Each column of subplots represents a specific level for the charge power capacity cost (\$/kW) assumption in the LDES parameter combination. Within each subplot the x-axis represents the discharge power capacity cost (\$/kW) and the y-axis the discharge efficiency (%).

**Figure SI-41.** Southern System: Percentage firm reduction as function of LDES parameter combination in the original 5-dimensional space compared to reference cases (scenarios 1-3 Table 4) using blue $H_2$ as low-carbon firm resource

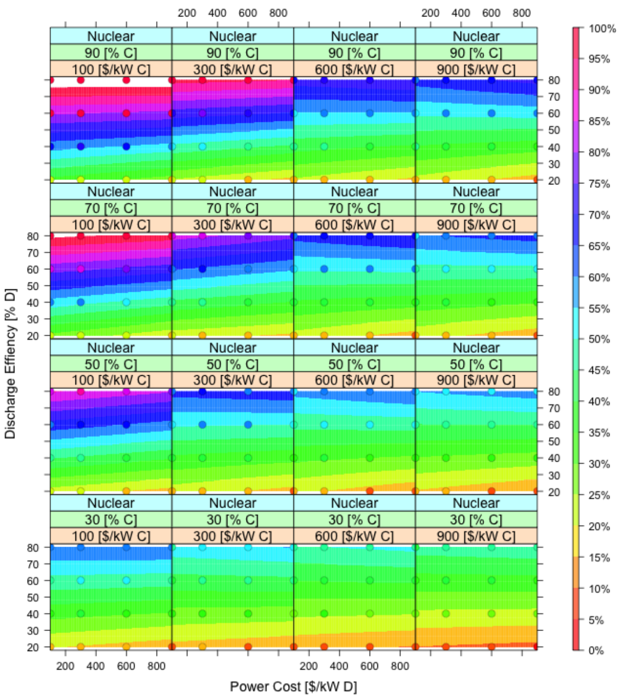


**(a)** 1 $/kWh

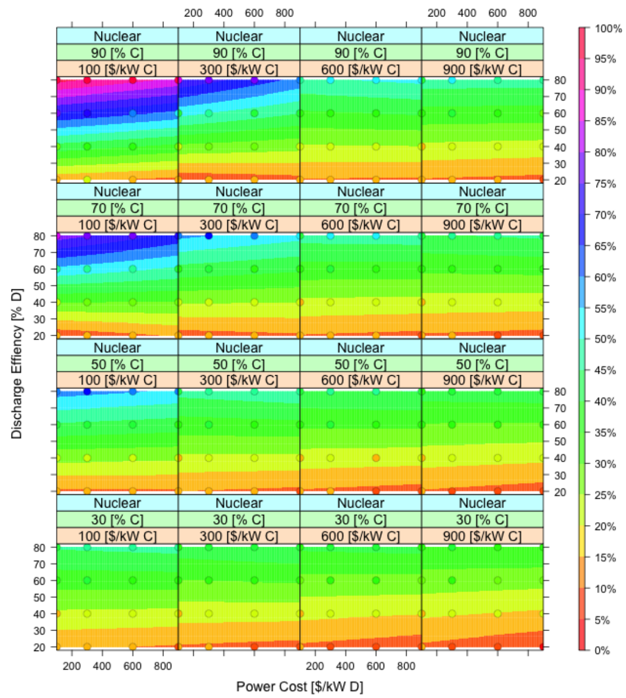


**(b)** 5 $/kWh

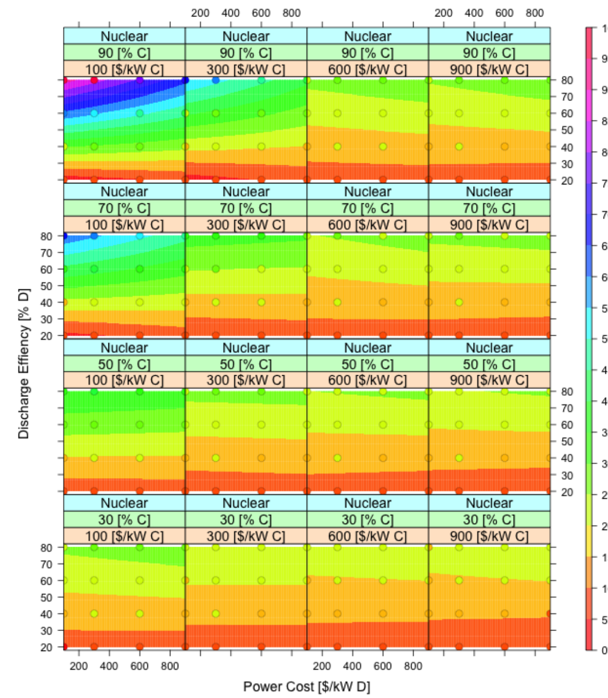


**(c)** 10 $/kWh

All plots for the same system with the same low-carbon firm resource. Each Figure for an specific energy capacity cost level ($/kWh). Each row of subplots represents a different level of charge efficiency (%). Each column of subplots represents a specific level for the charge power capacity cost ($/kW) assumption in the LDES parameter combination. Within each subplot the x-axis represents the discharge power capacity cost ($/kW) and the y-axis the discharge efficiency (%).

**Figure SI-42.** Northern System with Electrified Load: Percentage firm reduction as function of LDES parameter combination in the original 5-dimensional space compared to reference cases (scenarios 7-9 Table 4) using nuclear as low-carbon firm resource

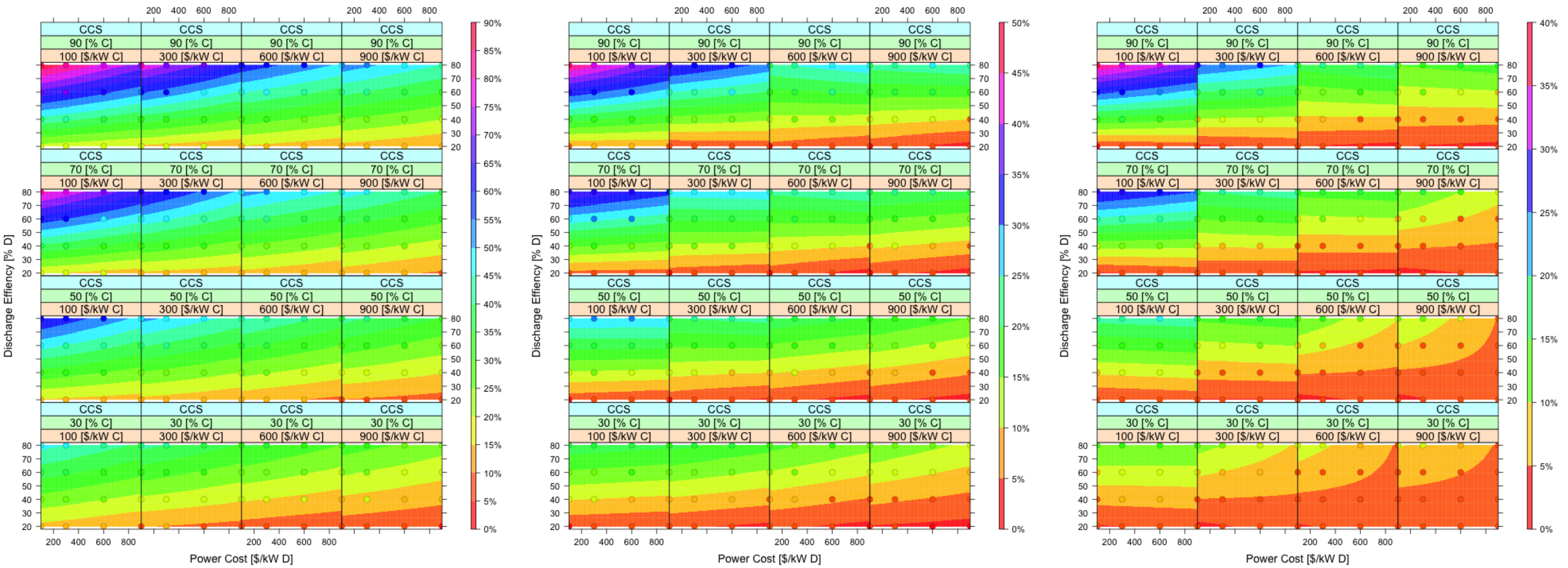


**(a)** 1 $/kWh **(b)** 5 $/kWh **(c)** 10 $/kWh

All plots for the same system with the same low-carbon firm resource. Each Figure for an specific energy capacity cost level ($/kWh). Each row of subplots represents a different level of charge efficiency (%). Each column of subplots represents a specific level for the charge power capacity cost ($/kW) assumption in the LDES parameter combination. Within each subplot the x-axis represents the discharge power capacity cost ($/kW) and the y-axis the discharge efficiency (%).

**Figure SI-43.** Northern System with Electrified Load: Percentage firm reduction as function of LDES parameter combination in the original 5-dimensional space compared to reference cases (scenarios 7-9 Table 4) using gas w/CCS as low-carbon firm resource

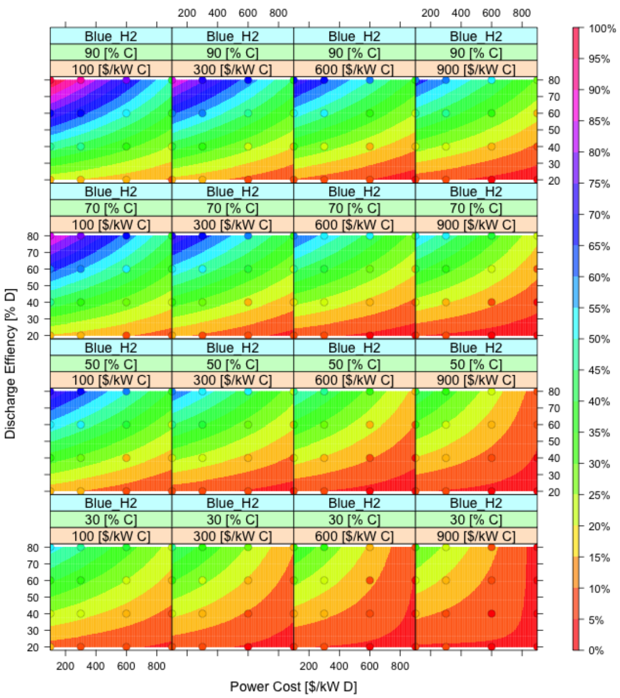


**(a)** 1 $/kWh

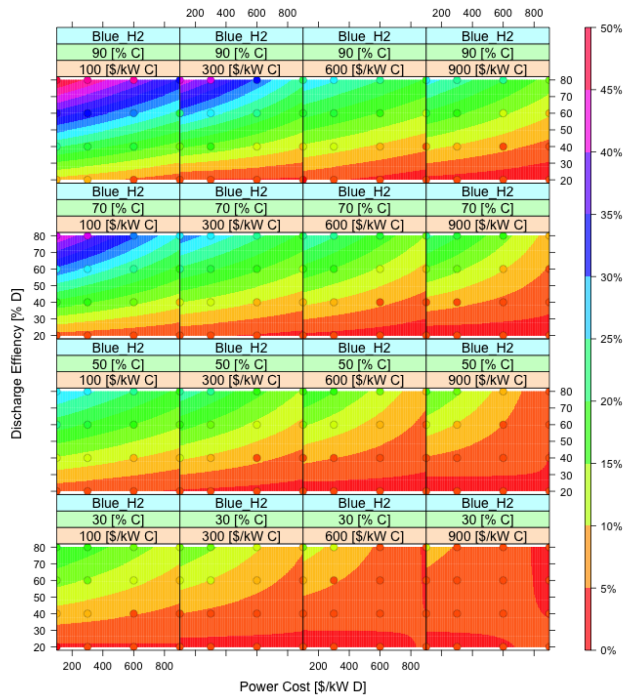


**(b)** 5 $/kWh

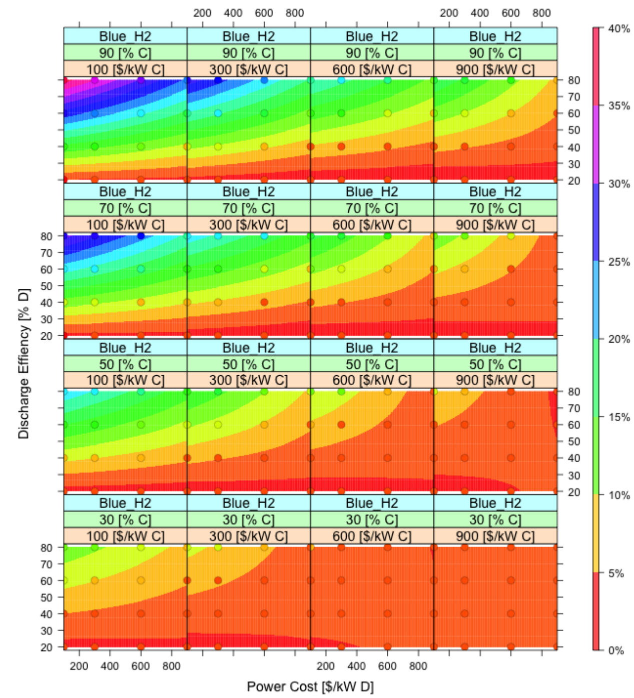


**(c)** 10 $/kWh

All plots for the same system with the same low-carbon firm resource. Each Figure for an specific energy capacity cost level ($/kWh). Each row of subplots represents a different level of charge efficiency (%). Each column of subplots represents a specific level for the charge power capacity cost ($/kW) assumption in the LDES parameter combination. Within each subplot the x-axis represents the discharge power capacity cost ($/kW) and the y-axis the discharge efficiency (%).

**Figure SI-44.** Northern System with Electrified Load: Percentage firm reduction as function of LDES parameter combination in the original 5-dimensional space compared to reference cases (scenarios 7-9 Table 4) using blue $H_2$ as low-carbon firm resource

# Supplementary Methods

## Reference Case Descriptors

**Table SI-1.** Base Cases Results

| Scenario # | System | Load/ Weather Condition | Firm Resource | VRE & Li-ion Cost | Total System Cost [bn$] | Avg. Cost [$/MWh] | Firm Capacity [MW] | Wind Capacity [MW] | Solar Capacity [MW] | Li-ion Power Capacity [MW] | Li-ion Energy Capacity [MWh] |
|---|---|---|---|---|---|---|---|---|---|---|---|
| 1 | S | B/B | Blue $H_2$ | L | $22.99 | $52.12 | 29,830 | 66,975 | 104,739 | 31,798 | 279,630 |
| 2 | S | B/B | Gas w/CCS | L | $23.44 | $53.14 | 32,967 | 59,890 | 82,961 | 28,294 | 220,939 |
| 3 | S | B/B | Nuclear | L | $29.95 | $67.90 | 28,948 | 55,208 | 97,013 | 35,581 | 355,808 |
| 4 | N | B/B | Blue $H_2$ | L | $10.17 | $56.02 | 15,901 | 31,629 | 37,271 | 11,131 | 91,984 |
| 5 | N | B/B | Gas w/CCS | L | $10.38 | $57.20 | 17,419 | 25,504 | 28,332 | 10,013 | 84,324 |
| 6 | N | B/B | Nuclear | L | $13.43 | $74.01 | 17,445 | 4,096 | 36,758 | 13,461 | 134,612 |
| 7 | N | E/B | Blue $H_2$ | L | $20.03 | $66.78 | 36,393 | 35,770 | 77,904 | 28,928 | 215,389 |
| 8 | N | E/B | CCS | L | $20.08 | $66.93 | 39,318 | 35,770 | 46,865 | 26,003 | 146,756 |
| 9 | N | E/B | Nuclear | L | $27.10 | $90.33 | 37,272 | 33,188 | 24,843 | 28,216 | 282,155 |
| 10 | N | B/H | CCS | L | $10.13 | $55.80 | 15,326 | 26,109 | 27,219 | 15,477 | 152,322 |
| 11 | N | B/L | CCS | L | $10.77 | $59.35 | 18,432 | 24,154 | 32,640 | 12,875 | 94,308 |
| 12 | N | E/B | Blue $H_2$ | M | $26.00 | $86.69 | 51,738 | 35,770 | 36,071 | 13,583 | 39,507 |
| 13 | N | E/B | CCS | M | $24.79 | $82.66 | 48,998 | 28,020 | 16,071 | 17,146 | 58,585 |
| 14 | N | E/B | Nuclear | M | $32.54 | $108.48 | 44,038 | 24,910 | 26,512 | 22,413 | 108,626 |

[1] Systems: (S) Southern(ERCOT), (N) Northern (ISONE)
[2] Load Profiles: (B) Base –linear growth, (E) Electrified
[3] Firm Resources: Nuclear, (CCS) Natural Gas with CCS, Blue $H_2$
[4] Weather Years: (B) Base, (H) Higher VRE CF,(L) Lower VRE CF
[5] Variable Renewable (VRE) and Li-ion Storage Cost: (L) Low 2018 NREL ATB, (M) 2018 Medium NREL ATB

## Model Configuration

The GenX electricity resource planning model [9] developed at MIT was used in the present research. For this analysis, we model a "greenfield" capacity plan –i.e., everything is built from scratch. The previous assumption is justified given the lifetime of existing generation assets (less than 30 years) and the explored year 2050. Arguably, the electricity generation resources operating in 2050 will have to be built in the decades to come and most current resources will not be in operation. In addition, we are not attempting to perform a planning study for a specific region. Instead, we use two "test systems" with differing climates as a way to explore the general impact of different demand profiles and wind and solar availability on outcomes of interest.

We model a time interval of one full year, divided into discrete one-hour periods and representing a future year (e.g., 2050). In this sense, the formulation produces a static long-run equilibrium outcome, because its objective is not to determine when investments should take place over time, but rather to produce a snapshot of the minimum-cost generation capacity mix under some pre-specified future conditions.

The model uses a linear relaxation of integer unit commitment constraints for thermal power plants. Integer unit commitment as developed in [12] and [13] is included in GenX. Linearization is accomplished by replacing the integer unit commitment and capacity addition variables with continuous variables, but subject to the same set of constraints. The integer unit commitment approach helps reducing the number of integer variables in a full binary unit commitment formulation (one binary variable for each thermal generator) to a more tractable formulation that uses integer variables to represent a set of resources of the same type in a cluster [13]. The linear relaxation of the unit commitment constraints set offers an additional significant improvement computational tractability while the increased abstraction error is kept below 1% as shown in [7].

We assume that transmission networks in both regional power systems are unconstrained with 19 VRE generation zones. That is, each system is represented as a "single node" without considering transmission losses or congestions between generators and demand. In principle, significant transmission reinforcements and expansions could take place in these systems by the year 2050 that would allow dispersed renewable resources, storage systems, and new generators to be accommodated. However, explicit consideration of transmission losses, congestions, and expansion decisions significantly increases model solution time. In addition, transmission networks typically represent a relatively modest share (around 5% [8]) of total power system costs. In the interest of computational tractability, explicit transmission power flows and expansion decisions are not considered. However, for each region, we model one additional wind cluster reflecting a higher quality resource and unlimited developable capacity but with higher transmission costs, as described in .

The model is fully deterministic and assumes perfect foresight in planning and operational decisions. The model is capable of modeling day-ahead commitment of frequency regulation and operating reserves, which are employed by system operators to deal with errors in renewable energy or demand forecasts or unanticipated failures of generators or transmission lines. However, we considered regulation and reserve requirements in several preliminary analyses and found that these requirements did not have a significant effect on outcomes. In the interest of computational tractability and the ability to model a greater number of total cases, we therefore do not consider regulation or reserve requirements in the cases reported.

## Economic and Operational Parameters

Tables SI-2 through SI-6 show the economic and technical assumptions used in this research. Where possible, values are extracted from the National Renewable Energy Laboratories (NREL) Annual Technology Baseline 2018 edition (ATB 2018) [11]. Any values that are not from NREL's ATB 2018 are indicated by citation. Capital costs are on a fully installed basis inclusive of installation labor and construction financing. Note that similar to other large-scale electricity system capacity expansion studies evaluating storage, we don't model storage capacity degradation as a function of operations, as this creates a non-convex formulation that is heavily computationally intensive and inconsistent with the linear programming framework employed in this study. Instead, the fixed O&M costs for Li-ion Battery resources described in Table SI-4 are inclusive of periodic replacement of battery cells to maintain usable capacity throughout the asset life as per [11].

Note that for long duration energy storage (LDES) resources, this paper assumes a 30 year asset life and 7.1% weighted average cost of capital (WACC) for charge power, discharge power, and energy storage. We convert capital costs to investment annuities using an annual capital recovery factor assuming continuously compounding interest. As real-world LDES technologies will undoubtedly present a range of asset lifetimes for power and energy capacity components, and cost of financing varies over time, we provide a conversion table Table SI-5 below, which reports the ratio of capital recovery factors under different asset life and WACC combinations relative to the 30 years/7.1% WACC assumptions used in this paper. To compare a resource with a different asset life or a different cost of capital assumption to the findings in this paper, use Table SI-5 to look up the ratio of capital recovery factors at different asset life/WACC assumptions, multiply the asset costs by the ratio above, and compare the resulting values to the figures and results presented in this study. As the range of LDES capital costs explored herein span 9x for charge and discharge power capacity and 50x for energy capacity, a wide range of alternative asset life and WACC assumptions fall within the design space considered herein.

**Table SI-2.** Technical Assumptions Thermal Resources

| Technology | Power Plant Size [MW] | Heat Rate [mmBTU/ MWh] | Min. Stable Output [%] | Hourly Ramp Rates [%] | Min Up /Down Times [h] | Startup Fuel [mmBTU/ start] |
|---|---|---|---|---|---|---|
| OCGT | 237 | 8.55 | 25 | 100 | 1/1 | 45 |
| CCGT | 573 | 5.97 | 33 | 100 | 4/4 | 4120 |
| CCGT with CCS | 400 | 7.17 | 50 | 100 | 4/4 | 3451 |
| Nuclear | 360 | 10.46 | 50 | 25 | 12/12 | 0 |

[1] Unless otherwise noted, all assumptions are from NREL 2018.

**Table SI-3.** Technical Assumptions: Non-Thermal Resources

| Technology | Power Plant Size [MW] | Min. Stable Output [%] | Hourly Ramp Rates [%] | Efficiency up / down [%] | Min/Max Duration Allowed [h] |
|---|---|---|---|---|---|
| Solar | Cont. | 0 | 100 | - | - |
| Wind | Cont. | 0 | 100 | - | - |
| Li-ion Battery | Cont. | 0 | 100 | 92.7/ 92.7 | 0.25 / 10 |
| LDES | Cont. | 0 | 100 | Varies | 10 / 1000 |

**Table SI-4.** Economic Assumptions for Different Resources

| Technology | Power Capital Cost [$/MW] | Power Investment Annuity [$/MW-yr] | Transmission Cost [$/MW-yr] | Energy Capital Cost [$/MWh] | Energy Investment Annuity [$/MW-yr] | Fixed O&M Cost [$/MW-yr] | Variable O&M Cost [$/MWh] | Start-up Cost[a] [$/start] |
|---|---|---|---|---|---|---|---|---|
| OCGT[b] | $681,296 | $57,000 | - | - | - | $7,010 | $11 | $8,058 |
| CCGT[b] | $961,890 | $80,400 | - | - | - | $10,000 | $3 | $45,267 |
| CCGT with CCS | $1,799,532 | $150,400 | - | - | - | $33,000 | $7 | $37,920 |
| Nuclear[g] | $4,570,756 | $382,100 | - | - | - | $99,000 | $2 | $46,080 |
| Solar[c] Tracking-AC | $651,000 / $1,062,000 | $55,600 / $90,700 | - | - | - | $4,000 | - | - |
| Solar Fixed Lat-AC[c] | $611,859 / $1,011,523 | $51,600 / $84,200 | - | - | - | $3,300 | - | - |
| Solar Fixed Winter-AC[c] | $611,859 / $1,011,523 | $51,600 / $84,200 | - | - | - | $3,300 | - | - |
| Onshore Wind[f] | $803,474 / $1,596,593 | $67,200 / $133,500 | - | - | - | $35,000 | - | - |
| Offshore Wind | $803,474[d]/ $1,596,593 | $67,200[d]/ $133,500 | $66,683[d] | - | - | $35,000[d] | - | - |
| | $2,095,658[e]/ $2,418,704 | $175,200[e]/ $202,200 | $32,327[e] | - | - | $125,000[e] | - | - |
| Li-ion [h] Battery | $276,617 / $415,447 | $31,100 / $46,700 | - | $68,447 / $180,824 | $7,700 / $20,300 | $2,660 | $0.532 | - |
| LDES | Varies | Varies | - | Varies | Varies | $2,660 | - | - |

[1] Unless otherwise noted, all assumptions are from NREL 2018 [11] Annual Technology Baseline for the year 2045.
[2] All assets are assumed to have 30-year lifetimes except for Li-ion battery which is 15 years.
[3] After-tax WACC of 7.1% assumed for all resources.
[a] Start-up costs are from NREL 2012 - Power plant cycling costs[10]; assumes warm starts and uses median estimated value.
[b] Blue hydrogen uses OCGT and CCGT technology inputs with the blue hydrogen fuel costs. NREL mid-range cost.
[c] Cost of solar reported in $/MW AC. AC to DC ratio of 1.5 for solar. NREL ATB '18 2045 low / medium cost utility-scale solar.
[d] Corresponds to Panhandle Wind in ERCOT. NREL ATB '18 2045 TRG6 low / medium cost.
[e] Corresponds to Off-Shore Wind in ISONE. NREL ATB '18 2045 TRG3 low / medium cost.
[f] Cost Assumptions for 15 different Wind Profiles. NREL ATB '18 2045 TRG6 low / medium cost.
[g] SMR type from [6].
[h] NREL ATB 2045 low / medium cost projections.

**Table SI-5.** Capital cost conversion ratios between different asset life and weighted average cost of capital (WACC) assumption

| | Asset life (years) | | | | | | | | | | | |
|---|---|---|---|---|---|---|---|---|---|---|---|---|
| WACC | 5 | 10 | 15 | 20 | 25 | 30 | 35 | 40 | 45 | 50 | 55 | 60 |
| 4% | 2.70 | 1.48 | 1.08 | 0.89 | 0.77 | 0.70 | 0.65 | 0.61 | 0.59 | 0.57 | 0.55 | 0.54 |
| 5% | 2.78 | 1.56 | 1.16 | 0.97 | 0.86 | 0.79 | 0.74 | 0.71 | 0.69 | 0.67 | 0.66 | 0.65 |
| 6% | 2.86 | 1.64 | 1.25 | 1.06 | 0.95 | 0.89 | 0.84 | 0.81 | 0.79 | 0.78 | 0.77 | 0.76 |
| 7% | 2.94 | 1.72 | 1.34 | 1.15 | 1.05 | 0.99 | 0.95 | 0.92 | 0.91 | 0.90 | 0.89 | 0.88 |
| 7.1% | 2.95 | 1.73 | 1.34 | 1.16 | 1.06 | 1.00 | 0.96 | 0.94 | 0.92 | 0.91 | 0.90 | 0.89 |
| 8% | 3.03 | 1.81 | 1.43 | 1.25 | 1.15 | 1.10 | 1.06 | 1.04 | 1.03 | 1.02 | 1.01 | 1.01 |
| 9% | 3.11 | 1.90 | 1.52 | 1.35 | 1.26 | 1.21 | 1.18 | 1.16 | 1.15 | 1.14 | 1.14 | 1.13 |
| 10% | 3.20 | 1.99 | 1.62 | 1.46 | 1.37 | 1.33 | 1.30 | 1.28 | 1.27 | 1.27 | 1.26 | 1.26 |

This study assumes 30 year asset life and 7.1% after tax WACC for all LDES resources. To compare a resource with different asset life or a different cost of capital to the findings in this table, use the above table to look up the ratio of capital recovery factors at different asset life/WACC assumptions, multiply the asset costs by the ratio above, and compare the resulting values to the figures and results presented in this study.

**Table SI-6.** Fuels Assumptions

| Fuel | Cost [$/mmBTU] | $CO_2$ emissions rate [kg/mmBTU] |
|---|---|---|
| Natural gas post-combustion CCS[a] | 5.45[b] | 5.31[c] |
| Uranium | 0.68 | 0.00 |
| Blue hydrogen[d] | 15.14 | 7.32 |

[a] U.S. Energy Information Administration. Annual Energy Outlook 2018 [1]
[b] Assumed to include a $10/metric ton $CO_2$ sequestration cost.
[c] CCS assumed to have a capture rate of 90%.
[d] IEA GHG program Technical Report 2017-02: "Techno-Economic Evaluation of SMR Based Standalone (Merchant) Hydrogen Plant with CCS" [5]. CCS High cost case.

## Variable Renewable and Demand Assumptions

For both wind and solar profiles we use the method developed in [2]. The year of 2009 was chosen as base year used for the renewable resource availability data. To establish the solar profiles, we assume that the county-level geographic distribution of solar installations in 2045 across the region of interest is the same as the current county-level distribution. An hourly PV generation profile for each county within the modeled area is generated using historical meteorological data from the National Solar Radiation Database (NSRDB) [14] as inputs to the open-source PV modeling package PVLIB [15]. These county profiles are weighted by the current county-level existing and proposed utility-scale solar capacity, taken from the U.S. Energy Information Administration (EIA) Form 860 database, and averaged for each region, resulting in a single spatially-averaged hourly PV profile for each region. Three PV technologies are modeled for each region, using the same geographic distribution: i) a tracking technology going from east to west (has the greatest solar capacity factor), ii) a fixed latitude technology which is fixed at an angle equal to latitude, and 3) a fixed winter tilt which is fixed at an angle equal to latitude plus an extra 23 degrees, to increase solar capacity during the wintertime. Both the Northern and Southern like systems each have three solar profiles based on this methodology.

To establish the wind profiles, data on wind capacity factors and availability is taken from NREL's Wind Integration National Dataset Toolkit (WIND Toolkit) [3]. This dataset includes hourly modeled wind capacity factor at 120,000 sites across the continental U.S. and an estimate of the maximum allowable wind capacity (from 2-16 MW) at each site. Wind capacity factors vary more significantly across the modeled regions than PV capacity factors, so rather than utilizing a single average wind profile, we cluster the modeled WIND Toolkit sites into 15 bins for each region. We first separate the available sites into 5 bins clustered by capacity factor, then subdivide each capacity-factor bin into 3 additional bins based on the distance of each modeled site to major population centers within the modeled region to create geographic variation in wind sites and capture variation in wind profiles across space. All modeled sites within each bin are then multiplied by the allowable wind capacity per site, summed, and divided by the total allowable wind capacity within the region, generating one hourly capacity-weighted capacity factor profile for each of the 15 bins. The allowable wind capacity in each bin is given by the sum of the allowable capacity at each of the sites included in the bin. One additional wind profile is included for each region to represent a higher-cost but potentially higher capacity factor wind development opportunity without any upper capacity constraint. For the Northern system this profile represents Massachusetts offshore wind while for the Southern system this profile represents sites located in the Texas panhandle region (due to the distance of this region to ERCOT network). These additional wind profiles include a capital expenditure cost adder of \$66,683/MW-year for the Southern system and \$32,327/MW-year for the Northern system to reflect the increased transmission cost associated with these sites. As noted elsewhere, we are modeling hypothetical systems, not specific regional power systems. Our intention in this study is to capture differences in temporal profiles of renewable energy (and demand) that might commonly be encountered at different latitudes and test the impact on the value/role of energy storage, rather than to capture planning challenges particular to the actual ISO New England or ERCOT power systems. We thus do not consider variation in transmission interconnection or spur line costs for the first 15 wind bins (or the three solar technology types), as these costs are idiosyncratic and location specific. Figure SI-45 shows the different duration curves for the solar and wind profiles used under base weather for each system.

The procedure described above was repeated in order to generate solar and wind profiles for “Higher Renewable Availability ” and “Lower Renewable Availability” scenarios. The years with highest and lowest overall wind availability between 2007 to 2013 were selected with the year 2010 identified as the year with highest availability and 2012 as the year with lowest availability. Figure SI-46 shows the different duration curves for the solar and wind profiles used under higher and lower weather conditions.

The base electricity demand profile uses real demand data from each region in 2009, to match the year used in the wind and solar profiles. To account for load growth, the demand in each hour is scaled up to 2045 assuming

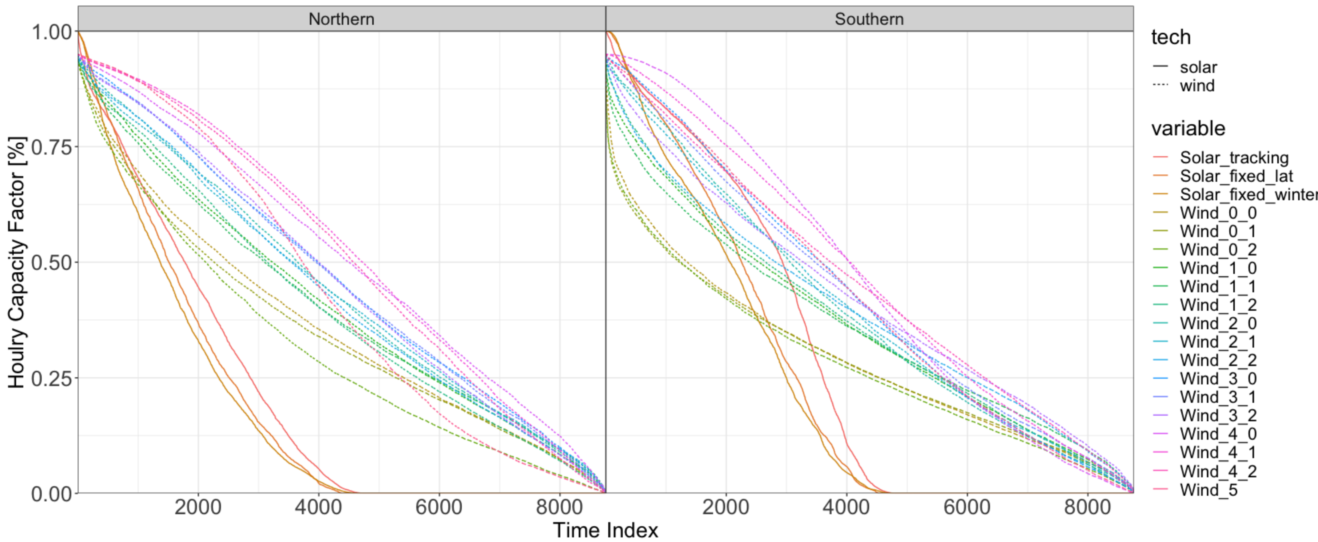


**Figure SI-45.** Duration Curves of VRE Hourly Profiles under Base Weather Conditions

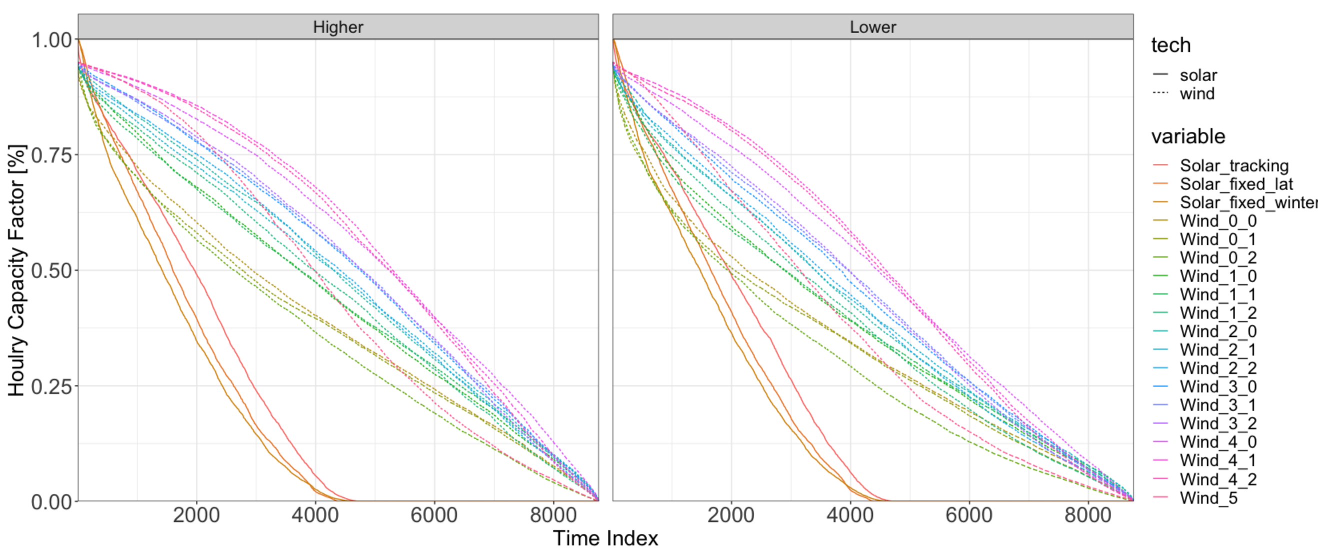


**Figure SI-46.** Duration Curves of VRE Hourly Profiles under Higher and Lower Weather Conditions Northern System a 1% growth rate each year. Additionally, an "electrification for deep decarbonization" profile was utilized for the corresponding scenarios. The 2050 Base Deep Decarbonization profile for New England from the " Deep Decarbonization in the Northeastern United States and Expanded Coordination with Hydro-Québec" study was used[16]. The profile was generated using the PATHWAYS model [4] by the authors of the report accounting for changes in LED lighting, EV penetration, heating electrification, among others. Figure SI-47 shows a comparison of both load profiles. It can be seen in the figure that electrification greatly increases the system peak and average demand. Moreover, electrification adds a strong seasonal component due to electrification of heating while at the same time it increases the short-time frequency due to the electrification of transportation among others.

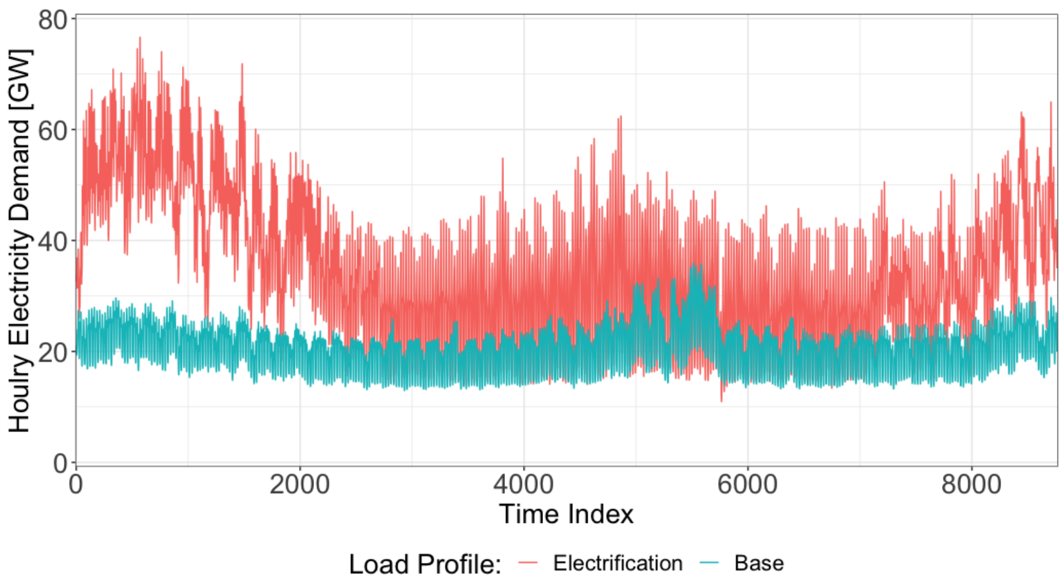


**Figure SI-47.** Comparison of "Base" and "Electrification for Deep Decarbonization" Load Profiles

## GenX Overview

Existing decision-making tools and technology valuation metrics are mainly cost-based and focus on the individual technology. The Levelised Cost of Electricity (LCOE) is an intuitive metric for technology-specific production cost, aggregating the investment and operational cost per unit of energy generated in $/MWh. This metric was practical in a $20^{st}$ century electricity system, containing exclusively dispatchable power plants. Today however, the LCOE has lost its meaning as it does not account for asset operability, prices and production variability, nor the impact that a plant's operation has on the electricity system in terms of reliability and operability as a whole (e.g., necessary back-up capacity, balancing and inertial services, reduced utilisation factors/increased emissions for other power plants). It is becoming clear that such services and technology features provide value to the power system but are not captured by existing valuation tools purely based on cost.

Rather than comparing different resources to one another based on cost (LCEO), the "Value-Cost Model" compares the marginal cost of each resource to the marginal value that the same resource provides to the system if is deployed. Technologies that might look promising from a purely cost-based perspective might present short-lived value in the system with "optimal" penetrations below expectations, and the other way around. The challenge is that although cost can be exogenously approximated, ultimately the incremental system value of a technology is a function of the prevalent system design and constraints and must be endogenously determined. Therefore, a centrepiece of value-based technology assessment methods are electricity system models which account for system integration effects and interrelated technology behaviour. The degree to which system requirements, environmental targets, and technical variety and detail are present in the model formulation must then be adequate for the decision-making or policy question.

For decarbonization and increasing penetration of variable renewable generation and battery storage it is essential to include enough operational detail in the model formulation. The reason for this is the need to capture challenges like the variable nature of wind and solar power, the different value sources of energy storage (energy, capacity deferral, network deferral, etc), the technical constraints of thermal plants (cycling, ramping limits, etc) and the synergies between different resources at the operational level. Systems value technical characteristics (flexibility, location, uncertainty, ability to provide services, etc) differently depending on the system's characteristics, consumption profiles and policies in place ($CO_2$ target, Clean Energy Standard or Renewable Standard).

Below we provide a summary of GenX, an electric power system investment and operations model described in detail elsewhere [9].

### Indices and Sets

**Table SI-7.** Model Indices

| Notation | Description |
|---|---|
| $h \in H$ | where $h$ denotes an hour and $H$ is the set of hours in a sub-period $w$. |
| $w \in W$ | where $w$ denotes a sub-period and $W$ is the set of sub-period within the year. |
| $z \in Z$ | where $z$ denotes a zone/node and $Z$ is the set of zones/buses in the network. |
| $l \in L$ | where $l$ denotes a line and $L$ is the set of transmission lines in the network. |
| $g \in G$ | where $g$ denotes a technology cluster and $G$ is the set of available resources. |
| $s \in S$ | where $s$ denotes a segment of consumers and $S$ is the set of all consumers segments. |

**Table SI-8.** Model Sets

| Notation | Description |
|---|---|
| $R \subseteq G$ | where $R$ is the subset of resources subject to ramping limitations. |
| $UC \subseteq G$ | where $UC$ is the subset of resources subject to Unit Commitment requirements. |
| $O \subseteq G$ | where $O$ is the subset of resources subject to energy balance requirements. |
| $STD_i \subseteq G$ | where $STD_i$ is the subset of resources qualified for some policy $i$. |
| $G_z \subseteq G$ | where $G_z$ is the subset of resources in zone $z$ . |

**Decision Variables**

**Table SI-9.** Model Variables

| Notation | Description |
|---|---|
| $y_g^{P+}$ | new power investments on resource cluster $g$. |
| $y_g^{P-}$ | retired power investments on resource cluster $g$. |
| $y_g^{P\Sigma}$ | total available power capacity in cluster $g$. |
| $y_l^{F+}$ | new investments on transmission capacity line $l$. |
| $y_l^{F\Sigma}$ | total available transmission capacity line $l$. |
| $x_{g,h,w}^{inj}$ | power injection from resource cluster $g$ during hour $h$ in sub-period $w$. |
| $x_{g,h,w}^{wdw}$ | power withdrawals from resource cluster $g$ during hour $h$ in sub-period $w$. |
| $x_{g,h,w}^{lvl}$ | energy balance level on resource cluster $g$ during hour $h$ in sub-period $w$. |
| $x_{s,h,w,z}^{nse}$ | curtailed demand segment $s$ during hour $h$ in sub-period $w$ at zone $z$. |
| $x_{l,h,w}^{flow}$ | power flow in line $l$ during hour $h$ in sub-period $w$. |
| $x_{g,h,w}^{commit}$ | commit state cluster $g$ during hour $h$ in sub-period $w$. |
| $x_{g,h,w}^{start}$ | start events cluster $g$ during hour $h$ in sub-period $w$. |
| $x_{g,h,w}^{shut}$ | shutdown events cluster $g$ during hour $h$ in sub-period $w$. |

**Parameters**

**Table SI-10.** Model Parameters

| Notation | Description |
|---|---|
| $voll$ | Maximum value for non-served energy in the system |
| $d_{h,w,z}$ | Electricity demand at hour $h$ of sub-period $w$ in zone $z$. |
| $n_s^{slope}$ | Cost of demand curtailment for segment $s$ as % of $voll$. |
| $n_s^{size}$ | Size of segment $s$ for demand curtailment as % of the hourly demand. |
| $\bar{y}_g^{P\wedge}$ | Maximum new power investments in cluster $g$. |
| $\bar{y}_g^{P\vee}$ | Existing brownfield power investments in cluster $g$. |
| $\bar{y}_g^{P\Delta}$ | Unit size of power investments in cluster $g$. |
| $\bar{y}_g^{F\wedge}$ | Maximum new transmission investments in line $l$. |
| $\bar{y}_g^{F\vee}$ | Existing brownfield transmission investments in line $l$. |
| $c_g^{Pi}$ | Annual amortization of capital cost for power investments in cluster $g$. |
| $c_l^{Fi}$ | Annual amortization of capital cost for transmission investments in line $l$. |
| $c_g^{Pom}$ | Fixed power O&M cost for units in cluster $g$. |
| $c_g^{o}$ | Variable O&M for units in cluster $g$. |
| | Continued on next page |

**Table SI-10 – continued from previous page**

| Notation | Description |
|---|---|
| $c_g^f$ | Fuel cost for units in cluster $g$. |
| $c_g^{st}$ | Cycling cost for units in cluster $g$. |
| $\epsilon_g^{CO_2}$ | $CO_2$ emissions rate for units in cluster $g$. |
| $\rho_{g,h}^{\wedge}$ | Hourly capacity factor in hour $h$ for cluster $g$. |
| $\rho_g^{\vee}$ | Minimum stable output for units in cluster $g$. |
| $\eta_g^0$ | Self discharge rate for units in cluster $g$ for energy balance. |
| $\eta_g^+$ | Efficiency up for units in cluster $g$ for withdraws. |
| $\eta_g^-$ | Efficiency down for units in cluster $g$ for injections. |
| $\delta_g$ | Ratio energy to power (duration) investments in cluster $g$. |
| $\kappa_g^+$ | Maximum ramp-up rate for units in cluster $g$ as % power capacity |
| $\kappa_g^-$ | Maximum ramp-down rate for units in cluster $g$ as % power capacity |
| $\tau_g^+$ | Minimum up-time for units cluster $g$ before new shutdown. |
| $\tau_g^-$ | Minimum down-time for units cluster $g$ before new restart. |
| $\mu_g^f$ | Maximum % of hourly demand that can be deferred . |
| $\tau_g^f$ | Maximum duration of demand deferral. |
| $\varphi_{l,z}^{map}$ | Network topology for each line $l$ $\begin{cases} 1 & \text{line leaving from zone } z \\ -1 & \text{line arriving at zone } z \\ 0 & \text{otherwise} \end{cases}$ |
| $\epsilon_z^{max}$ | $CO_2$ maximum emissions rate for zone $z$. |
| $\epsilon_{i,z}^{STD}$ | Policy standard energy requirement (% total energy) for policy $i$ in zone $z$. |

**Objective Function**

The Objective Function in Eq. (1) minimizes over 3 components that are jointly co-optimized.

$$\min_{y,x} \Bigg( \tag{1a}$$

$$\sum_{g\in G}(y_g^{P+}\cdot c_g^{Pi}\cdot \bar{y}_g^{P\Delta} + y_g^{P\Sigma}\cdot c_g^{Pom}) + \sum_{l\in L}(y_l^{F+}\cdot c_l^{Fi}) + \tag{1b}$$

$$\sum_{w\in W}\sum_{h\in H}\Big(\sum_{g\in G}(x_{g,h,w}^{inj}\cdot(c_g^{Po}+c_g^{f})) + \sum_{g\in O}(x_{g,h,w}^{wdw}\cdot c_g^{Po}) + \sum_{z\in Z}\sum_{s\in S} x_{s,h,w,z}^{nse}\cdot n_s^{slope}\Big) + \tag{1c}$$

$$\sum_{w\in W}\sum_{h\in H}\Big(\sum_{g\in UC} x_{g,h,w}^{start}\cdot c_g^{st}\Big)\Bigg) \tag{1d}$$

As shown in (1a) the method consist of minimizing the total system cost (or maximizing social welfare) with respect to investments variables $y$ (e.g., new investments in power capacity $y_g^{P+}$) and operational variables $x$ (e.g., power injections $x_{g,h,w}^{inj}$) over a one year period with $W$ sub-periods and $H$ hours per sub-period. The first component, Eq. (1b), of the objective function corresponds to the capacity expansion element of the problem. New investments in power ($y_g^{P+}$) and transmission capacity ($y_l^{F+}$) can be made at their respective investment costs $c_g^{Pi}$ and $c_l^{Fi}$. Note that in this study, we do not explicitly model transmission capacity expansion (transmission decisions are included here only to present a complete formulation of the model, as it may be used in other studies). Additionally, the total available power capacity ($y_g^{P\Sigma}$) is subject to the fixed operation and maintenance cost ($c_g^{Pom}$). The second term of the objective function, Eq. (1c), corresponds to the economic dispatch element of the problem. Power injections ($x_{g,h,w}^{inj}$) can be made at a cost equal to the variable operation and maintenance cost ($c_g^{Po}$) plus the fuel cost ($c_g^{f}$) from each resource cluster $g \in G$. Some resource clusters $g \in O$ have the ability to make power withdrawals ($x_{g,h,w}^{wdw}$) at their variable operation and maintenance cost ($c_g^{Po}$) (e.g., energy storage). Additionally, non-served demand ($x_{s,h,w,z}^{nse}$) from different consumer segments $s \in S$ might be necessary in some of the nodes of the system $z \in Z$ with a cost of unserved energy ($n_s^{slope}$) per segment $s$. The last component of the objective function, Eq. (1d), corresponds to the unit commitment element of the problem. Some resource clusters $g \in UC$ are subject to unit commitment constraints. These resources incur cycling costs ($c_g^{st}$) every time a startup event ($x_{g,h,w}^{start}$) is necessary.

**Constraints**

The optimization function defined in Eq. (1) is subject to different sets of constraints that define the feasible space for solutions to the variable sets $y$ and $x$. Without constraints like the Demand Balance constraints the solution to our problem would be no investments nor production and the objective value would be zero.

**Demand Balance Constraints** The Demand Balance constraints, Eq. (2), are among the main sets of constraints driving the optimization. For each hour $h \in H$, sub-period $w \in W$ and zone $z \in Z$ a constraint forces the electricity demand ($d_{h,w,z}$) to be equal to: (i) the power injections ($x^{inj}_{g,h,w}$) from resource clusters $g \in G_z$ belonging to zone $z$, (ii) minus power withdrawals ($x^{wdw}_{g,h,w}$) from resource clusters that can withdraw energy $g \in O$ and belong to zone $z$, $g \in G_z$, (iii) plus unserved energy ($x^{nse}_{s,h,w,z}$) across all consumer segments $s \in S$, and (iv) the net effect of power flows ($x^{flow}_{l,h,w}$) across lines $l \in L$ that are connected to zone $z$.

$$\begin{aligned} \sum_{g \in G_z} x^{inj}_{g,h,w} - \sum_{g \in (O \cap G_z)} x^{wdw}_{g,h,w} + \sum_{s \in S} x^{nse}_{s,h,w,z} - \\ \sum_{l \in L} \varphi^{map}_{l,z} \cdot x^{flow}_{l,h,w} &= d_{h,w,z} \end{aligned} \qquad \forall h \in H, w \in W, z \in Z \tag{2}$$

**Policy Constraints** Central to the motivation of this work are the policy constraints (e.g., clean or renewable energy mandates and $CO_2$ emission limits). These are sets of constraints that can broadly affect the feasible region for variable sets $y$ and $x$. Moreover, these constraints in most cases greatly increase the complexity of the problem by linking a great number of operational variables $x$ from different resource clusters $g$ across all sub-periods $w \in W$, all hours $h \in H$, and in some cases all regions $z \in Z$. There are two main types of policies considered in this methodology. The first type, Eq. (3), are the "direct decarbonization" policies that set a limit on the system's $CO_2$ emissions rate over the year. These policies can be implemented in two different ways Eq. (3a) and Eq. (3b). For Eq. (3a) the constraint is implemented for each zone $z \in Z$ independently. The total $CO_2$ generation at each zone $z$ is the product of the power injections ($x^{inj}_{g,h,w}$) and the emissions rate ($\epsilon^{CO2}_g$) across all clusters in the zone $g \in G_z$ summed over all sub-periods $w \in W$ and hours $h \in H$. The total $CO_2$ generation at each zone $z$ must be less or equal than the total $CO_2$ allowance for that zone, calculated as the total zonal demand times the maximum emissions rate ($\epsilon^{max}_z$) for that zone. Total zonal demand is calculated as the sum over all sub-periods $w \in W$ and hours $h \in H$ of the electricity demand of the zone ($d_{h,w,z}$) and the net energy losses ($x^{wdw}_{g,h,w} - x^{inj}_{g,h,w}$) across resources that can withdraw energy in the zone ($g \in (O \cap G_z)$). For Eq. (3b) the "direct decarbonization" policy constraint is implemented for the system as a whole. The change can be understood as if zones were pooling their $CO_2$ allowances together in order to reduce total system cost by improving the $CO_2$ allocation while ensuring that the total emissions in the system are kept to the same level. The change in going from Eq. (3a) to Eq. (3b) requires summing over all zones $z \in Z$ on both sides of the constraint.

$$\begin{aligned} \sum_{w \in W} \sum_{h \in H} \sum_{g \in G_z} x^{inj}_{g,h,w} \cdot \epsilon^{CO2}_g \leq \\ \epsilon^{max}_z \Big( \sum_{w \in W} \sum_{h \in H} \big( d_{h,w,z} + \sum_{g \in (O \cap G_z)} (x^{wdw}_{g,h,w} - x^{inj}_{g,h,w}) \big) \Big) \end{aligned} \qquad \forall z \in Z \tag{3a}$$

$$
\sum_{z \in Z} \sum_{w \in W} \sum_{h \in H} \sum_{g \in G_z} x^{inj}_{g,h,w} \cdot \epsilon^{CO2}_{g} \leq \sum_{z \in Z} \Big( \epsilon^{max}_{z} \sum_{w \in W} \sum_{h \in H} \big( d_{h,w,z} + \sum_{g \in (O \cap G_z)} (x^{wdw}_{g,h,w} - x^{inj}_{g,h,w}) \big) \Big) \tag{3b}
$$

The second type of policy, Eq. (4), are the "indirect decarbonization" policies or "energy standards" like renewable portfolio or clean energy standards or a combination of both. In this case we do not set a limit or allowance but instead set a minimum requirement ($\epsilon^{STD}_{i,z}$) on the fraction of total demand (electricity demand plus net energy losses) that must to be served by resources that qualify $g \in STD_i$ for each standard $i \in I$. As with Eq. (3) the implementation of these policies can be done in two ways Eq. (4a) and Eq. (4b). First, by zone as in Eq.(4a), power injections ($x^{inj}_{g,h,w}$) are summed over all sub-periods $w \in W$ and hours $h \in H$ for all resources that are in each zone $g \in G_z$ and that qualify for the specific standard $g \in STD_i$ for each standard $i$. These total injections must be greater than or equal to the minimum energy requirement set be the standard $i$. The minimum energy requirement set by the standard $i$ is calculated as the total zonal demand times the policy standard energy requirement ($\epsilon^{STD}_{i,z}$) for that zone. Total zonal demand, as was the case for Eq. (3), is calculated as the sum over all sub-periods $w \in W$ and hours $h \in H$ of the electricity demand of the zone ($d_{h,w,z}$) and the net energy losses ($x^{wdw}_{g,h,w} - x^{inj}_{g,h,w}$) across resources that can withdraw energy in the zone ($g \in (O \cap G_z)$). For Eq. (4b) each standard $i \in I$ is implemented for the system as a whole. The change can be understood as if zones were pooling their total requirements together in order to reduce total system cost by improving the allocation while ensuring that the total quotas in the system are kept to the same minimum level. The change in going from Eq. (4a) to Eq. (4b) requires summing over all zones $z \in Z$ on both sides of the constraint.

$$
\sum_{w \in W} \sum_{h \in H} \sum_{g \in (STD_i \cap G_z)} x^{inj}_{g,h,w} \geq \epsilon^{STD}_{i,z} \Big( \sum_{w \in W} \sum_{h \in H} \big( d_{h,w,z} + \sum_{g \in (O \cap G_z)} (x^{wdw}_{g,h,w} - x^{inj}_{g,h,w}) \big) \Big) \quad \forall z \in Z, i \in I \tag{4a}
$$

$$
\sum_{z \in Z} \sum_{w \in W} \sum_{h \in H} \sum_{g \in (STD_i \cap G_z)} x^{inj}_{g,h,w} \geq \sum_{z \in Z} \Big( \epsilon^{STD}_{i,z} \sum_{w \in W} \sum_{h \in H} \big( d_{h,w,z} + \sum_{g \in (O \cap G_z)} (x^{wdw}_{g,h,w} - x^{inj}_{g,h,w}) \big) \Big) \quad \forall i \in I \tag{4b}
$$

**Investment Related Constraints** Different constraints must be imposed on the investment related variables as shown in Eq. (5). First, for all resource clusters $g \in G$ power investment retirements ($y^{P-}_{g}$) times their unit size ($\bar{y}^{P\Delta}_{g}$) must be less than the initial existing or brownfield investments ($\bar{y}^{P\vee}_{g}$) in the cluster, Eq. (5a). Second, for all resource clusters $g \in G$ new power investment ($y^{P+}_{g}$) times their unit size ($\bar{y}^{P\Delta}_{g}$) must be less than the maximum deployable power investments ($\bar{y}^{P\wedge}_{g}$) in the cluster, Eq. (5b). Finally, for all resource clusters $g \in G$ the total available power capacity ($y^{P\Sigma}_{g}$) is equal to the sum of the initial existing or brownfield investments ($\bar{y}^{P\vee}_{g}$), plus the unit size ($\bar{y}_g^{P\Delta}$) times the net result of new investment ($y_g^{P+}$) and investment retirements ($y_g^{P-}$), Eq. (5c).

$$y_g^{P-} \cdot \bar{y}_g^{P\Delta} \leq \bar{y}_g^{P\vee} \qquad \forall g \in G \tag{5a}$$

$$y_g^{P+} \cdot \bar{y}_g^{P\Delta} \leq \bar{y}_g^{P\wedge} \qquad \forall g \in G \tag{5b}$$

$$y_g^{P\Sigma} = \bar{y}_g^{P\vee} + \bar{y}_g^{P\Delta} \cdot (y_g^{P+} - y_g^{P-}) \qquad \forall g \in G \tag{5c}$$

Additionally, investment related constraints for power lines must be imposed, Eq. (6). For all power lines $l \in L$ network reinforcements ($y_l^{F+}$) must be less or equal than the maximum deployable line reinforcements ($\bar{y}_l^{F\wedge}$) in the line, Eq. (6a). For all lines total available transmission capacity ($y_l^{F\Sigma}$) is equal to the sum of the initial existing or brownfield transmission capacity ($\bar{y}_l^{F\vee}$), plus the network reinforcements ($y_l^{F+}$), Eq. (6b).

$$y_l^{F+} \ \leq \ \bar{y}_l^{F\wedge} \qquad \forall l \in L \tag{6a}$$

$$y_l^{F\Sigma} \ = \ \bar{y}_l^{F\vee} + y_l^{F+} \qquad \forall l \in L \tag{6b}$$

Note that in this study, we do not explicitly model transmission capacity expansion (transmission decisions are included here only to present a complete formulation of the model, as it may be used in other studies).

**Economic Dispatch Constraints** A key component of this methodology compared to cost-based approaches is the inclusion of technical constraints on the Economic Dispatch Problem. Basic micro-economic analysis that intersects demand with the supply curves for each hour falls short in that all technologies are assumed to have similar (if any) limitations on chronological changes in demand and available supply (e.g., variable renewable energy). In the absence of these types of constraints the solution to the economic dispatch problem is simply the generation from lowest marginal cost resources in ascending order in the system, i.e., purely cost-based. However, when including operational constraints and hours are chronologically coupled the result is that resources are differentiated not only on the basis of their costs, and that technical characteristics such as location, flexibility, and the ability to provide a range of services also provide value — and that in different power systems these characteristics are valued differently.

The first group of constraints, Eq. (7), corresponds to the ramping, minimum stable output and maximum production limits. Ramping constraints are imposed in both directions. Ramp-down constraints, Eq. (7a), are set as the negative difference in power injections between consecutive hours ($x_{g,h-1,w}^{inj} - x_{g,h,w}^{inj}$) for each hour $h \in H$ in all sub-periods $w \in W$ for all resource clusters subject to ramping limits but not to unit commitment requirements $g \in (R - UC)$. For these resources the negative difference in power injections must be less than or equal to total available power capacity in the cluster ($y_g^{P\Sigma}$) times the maximum ramp-down rate ($\kappa_g^-$) of the cluster. Similarly, ramp-up constraints, Eq. (7b), are set as the difference in power injections between consecutive hours ($x_{g,h-1,w}^{inj} - x_{g,h,w}^{inj}$) for each hour $h \in H$ in all sub-periods $w \in W$ for all resource clusters subject to ramping limits but not to unit commitment requirements $g \in (R - UC)$. For these resources the difference in power injections must be less than or equal to total available power capacity in the cluster ($y_g^{P\Sigma}$) times the maximum ramp-up rate ($\kappa_g^+$) of the cluster.

$$x_{g,h-1,w}^{inj} - x_{g,h,w}^{inj} \leq \kappa_g^- \cdot y_g^{P\Sigma} \qquad \forall g \in (R - UC), h \in H, w \in W \tag{7a}$$

$$x_{g,h,w}^{inj} - x_{g,h-1,w}^{inj} \leq \kappa_g^+ \cdot y_g^{P\Sigma} \qquad \forall g \in (R - UC), h \in H, w \in W \tag{7b}$$

$$x_{g,h,w}^{inj} \geq \rho_g^{\vee} \cdot y_g^{P\Sigma} \qquad \forall g \in (G - UC), h \in H, w \in W \tag{7c}$$

$$x_{g,h,w}^{inj} \leq \rho_{g,h}^{\wedge} \cdot y_g^{P\Sigma} \qquad \forall g \in (G - UC), h \in H, w \in W \tag{7d}$$

$$x_{g,h,w}^{wdw} \leq y_g^{P\Sigma} \qquad \forall g \in O, h \in H, w \in W \tag{7e}$$

Minimum stable output limits, Eq. (7c), are also imposed on all resource clusters that are not subject to unit commitment requirements $g \in (G - UC)$. For each hour $h \in H$ in all sub-periods $w \in W$ power injections ($x_{g,h,w}^{inj}$) must remain above the minimum level determined by the total available power capacity in the cluster ($y_g^{P\Sigma}$) times the stable output rate ($\rho_g^{\vee}$) for the cluster. Note that this minimum output level ($\rho_g^{\vee}$) may be 0 for some resources (e.g. solar PV, wind, Li-ion batteries). Maximum power output, Eq. (7d), limits are imposed to all resource clusters that are not subject to unit commitment requirements $g \in (G - UC)$, including energy storage resources. For each hour $h \in H$ in all sub-periods $w \in W$ power injections ($x_{g,h,w}^{inj}$) must remain below the maximum production level determined by the total available power capacity in the cluster ($y_g^{P\Sigma}$) times the hourly capacity factor ($\rho_{g,h}^{\wedge}$) for the cluster. The hourly capacity factor, $\rho_{g,h}^{\wedge}$, varies in each hour for weather-dependent variable renewable resources (to reflect variations in e.g. wind speeds or solar insolation or stream flows) and is 1.0 in all periods for all other resources. For resources with the ability to withdraw energy $g \in O$, including Li-ion battery energy storage, Eq. (7e) imposes a limit on maximum withdraw at each hour $h \in H$ in all sub-periods $w \in W$ to be less than or equal to the power capacity of the resource.

The second group of constraints, Eq. (8), corresponds to the energy balance and operation requirements for resource clusters that can carry an energy balance $g \in O$ across time periods for all hours $h \in H$ and sub-periods $w \in W$, such as Li-ion batteries modeled in this study. The energy balance constraint, Eq. (8a) enforces that the energy balance difference between one hour and the next one ($x_{g,h+1,w}^{lvl} - x_{g,h,w}^{lvl}$) must be equal to increments minus reductions in energy stored. Energy is increased via energy withdrawals ($x_{g,h,w}^{wdw}$) multiplied by the corresponding efficiency ($\eta_g^+$) to account for losses. Energy is reduced via energy injections ($x_{g,h,w}^{inj}$) divided by the corresponding efficiency ($\eta_g^-$) to account for losses; and via internal losses calculated as the product between the energy balance ($x_{g,h,w}^{lvl}$) during that hour and the self discharge rate ($\eta_g^0$). Different operation limits must be imposed on these resource clusters. Eq. (8b) sets a limit on the maximum energy balance ($x_{g,h,w}^{lvl}$) to be always less or equal than total available power capacity in the cluster ($y_g^{P\Sigma}$) times the duration or energy-to-power ration ($\delta_g$). Eq. (8c) sets a limit on the injections ($x^{inj}_{g,h,w}$) to be less than or equal to the energy balance ($x^{lvl}_{g,h,w}$) times the injection efficiency ($\eta^{-}_{g}$). Eq. (8d) sets a limit on the withdrawals ($x^{wdw}_{g,h,w}$) to be less than the remaining energy capacity. This remaining capacity is determined by taking the difference between the energy capacity ($y^{P\Sigma}_{g} \cdot \delta_g$) and the energy balance ($x^{lvl}_{g,h,w}$).Finally, Eq (8e) limits the simultaneous operation of the injections ($x^{inj}_{g,h,w}$) and withdrawals ($x^{wdw}_{g,h,w}$) of the cluster to be less than or equal to the total available power capacity ($y^{P\Sigma}_{g}$). Note that simultaneous charging and discharging of a storage resource is possible because we are modeling an aggregation of many discrete storage units. Some storage units may be charging while others charging in a given time period. In practice, this occurs very rarely, as any positive marginal cost of energy in a given time period will encourage the model to only charge or discharge so as to avoid incurring additional costs associated with round-trip storage losses. Simultaneous charging and discharging only improves the objective function during rare periods when ramp down constraints or minimum stable output constraints along with minimum up/down time constraints on thermal generators would create a negative marginal energy prince at a time period in the absence of storage, indicating that increasing consumption would reduce the objective function or improve total costs by avoiding a thermal unit shut-down and later start-up costs upon restart of that unit. In these rare periods, the model may choose to charge and discharge at the same time to incur round-trip storage losses and reduce system costs. Eq. (8e) ensures that in these rare moments, the sum total of charging and discharging does not exceed installed storage power capacity and thus remains physically feasible. Note also that Eq. (8c) and (8d) are generally redundant with the combination of constraints in Eq. (8a)-(8b) and the non-negativity constraint on $x^{lvl}_{g,h,w}$. However, during periods of simultaneous charging and discharging (which may occur during negative price periods as discussed above), these constraints limit the maximum charge and discharge in each period to physically feasible values considering the available current storage state of charge and maximum capacity. In cases where the remaining storage capacity (considering charge losses), $(y^{P\Sigma}_{g} \cdot \delta_g) - x^{lvl}_{g,h,w}$, is $\leq$ the charge power capacity $y^{P\Sigma}_{g}$, then the charge (or withdrawl) power in that time step, $x^{wdw}_{g,h,w}$, will be constrained by Eq. (8d). Similarly, when the available energy for discharge (considering discharge losses), $x^{lvl}_{g,h,w} \cdot \eta^{-}_{g}$, is $\leq$ the storage discharge power capacity, $y^{P\Sigma}_{g}$, then Eq. 8c will be constraining on discharge power (or injection).

$$x^{lvl}_{g,h+1,w} - x^{lvl}_{g,h,w} = (x^{wdw}_{g,h,w} \cdot \eta^{+}_{g}) - (x^{inj}_{g,h,w}/\eta^{-}_{g}) - (x^{lvl}_{g,h,w} \cdot \eta^{0}_{g}) \qquad \forall g \in O, h \in H, w \in W \tag{8a}$$

$$x^{lvl}_{g,h,w} \leq y^{P\Sigma}_{g} \cdot \delta_g \qquad \forall g \in O, h \in H, w \in W \tag{8b}$$

$$x^{inj}_{g,h,w} \leq x^{lvl}_{g,h,w} \cdot \eta^{-}_{g} \qquad \forall g \in O, h \in H, w \in W \tag{8c}$$

$$x^{wdw}_{g,h,w} \leq (y^{P\Sigma}_{g} \cdot \delta_g) - x^{lvl}_{g,h,w} \qquad \forall g \in O, h \in H, w \in W \tag{8d}$$

$$x^{inj}_{g,h,w} + x^{wdw}_{g,h,w} \leq y^{P\Sigma}_{g} \qquad \forall g \in O, h \in H, w \in W \tag{8e}$$

The final group of economic dispatch constraints correspond to transmission constraints, Eq. (9). Constraints Eq. (9a) and (9b) impose the requirements that for all hours $h \in H$ and sub-periods $w \in W$ the power flow ($x^{flow}_{l,h,w}$) in either direction must be less than or equal to the total available transmission capacity ($y^{F\Sigma}_{l}$) for every line $l \in L$. Note that in this study, we do not explicitly model transmission power flows (transmission decisions are included here only to present a complete formulation of the model, as it may be used in other studies).

$$x^{flow}_{l,h,w} \leq y^{F\Sigma}_{l} \qquad \forall l \in L, h \in H, w \in W \tag{9a}$$

$$-x^{flow}_{l,h,w} \leq y^{F\Sigma}_{l} \qquad \forall l \in L, h \in H, w \in W \tag{9b}$$

**Unit Commitment Constraints** Another key component of this methodology that contrasts with to cost-based approaches is the inclusion of technical constraints associated with the Unit Commitment (UC) Problem. Unit commitment refers to the scheduling of resources to be available to operate ahead of time. Including UC details is important to reflect the increasing need for cycling as variable renewable energy is further increased in the system. Additionally, UC helps model increased flexibility by including startup and shutdown decisions that, if not included, would require all resources to always operate between their minimum stable output and their maximum output, without any ability to take resources offline and bring them back online later. The first of these constraints, Eq. (10), imposes limitations on the number of committed units ($x^{commit}_{g,h,w}$), startup events ($x^{start}_{g,h,w}$), and shutdown events ($x^{shut}_{g,h,w}$) for all resource clusters subject to UC constraints $g \in UC$ for all hours $h \in H$ and all sub-periods $w \in W$ to be less than or equal to the number of units in the cluster. The number of units is calculated as the total available power capacity ($y^{P\Sigma}_{g}$) divided by the unit size in the cluster ($\bar{y}^{P\Delta}_{g}$).

$$x^{commit}_{g,h,w} \leq y^{P\Sigma}_{g}/\bar{y}^{P\Delta}_{g} \qquad \forall g \in UC, h \in H, w \in W \tag{10a}$$

$$x^{start}_{g,h,w} \leq y^{P\Sigma}_{g}/\bar{y}^{P\Delta}_{g} \qquad \forall g \in UC, h \in H, w \in W \tag{10b}$$

$$x^{shut}_{g,h,w} \leq y^{P\Sigma}_{g}/\bar{y}^{P\Delta}_{g} \qquad \forall g \in UC, h \in H, w \in W \tag{10c}$$

Ramping, minimum stable output and maximum operation limits for clusters with UC requirements can be seen in Eq. (11) versus the same set of operating requirements for clusters without UC in Eq. (7). Ramp-down constraints are shown in Eq. (11a). The negative difference in power injections between consecutive hours ($x^{inj}_{g,h-1,w} - x^{inj}_{g,h,w}$) for each hour $h \in H$ in all sub-periods $w \in W$ for all resource clusters subject to UC $g \in UC$ must be less than or equal to the ramping down capacity of the committed units accounting for any start-up and shut-down events. Ramping capacity is calculated as the number of committed units that were not started-up in the same time period ($x^{commit}_{g,h,w} - x^{start}_{g,h,w}$) times the cluster's unit size ($\bar{y}^{P\Delta}_{g}$) times the maximum ramping rate ($\kappa^{-}_{g}$). The ramping down capacity is reduced by the number of start-up events in the cluster during the same period ($x^{start}_{g,h,w}$) since these units must operate above their minimum stable output ($\rho^{\vee}_{g}$) for units of size ($\bar{y}^{P\Delta}_{g}$). Ramping down capacity is increased by units that are shut down during the time period allowing a larger change in the cluster's output. Thus, the minimum between the maximum output ($\rho^{\wedge}_{g,h}$) and the maximum between the minimum stable output ($\rho^{\vee}_{g}$) or the maximum ramp-down rate ($\kappa^{-}_{g}$), times the cluster's unit size ($\bar{y}^{P\Delta}_{g}$) for all units shut down ($x^{shut}_{g,h,w}$) are added to the ramp-down capacity. In other words, an individual unit shutting down can result in a change in aggregate output for the cluster equal to the greater of either. Similarly, for ramp-up constraints, Eq. (11b), the difference in power injections between consecutive hours ($x^{inj}_{g,h,w} - x^{inj}_{g,h-1,w}$) for each hour $h \in H$ in all sub-periods $w \in W$ for all resource clusters subject to UC $g \in UC$ must be less than or equal to the ramping up capacity of the committed units accounting for any start-up and shut-down events. Ramping up capacity is calculated as the number of committed units that were not started up in the same time period ($x^{commit}_{g,h,w} - x^{start}_{g,h,w}$) times the cluster's unit size ($\bar{y}^{P\Delta}_{g}$) times the maximum ramping rate ($\kappa^{+}_{g}$). The ramping up capacity is increased by the number of start-up events in the cluster during the same period ($x^{start}_{g,h,w}$). Newly started units increase output up to the minimum between their maximum output ($\rho^{\wedge}_{g,h}$)and the minimum between their minimum stable output ($\rho^{\vee}_{g}$) and the ramp-up rate ($\kappa^{+}_{g}$), times the cluster's unit size ($\bar{y}^{P\Delta}_{g}$) for started units ($x^{start}_{g,h,w}$). Units shut down reduce the ramping up capacity by the total number of shut-down units ($x^{shut}_{g,h,w}$) times the minimum stable output of this units ($\rho^{\vee}_{g}$) and the unit's size ($\bar{y}^{P\Delta}_{g}$).

$$
\begin{aligned}
x^{inj}_{g,h-1,w} - x^{inj}_{g,h,w} \;\leq\;& (x^{commit}_{g,h,w} - x^{start}_{g,h,w})\kappa^{-}_{g} \cdot \bar{y}^{P\Delta}_{g} && \\
& - x^{start}_{g,h,w} \cdot \bar{y}^{P\Delta}_{g} \cdot \rho^{\vee}_{g} && \forall g \in UC, h \in H, w \in W \qquad \text{(11a)} \\
& + x^{shut}_{g,h,w} \cdot \bar{y}^{P\Delta}_{g} \cdot \min(\rho^{\wedge}_{g,h}, \max(\rho^{\vee}_{g}, \kappa^{-}_{g})) && \\
x^{inj}_{g,h,w} - x^{inj}_{g,h-1,w} \;\leq\;& (x^{commit}_{g,h,w} - x^{start}_{g,h,w})\kappa^{+}_{g} \cdot \bar{y}^{P\Delta}_{g} && \\
& + x^{start}_{g,h,w} \cdot \bar{y}^{P\Delta}_{g} \cdot \min(\rho^{\wedge}_{g,h}, \max(\rho^{\vee}_{g}, \kappa^{+}_{g})) && \forall g \in UC, h \in H, w \in W \qquad \text{(11b)} \\
& - x^{shut}_{g,h,w} \cdot \bar{y}^{P\Delta}_{g} \cdot \rho^{\vee}_{g} && \\
x^{inj}_{g,h,w} \;\geq\;& x^{commit}_{g,h,w} \cdot \bar{y}^{P\Delta}_{g} \cdot \rho^{\vee}_{g} && \forall g \in UC, h \in H, w \in W \qquad \text{(11c)} \\
x^{inj}_{g,h,w} \;\leq\;& x^{commit}_{g,h,w} \cdot \bar{y}^{P\Delta}_{g} \cdot \rho^{\wedge}_{g,h} && \forall g \in UC, h \in H, w \in W \qquad \text{(11d)}
\end{aligned}
$$

Minimum stable output, Eq. (11c), for clusters $g \in UC$ is sets for power injections ($x^{inj}_{g,h,w}$) to be greater than or equal to the number of units committed in the cluster ($x^{commit}_{g,h,w}$) times the cluster's unit size ($\bar{y}^{P\Delta}_{g}$) and the minimum stable output rate ($\rho^{\vee}_{g}$). Similarly, maximum operation limits, Eq. (11d) are set for power injections ($x^{inj}_{g,h,w}$) to be less or equal than the number of units committed in the cluster ($x^{commit}_{g,h,w}$) times the cluster's unit size ($\bar{y}^{P\Delta}_{g}$) and the maximum output rate ($\rho^{\wedge}_{g,h}$).

Finally, constraints on the UC states and limitations accounting for minimum Up and Down Times must be included. Eq. (12a) sets the relationship for commitment state changes between consecutive hours ($x^{commit}_{g,h,w} - x^{commit}_{g,h-1,w}$) to be equal to the net change in start-up and shut-down events ($x^{start}_{g,h,w} - x^{shut}_{g,h,w}$) in the cluster $g \in UC$ for all hours $h \in H$ and sub-periods $w \in W$. Minimum down-time requirements are imposed in Eq. (12b) setting the number of units offline ($y_g^{P\Sigma}/\bar{y}_g^{P\Delta} - x_{g,h,w}^{commit}$) to be greater than or equal to the total number of shut-down events ($x_{g,h,w}^{shut}$) during the preceding hours ($h - \tau_g^-$) and the current hour ($h$), where $\tau_g^-$ is the minimum down-time for units in cluster $g$. Minimum up-time requirements are imposed in Eq. (12c) setting the number of committed units ($x_{g,h,w}^{commit}$) to be greater than or equal to the total number of start-ups ($x_{g,h,w}^{start}$) during the preceding hours ($h - \tau_g^+$) and the current hour ($h$), where $\tau_g^+$ is the minimum up-time for units in cluster $g$.

$$x_{g,h,w}^{commit} - x_{g,h-1,w}^{commit} = x_{g,h,w}^{start} - x_{g,h,w}^{shut} \qquad \forall g \in UC, h \in H, w \in W \tag{12a}$$

$$y_g^{P\Sigma}/\bar{y}_g^{P\Delta} - x_{g,h,w}^{commit} \geq \sum_{h \in (h-\tau_g^-:h)} x_{g,h,w}^{shut} \qquad \forall g \in UC, h \in H, w \in W \tag{12b}$$

$$x_{g,h,w}^{commit} \geq \sum_{h \in (h-\tau_g^+:h)} x_{g,h,w}^{start} \qquad \forall g \in UC, h \in H, w \in W \tag{12c}$$

**Time Wrapping and Coupling** Our modeling approach does not assumes exogenous initial conditions for any of the time related components (e.g. unit commitment, ramping, energy storage balance, etc). Instead, we wrap-up initial and final conditions by setting the previous hour to the first hour of the first sub-period ($h-1, w|h = 1, w = 1$) to be equal to the last hour of the last sub-period ($h, w|h = H, w = W$) in the time horizon –e.g. the storage level at the end of the planning horizon is equal to the initial condition for the first hour of the planning horizon. Additionally, our methodology keeps the chronological coupling across different sub-periods $w$ (e.g. weeks) ensuring the operation is consistent and optimized simultaneously for the full year. This is done by setting the previous hour to the first hour of each sub-period ($h - 1, w|h = 1, w \in \{2, .., W\}$) to be equal to the last hour of the previous sub-period ($h, w - 1|h = H, w \in \{2, .., W\}$) –e.g. the commitment state at the end of a sub-period is the initial commitment state for the next sub-period.

## Long-duration Energy storage Implementation

In order to investigate LDES resources the methodology developed in [9] requires some modifications. An important difference between LDES technologies and Li-ion batteries is that the former has the ability to scale power and energy capacity independently. As mentioned previously the "LDES Technology Space" includes a variety of technologies, with some technologies decoupling energy and power scaling, while others can also decouple charge and discharge power scaling. Given the exploratory nature of our analysis, our LDES Technology Space exploration assumes that the three scaling dimensions – energy capacity, discharge power capacity, and charge power capacity– are independent.

In order to account for these differences new decision variables for investments for energy capacity, and charge power capacity must be included together with additional parameters (discharge power capacity was already implemented for short-term storage). The Objective function must include the additional variables and some operational constraints need to be modified.

### Decision Variables

Table SI-11 shows the new variables to account for independent energy capacity and charge power capacity investments, retirements and total available capacity.

**Table SI-11.** New Model Variables

| Notation | Description |
|---|---|
| $y_g^{E+}$ | new energy investments on resource cluster $g$. |
| $y_g^{E-}$ | retired energy investments on resource cluster $g$. |
| $y_g^{E\Sigma}$ | total available energy capacity in cluster $g$. |
| $y_g^{C+}$ | new charge power investments on resource cluster $g$. |
| $y_g^{C-}$ | retired charge power investments on resource cluster $g$. |
| $y_g^{C\Sigma}$ | total available charge power capacity in cluster $g$. |

### Parameters

Table SI-12 shows the new parameters for energy capacity and charge power capacity maximum new investments, existing capacity, as well as, cost parameters for new investment and fixed operation and maintenance for total capacity. Additionally, we must include maximum and minimum durations parameters.

**Table SI-12.** New Model Parameters

| Notation | Description |
|---|---|
| $\bar{y}_g^{E\wedge}$ | Maximum new energy investments in cluster $g$. |
| $\bar{y}_g^{E\vee}$ | Existing brownfield energy investments in cluster $g$. |
| $c_g^{Ei}$ | Annuity of capital cost for energy investments in cluster $g$. |
| $c_g^{Eom}$ | Fixed energy O&M cost for units in cluster $g$. |
| $\bar{y}_g^{C\wedge}$ | Maximum new charge power investments in cluster $g$. |
| $\bar{y}_g^{C\vee}$ | Existing brownfield charge power investments in cluster $g$. |
| $c_g^{Ci}$ | Annuity capital cost for charge power investments in cluster $g$. |
| $c_g^{Com}$ | Fixed charge power O&M cost for units in cluster $g$. |
| $\delta_g^{\wedge}$ | Maximum duration (ratio energy to discharge power) investments in cluster $g$. |
| $\delta_g^{\vee}$ | Minimum duration (ratio energy to discharge power) investments in cluster $g$. |

### Objective Function

The original Objective Function in Eq. (1) must be modified to include new investment variables. Eq. (1b) is updated with additional terms to account for the total cost of energy capacity related investments ($y_g^{E+}c_g^{Ei}$ +

$y_g^{E\Sigma} c_g^{Eom}$) and charge power capacity related investments ($y_g^{C+} c_g^{Ci} + y_g^{C\Sigma} c_g^{Com}$) resulting in the updated Eq. (13b). The Objective Function of the problem becomes (13).

$$\min_{y,x} \Bigg( \tag{13a}$$

$$\sum_{g \in G} (y_g^{P+} \cdot c_g^{Pi} \cdot \bar{y}_g^{P\Delta} + y_g^{P\Sigma} \cdot c_g^{Pom}) + \sum_{g \in O} (y_g^{E+} c_g^{Ei} + y_g^{E\Sigma} c_g^{Eom} + y_g^{C+} c_g^{Ci} + y_g^{C\Sigma} c_g^{Com}) +$$

$$\sum_{l \in L} (y_l^{F+} \cdot c_l^{Fi}) + \tag{13b}$$

$$\sum_{w \in W} \sum_{h \in H} \Big( \sum_{g \in G} (x_{g,h,w}^{inj} \cdot (c_g^{Po} + c_g^{f})) + \sum_{g \in O} (x_{g,h,w}^{wdw} \cdot c_g^{Po}) + \sum_{z \in Z} \sum_{s \in S} x_{s,h,w,z}^{nse} \cdot n_s^{slope} \Big) + \tag{13c}$$

$$\sum_{w \in W} \sum_{h \in H} \Big( \sum_{g \in UC} x_{g,h,w}^{start} \cdot c_g^{st} \Big) \Bigg) \tag{13d}$$

**Investment Related Constraints**

New investment decisions require including additional constraints to the problem described in the previous section. First, for Long Duration Energy Storage resources clusters $O^2 \subseteq O$ energy investment retirements ($y_g^{E-}$) must be less than the initial existing or brownfield energy investments ($\bar{y}_g^{E\vee}$), Eq. (14a). Second, new energy investment ($y_g^{E+}$) must be less than the maximum deployable energy investments ($\bar{y}_g^{E\wedge}$), Eq. (14b). The total available power capacity ($y_g^{E\Sigma}$) is equal to the sum of the initial existing or brownfield investments ($\bar{y}_g^{E\vee}$), plus the net result of new energy investment ($y_g^{E+}$) and energy investment retirements ($y_g^{E-}$), Eq. (14c). The exact same logic must be applied to charge power investments through Eq. (14f) to (14h).

$$y_g^{E-} \leq \bar{y}_g^{E\vee} \qquad \forall g \in O^2 \tag{14a}$$

$$y_g^{E+} \leq \bar{y}_g^{E\wedge} \qquad \forall g \in O^2 \tag{14b}$$

$$y_g^{E\Sigma} = \bar{y}_g^{E\vee} + (y_g^{E+} - y_g^{E-}) \qquad \forall g \in O^2 \tag{14c}$$

$$y_g^{P\Sigma} \cdot \delta_g^{\vee} \leq y_g^{E\Sigma} \qquad \forall g \in O^2 \tag{14d}$$

$$y_g^{P\Sigma} \cdot \delta_g^{\wedge} \geq y_g^{E\Sigma} \qquad \forall g \in O^2 \tag{14e}$$

$$y_g^{C-} \leq \bar{y}_g^{C\vee} \qquad \forall g \in O^2 \tag{14f}$$

$$y_g^{C+} \leq \bar{y}_g^{C\wedge} \qquad \forall g \in O^2 \tag{14g}$$

$$y_g^{C\Sigma} = \bar{y}_g^{C\vee} + (y_g^{C+} - y_g^{C-}) \qquad \forall g \in O^2 \tag{14h}$$

$$\tag{14i}$$

Eq. (14d) and (14e) impose upper and lower bounds on the duration of the storage. The total power capacity ($y_g^{P\Sigma}$) times the minimum duration parameter ($\delta_g^{\vee}$) must be less or equal than the total available energy capacity

$(y_g^{E\Sigma})$. At the same time, the total power capacity $(y_g^{P\Sigma})$ times the maximum duration parameter $(\delta_g^{\wedge})$ must be greater or equal than the total available energy capacity $(y_g^{E\Sigma})$.

**Economic Dispatch Constraints**

Two constraints formulated in the previous section for the Economic Dispatch Problem need to be updated to account for independent decisions in power and energy for energy storage. These constraints are Eq. (8b) and (8d). An updated version is presented below in Eq. (15a) and (15b), respectively. Additionally, constraint Eq. (15c) must be included to account for the independent deployment of charge power capacity investments that will limit the ability of charging the system.

$$x_{g,h,w}^{lvl} \le y_g^{E\Sigma} \qquad \forall g \in O^2, h \in H, w \in W \tag{15a}$$

$$x_{g,h,w}^{wdw} \le y_g^{E\Sigma} - x_{g,h,w}^{lvl} \qquad \forall g \in O^2, h \in H, w \in W \tag{15b}$$

$$x_{g,h,w}^{wdw} \le y_g^{C\Sigma} \qquad \forall g \in O^2, h \in H, w \in W \tag{15c}$$

# References


[1] U.S. Energy Information Administration. Annual Energy Outlook 2018 with Projections to 2050. Technical report, U.S. Department of Energy, Washington, D.C., 2018.

[2] Patrick R. Brown and Francis M. O'Sullivan. Spatial and temporal variation in the value of solar power across United States electricity markets. *Renewable and Sustainable Energy Reviews*, 121(June 2019):109594, 2020.

[3] Caroline Draxl, Andrew Clifton, Bri Mathias Hodge, and Jim McCaa. The Wind Integration National Dataset (WIND) Toolkit. *Applied Energy*, 151:355–366, 2015.

[4] Evolved Energy Research. EnergyPATHWAYS Model.

[5] IEA Greenhouse Gas R&D Programme (IEAGHG). Techno - Economic Evaluation of SMR Based Standalone (Merchant) Hydrogen Plant with CCS. Technical Report February, International Energy Agency (IEA), 2017.

[6] International Energy Agency and Nuclear Energy Agency. Projected Costs of Generating Electricity. Technical report, Organisation for Economic Co-operation and Development (OECD), 2015.

[7] Jesse D Jenkins. *Electricity system planning with distributed energy resources : new methods and insights for economics, regulation, and policy.* Doctoral dissertation, Massachusetts Institute of Technology, 2018.

[8] Jesse D. Jenkins, Max Luke, and Samuel Thernstrom. Getting to Zero Carbon Emissions in the Electric Power Sector. *Joule*, 2(12):2498–2510, 2018.

[9] Jesse D Jenkins and Nestor A Sepulveda. Enhanced Decision Support for a Changing Electricity Landscape : The GenX Configurable Electricity Resource Capacity Expansion Model. 2017.

[10] N. Kumar, P. Besuner, S. Lefton, D. Agan, and D. Hilleman. Power Plant Cycling Costs. Technical Report April, NREL (National Renewable Laboratory), 2012.

[11] NREL (National Renewable Energy Laboratory). 2018 Annual Technology Baseline. `https://atb.nrel.gov/electricity/2018/`, 2018.

[12] Bryan S. Palmintier. *Incorporating Operational Flexibility Into Electric Generation Planning: Impacts and Methods for System Design and Policy Analysis.* Phd dissertation, Massachusetts Institute of Technology, 2013.

[13] Bryan S Palmintier and Mort D Webster. Impact of Operational Flexibility on Electricity Generation Planning with Renewable and Carbon Targets. *IEEE Transactions on Sustainable Energy*, 7(2):672–684, 2016.

[14] Manajit Sengupta, Yu Xie, Anthony Lopez, Aron Habte, Galen Maclaurin, and James Shelby. The National Solar Radiation Data Base (NSRDB). *Renewable and Sustainable Energy Reviews*, 89(September 2017):51–60, 2018.

[15] Joshua S. Stein, William F. Holmgren, Jessica Forbess, and Clifford W. Hansen. PVLIB: Open source photovoltaic performance modeling functions for Matlab and Python. *Conference Record of the IEEE Photovoltaic Specialists Conference*, 2016-Novem:3425–3430, 2016.

[16] James H. Williams, Ryan Jones, Gabe Kwok, and Benjamin Haley. Deep Decarbonization in the Northeastern United States and Expanded Coordination with Hydro-Quebec. Technical Report April, A report of the Sustainable Development Solutions Network in cooperation with Evolved Energy Research and Hydro-Quebec, 2018.